HOLOCENE DEVELOPMENT AND SEDIMENT TRANSPORT ON THE NORTHEASTERN GRAND BANKS OF NEWFOUNDLAND

BY

J.V. BARRIE

W.T. COLLINS

M.P. SEGALL

C.F.M. LEWIS

"This work was supported by the Federal Panel on Energy R & D (PERD)."

The Centre for Cold Ocean Resources Engineering (C-CORE) was established at Memorial University of Newfoundland in St. John's in 1975. Its initial funding was provided by the Devonian Group of Charitable Foundations of Calgary. Ongoing funding now comes from government and industry.

The Centre's mandate is to undertake research that will assist the safe and orderly development of Canada's resources in cold and ice frequented oceans.

J. V. Barrie
Leader, Seabed Group
C-CORE and Department of Earth Sciences
Memorial University of Newfoundland

W.T. Collins
Researcher, Marine Geology
C-CORE

M.P. Segall
Researcher, Marine Geology
C-CORE

C.F.M. Lewis
Geological Survey of Canada
Bedford Institute of Oceanography
Dartmouth, Nova Scotia

Disclaimer

The contents of this report do not necessarily reflect the views, opinions, or policies of the Government of Canada.

ABSTRACT

Five sediment facies are recognized for the northeastern Grand Banks of Newfoundland based on sediment and bedform distributions (Barrie et al., 1984). Sediments from grab samples, boreholes and vibrocores obtained in each of these facies were examined for texture, pebble lithology, mineralogy of sands, and quartz-grain surface textures. Results indicate a predominant local Tertiary and Cretaceous source of the material with a minor input from ice/iceberg rafting in the deeper shelf edge region. From the late Pleistocene-Holocene transgression to the present, the shelf surficial sediments have been highly reworked resulting in mature sand for which the various mineral size components are hydraulically equivalent. The pre-transgression subaerial surface can be laterally traced above -100m, the lowest stand of sea level, by the distinct change in heavy mineralogy from a dominance of garnet to iron hydroxide opaques, the intensity of quartz iron staining, and an increase in silt content.

During the winter months, in a water depth of 70 m, the critical threshold of sand transport under oscillatory flow is exceeded up to 70% of the time. Unidirectional velocities, 0.5 m above the seabed, are generally low with extreme velocities exceeding 0.45 m/sec. Both wave-generated and ocean currents have mean flow directions to the south-southeast. This motion results in sediment transport in this direction and in the formation and movement of observed oscillation ripples, megaripples and sand waves (parallel to the bathymetric contours). The larger sand ridges also appear to respond to the

southeasterly transport as evidenced by increasingly younger C^{14} dates towards the southeast throughout the ridge. Investigations, including tracer sand studies are presently underway to quantify the conditions under which these bedforms move.

ACKNOWLEDGEMENTS

We gratefully acknowledge G.B. Fader, C.L. Amos, D.R. Parrott, and B. Petrie for improving the manuscript with their helpful comments. The authors wish to thank Senior Scientist G. Vilks and the Captain and crew of **CSS HUDSON** for their cooperation and guidance through field operations. We extend our appreciation to C.M.T. Woodworth-Lynas for compilation of the isopach map, G. Stapleton and A. Simms for programming and D. King for drafting.

TABLE OF CONTENTS

LIST OF FIGURES

PAGE

LIST OF TABLES

INTRODUCTION

The northeastern Grand Banks of Newfoundland, in the area of the Hibernia discovery, is representative of a dynamic shelf vulnerable to iceberg scouring and wave and current sediment transport (Fig. 1). The seabed is particularly subject to shear stress from oceanic swell (water depths in the study area range from 60 m to about 140 m), storm driven waves, currents and the intrusion of the central arm of the Labrador Current. Further disruption of the seabed takes place when southward drifting icebergs ground and scour the seabed sediments.

Previous studies have noted and discussed the distribution of sediment erosion and transport events and iceberg disturbance for the northeastern Grand Banks centred in the Hibernia region (e.g. Amos and Barrie, 1980; Fader and King, 1981; Lewis and Barrie, 1981; Syvitski et al., 1983; Barrie et al., 1984). From results of sidescan sonar, Huntec DTS high resolution seismic reflection profiling, bottom photography, grab samples and submersible observations these studies have established a suite of five bathymetrically-controlled sediment facies based on sediment texture and bedform distribution. Above 140 m water depth the facies range from continuous fine sand, through lag gravel with sand ribbons, to a narrow contour-paralleling sand body (Boundary Sand) lying along the upper edge of a terrace at 100 m water depth. This terrace is thought to represent the late glacial low sea level stand (Fader and King, 1981; Lewis and Barrie, 1981; Barrie et al., 1984). Above 90 m, alternating sand ridges up to 4 m thick and mobile gravels occur. These post sea

level transgressive units unconformably overlie Tertiary beds with an angular discordance.

From analysis of these sediment distributions a qualitative assessment of the magnitude and distribution of sediment transport and iceberg grounding events has been made. Evidence from these previous studies implies that the larger bedforms (sand ribbons and sand ridges) are relict and were formed during the early Holocene when sea level stands were lower. The smaller bedforms (ripples, megaripples and sand waves) represent the modern hydrodynamic regime in the Hibernia area (Barrie et al., 1984).

Several questions remained unanswered from these studies. One important question is to determine how sediment dispersal relates to the understanding of the modern hydrodynamic regime. Can these sediment movements be accounted for under present wave and current conditions? The present model of Holocene sedimentological development of the northeastern Grand Banks is based on interpreted acoustic geophysical data, site specific and regional bottom photographs and surface grab samples. Another question then is, would stratigraphic samples analysed using several sedimentological techniques support the model and add further understanding to the long-term development of the larger sand bodies found in the Hibernia area?

Further questions related to the first query above are;

1) What is the depth of the potential mobile layer during a sediment transport event? Is it due to dynamic loading or sediment entrainment and what are the magnitude and

direction of the potential movements?

2) What is the erosive capability of normal yearly extreme velocities and of maximum predictable velocities for a combination of unidirectional and oscillatory currents?

3) Are the large bedforms (sand ridges and ribbons) relict (formed during earlier times of lower sea level)?

The understanding of these scientific questions is beneficial in assessing constraints for the engineering of offshore development.

In July 1983, eleven vibrocores (Appendix II) were obtained across the study area (Lewis, 1983) with special consideration to the P-15 sand ridge where six vibrocores were collected. In 1980, Geocon drilled geotechnical boreholes at the B-08, O-35 and I-45 wellsites (Geocon, 1980a, b, c). On a cruise of the **CSS HUDSON** in October, 1983 (Vilks, 1984) the BRUTIV camera sled system was used to survey 52 km along with both the 100 kHz (180 km) and 500 kHz (30 km) sidescan sonars, as well as the Huntec DTS (180 km), and 1.12 m^3 air gun (180 km) seismic profiles. Based on these new data the following analyses were completed.

METHODOLOGY

Data compiled and used for this report comes from many sources summarized by Barrie et al. (1984). In addition vibrocores, grab samples, high resolution (100 and 500 kHz) sidescan sonograms, Huntec DTS high resolution seismic profiles, 1.12 m^3 air gun records, BRUTIV camera sled photographs (Foulkes,

1984) and borehole data were collected during the previously mentioned cruises.

The Huntec Deep Tow shallow seismic reflection system with Acoustic Reflectivity Module calculates and displays the energy reflected from the seafloor as a percentage of incident acoustic energy (Parrott et al., 1980). The reflectivity measurements assist in the interpretation of sediment type and distribution of bed features (Appendix I). The acoustic reflectivities R_1 and R_2, measured in percentiles, indicate the amount of coherent energy reflected from the seafloor (R_1) and the amount of scattered energy (R_2) (Parrott et al., 1980; Fader and King, 1981). These values for the Hibernia area of the Grand Banks show that for gravelly substrates, the R_1 median profile is highly variable, ranging from 35 to 60%. R_1 median profiles for sand range from 25 to 45% and R_2 profiles range from 2 to 10%. Where shells, ripples and/or megaripples occur, R_1 values commonly decrease because of the decreasing amount of coherent energy reflected from the seafloor (from 25 to 45% to approximately 15 to 30%) and R_2 values commonly increase to approximately 20% from 2 to 10% as a result of the increase in the amount of scattered energy.

Twelve vibrocores were split, logged (Appendix II), photographed, and finally subsampled for further analysis. This included textural analysis on all samples, heavy mineral analysis on selected samples, lithic identifications (Appendix III) and 13 radiocarbon dates (Table 1). Textural analysis was as described for surface samples except for cores 4, 9, 11 and 15 where

textural analysis was carried out on the C-CORE settling tube (Gillespie and Rendell, 1985). Heavy mineral separations were undertaken for each 1/2Ø size interval between 0.063 and 0.35 mm on selected samples, otherwise only the 3Ø (0.105-0.149 mm) size was separated. Mineralogical identification was done on the 3Ø fraction of the separated samples only.

From the over 200 sieved surficial samples previously collected in the greater Hibernia area of the Grand Banks, 26 samples, representing a transect through the area, were selected for further analysis. Standard grain size analysis by sieving was carried out on all samples at 1/2 phi intervals. Heavy mineral separation was carried out on nine samples from the 2 to 4 phi sand fraction (0.063 to 0.35 mm) using tetrabromethane (S.G. = 2.9 g/cm^3) and the standard gravity separation method (Carver, 1971) (Appendix IV). Weight percent values of the total heavy mineral residue were determined and used to produce heavy and light mineral frequency curves. The 3 phi (0.105 - 0.149 mm) heavy mineral fraction was mounted in Canada balsam and a total of 200 non-opaque minerals counted using the ribbon method of Galehouse (1971). Two samples, 21 and 82 (Fig. 21), were examined in individual 1/2Ø fractions between 0.063 and 0.35 mm. These narrow fraction separations and mineral identifications are required both to calculate hydraulic size in accordance with the method described by Briggs (1965), and to infer mineral size restrictions in the overall sedimentary dispersal basin. Opaque minerals were identified under reflected light. Two core sub-samples were diagnosed using X-ray diffraction techniques.

Evaluation of grain roundness and form was carried out, for the same 26 samples, by a visual examination of the whole sample in comparison with photographic charts for sand grains (Powers, 1953). Scanning electron microscope (SEM) examination of 177 quartz grains was carried out for 10 representative samples across the study area. Preparation of the samples followed the methods of Krinsley and Doornkamp (1973). At least 15 coarser than 1 phi grains (2 mm) were selected at random using a binocular microscope.

The separated gravel fraction (greater than 2.0 mm) was visually inspected and each lithic fragment was weighed, measured and classified. Carbonate clasts of sufficient size were sectioned, stained and examined petrographically.

SURFICIAL GEOLOGY OF THE HIBERNIA AREA

INTRODUCTION

Barrie et al. (1984) have divided the surficial sediments of the Hibernia area on the northeastern Grand Banks of Newfoundland into five depth-controlled facies units. This report as depicted in Figure 2 incorporates the compilation of data obtained during the cruises of **CSS HUDSON** 83-017 and 83-033, with previous grab samples (Amos and Barrie, 1980).

Although small scale bedform ripples have not been studied throughout the entire area to date, it is felt that they are characteristic of the facies in which they are found. For this paper we have initially classified these ripples according to

wavelength based on BRUTIV photographs as noted below. In most cases these are wave-generated ripples; exceptions are noted in the detailed facies description.

Ripple Type	Wavelength (m)
Class A	0-0.15
Class B	0.15-0.45
Class C	0.45-0.7
Class D	>0.7

The major facies found within the study area generally adhere to the contacts and descriptions noted by Barrie et al. (1984). Subtle variations from that interpretation are the result of BRUTIV data, which resolve small scale bedforms that cannot be identified with the use of the Huntec DTS profiles and side scan sonograms, alone. These variations are described in Appendix 1.

UNIT A (CONTINUOUS SAND)

Unit A has been described by Barrie et al. (1984) as a smooth seabed covered by fine sand at the eastern edge of the region (Fig. 2). Water depths range from 110 to 140 m.

Stratigraphy

Vibrocores 14 (1.25 metres) and 15 (1.24 metres) were collected in Unit A (Figs. 2 and 3). The sediments are light to medium grey except for an olive yellow coloration in the upper 0.19 m. Pebbles and granules are dispersed and less abundant than in cores from the Boundary Sand (Unit C) and Sand Ridge

(Unit E) except at the bottom of core 14 where granules to cobbles of limestone and siltstone are found. By visual examination, the shell content increases down core from mean 0% to 10% at the bottom of the cores.

Grain size analyses show greater than 95% fine sand with an average sample mean of 2.25Ø (0.21 mm) (Fig. 3). There is less than 1% gravel except at the bottom of core 14 where 7% gravel occurs. The abundance of silt and clay is variable up to 3%. The sediments are moderately sorted becoming poorly sorted towards the bottom. The sands show a unimodal grainsize distribution skewed towards the coarser fraction. The cores also show a general fining upward trend.

Two subsamples were analysed for heavy minerals. The 3.0Ø (1.25 mm) fraction from the 1.66-0.70 m interval and the 2.0-4.0Ø (0.25-0.063 mm) fraction from 0.148-0.153 m of core 14 were analysed (Fig. 4). The abundance of heavies was 0.86% and 0.52% of the total sample respectively.

UNIT B (LAG GRAVEL AND SAND RIBBONS)

Unit B lies on the lower terrace at a water depth of 95 m and extends eastwards to Unit A (Fig. 2). Minimum and maximum widths of this unit are 13 and 30 km respectively. BRUTIV, sidescan and Huntec DTS data collected during the **CSS Hudson** 83-033 cruise suggest this is a hydrodynamically more complex area than elsewhere in the study area shown in part by a greater number of possible current generated ripples along its margin.

This unit is represented by alternating sand ribbons, less than 1 m thick, and gravel lag. Arcuate sand waves and megaripples with wave fronts normal to the long axis of the ribbons are abundant on the flanks of the ribbons, all showing a southeasterly transport direction, parallel to the facies (Barrie et al., 1984). Gravelly sand is the predominant sediment type (Amos and Barrie, 1980). R_1 and R_2 median profiles are highly variable.

Contacts between the sand and gravel tracts within this unit are gradational. The contact most easily observed on the side scan sonogram is formed by sand stringers or megaripples migrating across a lag gravel seabed under the influence of apparent south-southeasterly and southeasterly currents. Finer scale resolution of this contact, by BRUTIV camera transects shows a pebble/gravel seabed which grades outward from a dense inner core to a region where the pebble/gravel cover is only slight. R_1 values are relatively high for sand (Parrott et al., 1980) ranging from 30 to 60%. BRUTIV photographs show ripples of two wavelengths in areas where the Huntec DTS profiles show the sand ribbons to be less than 0.4 m thick:

1) northeast-southwest bifurcating, wave generated, Class C ripples cut obliquely by
2) smaller scale (Class A) north northeast to south southwest trending ripples (Fig. 5). Through Unit B, in areas of thinner sand, the quantity of ripple trough infill material increases and ripples become more sinuous (Fig. 6).

Lag material varies from a 100% gravel/shell armoured seabed (Fig. 7a) to moderate gravel/shell cover on sand. Where BRUTIV photographs show sand within the lag units, the sand appears as small scale ripples surrounded by the lag with fresh and degraded megaripples at the outer margins of the lag (Fig. 7b and c). There does not appear to be a change in the type or extent of rippling within Unit B from north to south.

UNIT C (BOUNDARY SAND)

Unit C or Boundary Sand follows a northeast-southwest trending curvilinear path in the east-central portion of the study area (Fig. 2). It is characterized by very thin to 2 m thick sand making up the slightly irregular seabed which is marked by crests and troughs of sand waves as well as possible current scours. Unit C widens from approximately 1 km at 46°45'N to 9 km at 46°37'N, possibly as a result of the greatly reduced seafloor gradient to the south. Between 100 and 90 m depth the decreased spacing of bathymetric contours indicate an increase in slope from south to north.

Sediment texture is consistent from north to south throughout Unit C. Grab samples described by Amos and Barrie (1980) as well as vibrocore samples indicate that fine to medium grained sand predominates throughout the area. Large scale bedforms consist of sand waves with wavelengths averaging 100-400 m, megaripples ranging from 5 to 50 m wavelength, and strongly reflective shell beds. Sand wave troughs vary sightly in orientation from the north to the south in Unit C. Sand bodies (1.4

to 1.8 m thick) have sand wave troughs oriented in an east to west and an east northeast to west southwest fashion. Transport direction is south to southeast. They are found in the northern and southern sectors of the study area. The central portion of the region is pinched into a very narrow corridor of 1.1 m thick sand with north-south trending sand wave troughs.

Three sets of ripples have been observed locally within the thinner areas of sand. These ripples produce a "washboard" effect on the seabed (Fig. 8). This type of seabed is not always resolved as sand on the Huntec profile due to its locally shallow nature. North-northeast to south-southwest oriented Class C ripples with shell hash and pebble filled troughs dominate the area. As the sand is remobilized, it is possible that these shells and pebbles will remain as indicators of degraded ripples. Smaller scale Class B ripples which trend northwest-southeast, occupy positions between the previously mentioned ripples. Minor occurrences of northwest-southeast oriented Class A ripples are found within the troughs of these smaller ripples.

Stratigraphy

Cores 10, 11 and 16 were collected from between 78 and 85 metres water depth (Fig. 2 and 3) on the southern Boundary Sand. The cores describe an east-west cross section for the unit. Core 16 has a length of 2.0 metres while 10 and 11 have lengths of 0.9 and 1.02 m, respectively. Granules and pebbles, including carbonate rock fragments, are dispersed throughout the cores. Large shell fragments are found in association with large lithic

rock fragments. The shell content is about 15% throughout the cores, and in places is aligned parallel to bedding. Both gradational and sharp contacts occur. Laminations of medium to fine sand alternating with coarser grained more poorly sorted sand, are present in the lower portion of Core 16 (Fig. 3).

Grain size analysis shows over 95% medium sand with an average mean grain size of 1.42Ø (.357 mm) (Fig. 3). The gravel content is generally less than 5% except for thin units found in cores 11 (0.53-0.61 m) and 16 (0.8-0.9 m) where approximately 40% gravel occurs. Silt and clay account for less than 1% of the sediment in these cores. The cores show moderate sorting and a unimodal grainsize distribution which is slightly skewed towards the coarser size fraction and an overall coarsening of grain size down core.

Heavy mineral analysis shows the amount of heavies in these cores is less than 1.0% with one sample as low as .01%. Mineralogical analysis shows consistency in mineral species abundance throughout the section. Garnet and zircon form the dominant mineral assemblage and magnetite is present as the dominant opaque mineral (Fig. 4).

UNIT D (GRAND BANKS GRAVEL)

Unit D on the upper terrace (80 m) is composed primarily of thin (0.5 m) gravel, sandy gravel, and gravelly sand (Amos and Barrie, 1980; Barrie et al., 1984), the medium sand being moderately to well sorted. It occupies north-south and north-

northwest to south-southeast trending extensive linear tracts in the central and western portions of the study area (Fig. 2).

Sonogram backscatter for Unit D is moderate to strong. This is in part the result of a slightly irregular seabed morphology, the gravelly texture of the surficial sediments, and numerous boulders and shell beds found throughout the region (Fig. 9). The percentage of pebble/shell cover over sand varies throughout the unit. In areas of moderate to dense gravel cover, the underlying sand is somewhat stabilized and not as easily reworked by bottom currents and storm surges as in areas with less dense cover. Only spatially limited tracts exist where the seabed consists of 100% gravel armour. R_1 values in Unit D range from 45 to 65%.

Where Huntec DTS profiles indicate areas of thicker sand within Unit D extensive fields of both two and three dimensional megaripples and small sand waves (wavelength 100 m) exist. Erosional features such as those shown in Figures 9 and 10 are also evident. Ripple troughs trend north-south and northeast-southwest. These troughs increase in backscatter with increased linearity. North-south and northeast-southwest trending degraded Class C ripples and Class D megaripples are evident in BRUTIV photographs (Fig. 11a). These larger megaripples (Class D) are likely those seen on the sonograms. Within the larger megaripple troughs, wave induced Class B ripples trending northeast-southwest and Class A ripples orientated both east-west and northeast-southwest can be seen (Fig. 11b).

UNIT E (SAND RIDGE FIELD)

Unit E, the westernmost unit is dominated by medium to coarse sand which has accumulated in north-south ridges up to 3.7 m in thickness over a relatively smooth seabed. Throughout Unit E the surficial sediments become progressively coarser towards the west. The ridges themselves show a bimodal grain size distribution with coarse, moderately sorted sands on the ridge crests and well to moderately well sorted, medium grained sands on the ridge flanks (Barrie et al., 1984). Thick shell beds, characterized by decreased R_1 and increased R_2 values form on the flanks of some ridges (Fig. 12). The morphology of the sand ridge shown in Figure 12 could in part be controlled by the unconformable surface of underlying Tertiary beds. Huntec DTS profiles show what is interpreted to be the Tertiary surface shallowing upward, coinciding with a thinning of the sand ridge. The ridges generally seem to decrease in thickness from north to south. Maximum sand ridge thicknesses in the northern sector of the study area range from 1.8 to 3.7 m, while to the south the maximum thickness is 1.8 m. The ridges can be classified as "characteristically mixed" (between moribund and active) according to Amos and King (1984).

Acoustic backscatter on sonograms from sand wave troughs is greater than anticipated for sand. This effect is attributed in part to the presence of closely-spaced small-scale ripples (Fig. 13) which provide a rougher seabed surface.

R_1 values within Unit E are relatively constant at 50%. It is felt that the boundaries between Units D and E are not

consistent from survey to survey due to the relative ease with which fine to medium sand can be mobilized along the borders during periods of storm activity. Grab sample and vibrocore data (Amos and Barrie, 1980; Appendix II) show the sand to fine southward, indicating transport from north to south as is also indicated by the orientation of megaripples and sand waves.

Northwest-southeast trending, 2-D megaripples with highly reflective troughs are found on the gently sloping flanks of the ridges where the sand thins to less than 0.4 m. This feature is found in both the northern and southern portions of the study area. Arcuate sand waves and megaripples (Barrie et al., 1984) are modified by low amplitude, sinuous Class B ripples which trend north-northeast to south-southwest (Fig. 14). Within these ripples lie northwest-southeast trending Class A ripples.

Stratigraphy

Cores 6 through 9 were collected from an area just east of the Hibernia P-15 discovery well (Fig. 2, 15 and 16). They are situated in approximately 75 metres water depth on a north-south trending sand ridge approximately 1.5 to 2.0 metres in thickness (Fig. 15). Cores 4 and 5 were collected from a southern extension of the same sand ridge in about 67 metres of water. The northern sand ridge cores (6-9) consist of sand which is buff in the upper 0.1-0.18 m to light grey through the rest of the core. Granules and pebbles are dispersed throughout each core. The shell content is variable and consists of angular bivalve and echinoderm fragments. An intact gastropod was collected from the

0.38 m interval in core 6. In places the shells are aligned parallel to bedding. Both gradational and well defined contacts are present and are based on observed differences in grain size, percentage of lithic and shell fragments and to a lesser extent on color change. Laminations are present in the lower portions of the northern sand ridge cores. These are found as alternating bands of coarser grained material, usually containing a larger percentage of lithic and shell fragments.

Cores 4 and 5, the longest cores recovered, are similar in lithology to cores 6-9 except that no laminations are found. At 2.03 m in core 5 a sharp contact occurs below which no shells are found and the color changes to an olive brown. The contact zone itself is dark grey and contains a large amount of fine material that is very compact and partially cemented.

Grain size results are presented in Figure 16. The results showed greater than 92% sand across the ridge. The medium grained sand has an averaged mean of 1.26Ø (0.42 mm) with a general decrease in grain size down core. Less than 8% gravel occurs, the majority of which is found in the upper few centimetres. There is generally less than 1% silt and clay except below 2.03 metres in core 5 where approximately 6% silt is found. Sorting values are highly variable with the average being moderate to poorly sorted. When weight percent is plotted against phi size for all cores the results is a unimodal grainsize distribution slightly skewed toward the coarser size fraction, except for the interval below 2.03 metres in core 5 where a fine grained "tail" is apparent.

The amount of heavy minerals in the sand ridge cores varies from 1% to as low as .07% with the average at 0.5%. The heavies increase in abundance with depth in the core and show little difference across the sand ridge. Mineralogical analyses show the dominant mineral assemblage to be garnet and zircon which is consistent with surface samples (Fig. 17). Weight percent versus phi size plots for heavy and light minerals show a 0.5 to 1.00Ø separation indicating hydraulic equilibrium of the sands.

In a subsample from the 2.67-2.70 m interval of core 5 the mineralogy is dominated by iron-aluminum hydroxide minerals tentatively interpreted as goethite and possibly gibbsite and the quartz grains are highly iron stained. Garnet and zircon make up minor constituents.

Vibrocores from sand ridges along the New Jersey Shelf (Rine and Tillman, 1983); Stubblefield et al., 1983) showed a general decrease in grain size downcore as is noted in the Grand Banks cores. Similarly, laminations and non-laminated beds were found in the New Jersey cores, as well as skeletal-rich and non-skeletal lithologies. Rine and Tillman (1983) found that the middle shelf ridges directly overlie sediments without skeletal remains as seen in vibrocore 5.

RADIOCARBON DATES

Radiocarbon analysis was carried out for the Geological Survey of Canada on shells mollusc fragments from subsamples selected throughout the vibrocores (Table 1). The dates range

from 3610 years B.P. in the south Sand Ridge to 22,780 years B.P. in the Continuous Sand Zone (Fig. 3 and 16). Duplicate dates on separate samples from the same level in two cores indicate the overall resolution in the dating is approximately 1000 years.

Table 1. Radiocarbon dates from selected vibrocore samples.

Lab Number	Subsample Number and Depth*	Age	Unit/Facies
Beta 8888	83017-5-187	3760 ±130 B.P.	SOUTH
Beta 8886	83017-4-174A	2610 ±150 B.P.	SAND
Beta 8884	83017-4-174B	3730 ±130 B.P.	RIDGE
Beta 8887	83017-6-40A	8070 ±130 B.P.	NORTH
Beta 8877	83017-6-40B	7230 ±120 B.P.	SAND
Beta 8876	83017-7-109	5820 ±120 B.P.	RIDGE
Beta 8885	83017-9-137	6270 ±160 B.P.	
Beta 8878	83017-16-116	7150 ±240 B.P.	BOUNDARY
Beta 8883	83017-16-199	10570 ±370 B.P.	SAND
Beta 8879	83017-11-57	9840 ±200 B.P.	
Beta 8880	83017-10-67	9470 ±280 B.P.	
Beta 8881	83017-14-150	16860 ±720 B.P.	CONTINUOUS
Beta 8882	83017-15-178	22780 ±620 B.P.	SAND

*Depth in cm is given by the last group of digits in the subsample number. The middle group of digits is the vibrocore station number.

Dates from the north P-15 Sand Ridge indicate progressively older sediments to the eastern flank (6,000 to 8,000 years, B.P.) though this same trend corresponds to the thinning of the ridge to the trough. These older dates at the surface of the eastern flank imply a correlation with sediments deeper in the central portion of the sand ridge, and suggest westward or southwestward early to mid-Holocene migration. Further radiocarbon dating is required to define time-stratigraphic units across the ridge. Shells at the base of the southern end of the same ridge are even younger (approx. 3,000 years, B.P.) than the northern samples, and suggest mid to late Holocene ridge migration to the south.

Samples obained from the three Boundary Sand cores are generally older (7150 to 10,570) than the P-15 sand ridge dates as expected for a sand ridge in deeper waters. Dates from 1.16 and 1.99 m of core 16 give a sediment depositional rate of about 0.2-0.3 cm per year. Assuming the top of the core to be modern, the depositional rate would be uniform at a very slow rate. The oldest dates (ca. 20, 000 B.P.) as anticipated, were found at the bottom of cores 14 and 15 in the deepest water sand facies, the Continuous Sand Unit.

Taken together, the radiocarbon-dated cores define a set of sand bodies which are progressively younger in shallower water over the period of Late Wisconsinan to mid-Holocene time. This progression was expected and is entirely conformable with the hypothesis that many surface sand deposits on the continental shelf originate in the high energy shore zone of the transgressing post glacial sea level, though they are

subsequently modified by oceanographic processes. The basal dates for the Continuous Sand Facies correspond with the previously inferred time of low sea level stand (Fader and King, 1981; Lewis and Barrie, 1981; Barrie et al., 1984) for northeastern Grand Bank.

SEDIMENTOLOGY

TEXTURAL DISTIRBUTION

Based on the discussions of the sediment facies it can be seen that there is a general decrease in surficial-sediment grain size down slope between 70 and 140 m (Fig. 18). Gravel content decreases in the same manner. The facies boundary between Unit B and Unit A demarcates the change from medium to fine sand. Generally the whole area is moderately well sorted becoming moderately sorted at the western end of Unit E where the mean grain size is coarse. This same general fining of surficial sediment downslope along the northeastern continental shelf edge of Grand Bank was displayed on a regional basis by Slatt (1977).

The sediment found in the vibrocores consists almost exclusively of quartz sand. This sand is grey to light grey except for the upper 0.2 m where it appears as buff color. The sand to gravel ratio is usually greater than 9:1 except in the upper centimeters of the Sand Ridge cores where gravel contents up to 50% occur. The gravel content also increases at the bottom of the Sand Ridge cores as well as down core 14 within the Continuous Sand facies. This lower sand and gravel unit was probably responsible for the refusal of the vibrocorer. The silt

and clay fraction is less than 1% of the total except for the lower unit of core 5 where it is over 5%.

The shell content is variable and averages 15% of the total sediment in the cores. The dominant shell types are mollusc, bivalve, and gastropod fragments with lesser numbers of echinoderm and bryozoan fragments. The shells are found both in specific units within a core and dispersed throughout the core. Specific shell beds could not be correlated.

Laminations consist of alternating fine-grained and coarser sediment layers sometimes including granules. The majority of laminations occur in the Sand Ridge cores where they appear to be due to an irregular influx of sediment. Laminations found at the 1.42-1.67 m interval in core 16 (Boundary Sand) are evenly-spaced and appear to represent uniform sedimentary cycles.

The standard deviation values, on average, indicate poorly sorted sediments. According to Folk (1974) these would be classed as submature sediments. In a plot of grain size versus standard deviation (sorting) a linear relationship can be seen (Fig. 19). The general trend is for finer material to exhibit better sorting. Samples from the northern P-15 sand ridge show complete variability between sorting and mean grain size as do the cores from the Boundary Sand. Values from the southern sand ridge show less variability in sorting and more consistency in grain size; this could indicate that the extension of the ridge to the south is a more recent event and that the northern ridge is more relict in nature as evidenced by the radiocarbon dates.

Cores from the Continuous Sand zone are distinctive in that they show much less variability in grainsize and sorting.

Grain Roundness

Evaluation of grain roundness in surficial samples was carried out by a visual examination in comparison with photographic charts of sand grains of known roundness (Powers, 1953). The analysis of the samples shows a unimodal distribution with 45% of the grains being sub-round, 28% of the grains sub-angular, 15% round, 10% angular, and 2% being very round. Scanning electron microscope examination of 177 quartz grains confirms this distribution. When comparing grain roundness with water depth two modes are found (Fig. 20). Samples taken from above the 110 metre water depth range from angular to very well rounded and correspond to an area above the late Wisconsinan low sea-level stand (Fader and King, 1981; Barrie et al., 1984). The broad range in roundness is probably due to the variety of processes that acted on the sediments such as the early Holocene aeolian transport of sands and the increased wave action of the littoral zone. Below the 110 metre depth the samples are generally subround to subangular and could represent sands from a sub-littoral zone.

Grain Form

A visual evaluation of grain form was carried out by comparing the average shape of the grains in a whole sample with the shapes on a form triangle (Folk, 1974). The results show the

majority of samples are compact bladed, and compact elongate.

PEBBLE LITHOLOGY

The majority (62%) of the rock fragments larger than -2 phi (4 mm) identified from 23 sample locations over the Hibernia study area are sedimentary (siliclastics and carbonates) in origin (predominantly sandstones and siltstones). The next largest type (32%) lithic type is igneous (predominantly granites) (Fig. 21). Metamorphic fragments are noticeably reduced in all samples (6% average). Typical metamorphic fragments found are metasediments and gneisses.

Pebbles found within the eleven vibrocores are nearly identical in type and abundance as those found in the surficial samples. There the total sedimentary fraction makes up 59% while igneous fragments total 32% and metamorphics 8% (Figs. 4 and 17).

The sandstones are typically fine to medium grained and green, grey and reddish brown in color while the siltstones are grey to grey-green. The sedimentary fraction other than sandstones and siltstones is made up of shales, mudstones and carbonates. The carbonate lithics are displayed independently of the sedimentary group in Figure 21 because of the potential significance they have in identifying sediment provenance. Carbonates average about 7% of the lithic fragments and consist of very fine grained, grey to buff limestone and dolomitic limestone. In the subsurface, carbonate content increases to 18%. Concentric zoning of limestones due to weathering was observed. The igneous components are largely made up of fine-,

medium- and coarse-grained biotite-hornblende granites with lesser amounts of gabbros and basic volcanics.

Both igneous and metamorphic fragments from the grab samples can have multiple sources, most of which are not local. Most probable origins are from the Precambrian rocks of Newfoundland, Labrador, the Canadian Arctic Islands and Greenland. Only the Canadian Arctic Islands and Greenland presently provide a contemporary source, due to iceberg rafting. Earlier proglacial and fluvial deposition could have provided igneous and metamorphic material derived from crystalline rocks from the island of Newfoundland and the Avalon Channel (Fig. 1) to the outer bank region, both during the Wisconsinan and earlier Pleistocene times. These same mechanisms plus fluvial action during the early Holocene would have provided quartzites and granites from the Virgin Rocks/Eastern Shoals region (Fig. 1) (King et al., 1986) as these were the topographic highs on the island of Grand Bank. Seismic evidence exists (**CSS HUDSON** cruise 83-033) for large fluvial channels across the bank; small fluvial channels were likely obliterated during transgression. The high quartz content, up to granule size, indicates mid to early Pleistocene glacial erosion of the Virgin Rocks/Eastern Shoals region and/or early Holocene fluvial action.

The major lithic fragments (the sandstones and siltstones) are very much a product of local derivations. The underlying Tertiary beds predominantly consist of sandstones, siltstones and mudstones (Jansa and Wade, 1974). Closer inshore, the near-surface Paleozoic rocks would be an excellent source of

sedimentary lithics. Ordovician to Devonian beds are predominantly grey to red siltstones and to a lesser degree sandstones (King et al., 1986), the redbeds are thought to be Devonian in age. Most of these beds lie close to the seabed in the inner bank region (Fig. 1) (King et al., 1986). Again, early Pleistocene glacial action or Wisconsinan proglacial mechanisims could have transported these fragments to the outer shelf area.

Slatt (1977) found that grab samples from his 'Outer Sand Facies' in which the samples described here would fall, contain the same distribution of gravel types. Carter (1979) also found a similar suite of gravel lithologies on the upper continental slope adjacent to the Grand Banks with the exception of a greater abundance of gneisses. He attributed the majority of these clasts to the Proterozoic and Paleozoic rocks of Newfoundland and their offshore equivalents. Carter et al., (1979) reasoned that a smaller quantity of the granite and gneiss was ice-rafted from Proterozoic crystalline rocks in northern Greenland and the eastern Canadian Arctic.

The minor distinctive carbonate fraction (7%) again has potential local source derivation. Carbonates are known in the Eocene of the Banquereau Formation (Arthur et al., 1982; Jansa and Wade, 1974; Williams, 1974; McIver, 1972), and are encountered throughout the Jurassic and Cretaceous of the northeastern Grand Banks (Arthur et al., 1982). These predominately limestone beds are relatively thin. During early Holocene or mid to late Pleistocene glacial or fluvial mechanisms could have removed carbonate material in the central Banks region

where Eocene and older rocks are near the surface (Williams and Brideaux, 1975). The second possible source area, is the Canadian Arctic Islands (Thorsteinsson and Tozer, 1969) and northern Greenland (Johnson et al., 1972) where extensive carbonate Paleozoic-Mesozoic platformal strata occur. This source area involves an ice transport mechansism.

Carter (1979) found a substantial increase in the carbonate content of lithic fragments with increasing depth down the continental slope off the northern Grand Banks. On the lower slope and rise the average concentration exceeds 50% (Carter, 1979). The carbonates are primarily composed of limestone (micrite) with lesser amounts of dolomite. The trend of an increased carbonate-dominated gravel assemblage on the slope and beyond generally holds true for the entire eastern Canadian continental margin (Carter, 1979). Carter et al. (1979) attributes these concentrations to iceberg rafting from Paleozoic rocks in the eastern Arctic. The clasts found on the slope resemble the Paleozoic carbonates. Deposition of the majority of the carbonate is dated at mid-Holocene (Carter, 1979; Carter et al., 1972). This would coincide with rapid deglaciation in the two major source areas, Baffin Island and the Foxe Basin (Andrews et al., 1972). The increase of carbonates found in the subsurface subsamples correlates with earlier high fluxes of icebergs bringing carbonates to the shelf.

The provenance of the surficial sediments on the Grand Banks based on gravel identifications can then be divided into three depositional areas. The inner shelf areas, defined by Slatt

(1977) as the 'Inner Gravel Facies', is dominated by material primarily deposited by glacial and glaciomarine mechanisms from the nearby island of Newfoundland and adjacent offshore areas. The total percentage gravels making up the surficial sediments of the Inner Gravel Facies varies from 50-80% compared with an average of less than 10% for the Outer Sand Facies, (Slatt, 1974). This gravel abundance and type change is used as a major factor in the definition of the late Wisconsin extent of the Avalon ice cap onto the Grand Banks according to Slatt (1977). The rest of the broad shallow shelf area to approximately the upper continental slope area is covered in material of local derivation and westward sources from the island of Newfoundland. Slatt's (1977) definition of this broad area, the 'Outer Sand Facies' allows for little glaciofluvial deposition. Towards the outer shelf/upper slope area the influence of iceberg rafted material increases. The third area, as defined by Carter (1979), is the lower slope and rise, dominated by carbonate originating in the eastern Arctic and transported south in the Holocene by icebergs.

Sample analysis from the Hibernia area does not entirely agree with Slatt's (1977) description of total autochthonous shelf sedimentation of the 'Outer Sand Facies'. Though a greater percentage of the gravel sized material is of local derivation some of the igneous and probably all of the carbonates and metamorphics have undergone some transportation whether by ice/iceberg rafting, glaciomarine or glaciofluvial transport. This is graphically apparent when looking at the regional

distribution of lithic fragments and heavy minerals in the Hibernia area (Fig. 21).

In deeper waters (Units A and B) below the 90-100 m interterrace slope, metamorphic fragments are always present in quantities greater than 5% and the sedimentary fraction is reduced to 50% or less on average. The opposite is true on the upper terrace (Units D and E) where the sedimentary fraction is greater than 60% and there are no metamorphic rock fragments showing in the surface samples. The distributional variation has two possible mechanisms. Firstly, the increase in all sedimentary gravels inshore of the 90-100 m water depth reflects the high energy nearshore environment prevalent during the Holocene transgression in which the underlying Tertiary sediments rich in sandstone and siltstone lithics were eroded and reworked by the mechanism described by Slatt (1977). The 90-100 m water depth marks the lowest stand of the late Wisconsinan sea level. The second mechanism causing this variation is the modern and Holocene travel paths of icebergs. Icebergs take two dominant paths over the Newfoundland shelf (Murray, 1969; Dinsmore, 1972). The shelf edge branch concentrates most of the icebergs in a southerly flow just east of the area under study (Lewis and Barrie, 1981) (Fig. 22). Consequently iceberg incursions are less likely as one moves upslope to the west as can be seen by the distribution of iceberg scouring (Lewis and Barrie, 1981). This distribution of icebergs and grounding icebergs should also correlate in iceberg rafted sediment. The increase of metamorphic rock fragments downslope and the decrease in

sedimentary lithics correspond to this distribution. The metamorphics below 100 m are then considered to be largely iceberg rafted from northern sources of iceberg rafting and the lesser quantities of sedimentary lithic fragments are thought to reflect an abundance of substrate erosion as this area was not transgressed by a high energy surf zone. This increase of iceberg rafted material towards the shelf break of the northeastern Grand Banks was also seen by Carter (1979) and Carter et al. (1979).

HEAVY MINERALS

Garnet is the dominant mineral on the northeastern Grand Banks (Figs. 4 and 17). It comes in two varieties, a dominant, colorless type (45%) and a characteristic pink garnet (13%). Slatt (1977) noted the same mineralogical domination in his 'Outer Sand Facies' of the Grand Banks. Secondary minerals include zircon, amphibole, rutile, glauconite and sphene (Fig. 21). The two main minerals, garnet and to a much lesser extent zircon make up nearly 80% of the non-opaque assemblage. Both minerals are very stable and resistant to destructive sedimentary processes and therefore have a high ZTR index (Hubert, 1962). Opaques, mainly magnetite, make up 30% of the total heavy minerals. Minerals that are included as 'others' are tourmaline, andalusite, epidote, kyanite, apatite and monazite.

Garnet also dominates the subsurface samples with both colorless (39%) and pink (12%) varieties (Fig. 4 and 17). The interesting difference in the subsurface mineralogy is at the

bottom core 5 where iron-aluminum hydroxides (goethite and gibbsite) are the ubiquitous mineral assemblage. This zone is interpreted to be the old erosional surface during subaerial exposure and the hydroxide minerals could have resulted from weathering of iron and aluminium bearing rocks. Samples analysed from the 0-35 and B-08 boreholes (Geocon, 1980a, b) reveal similar results. This same stratigraphic unit displays intense quartz iron staining, again a strong indication of subaerial exposure (Judd et al., 1970; James and Stanley, 1967; 1968).

The provenance of the dominant garnet is the underlying Tertiary sands which are rich in garnet. The glauconite found in surficial sediments is also indicative of a Tertiary source. Similar glauconite grains occur in the Tertiary coastal plain strata directly underlying the Quaternary sands (Bartlett and Smith, 1971; Jansa and Wade, 1974; Slatt, 1977).

The garnet heavy mineral suite demonstrates that the surficial sands of the northeastern Grand Banks are extemely mature, a result of continuous reworking over a substantial period of time, regardless of the water depth. This interpretation is reinforced by the textural evidence and the presence of a full range of hydrodynamic sedimentary bedforms (Barrie et al., 1984). Alam and Piper (1981) indicate that the Grand Banks is the major source of the mature upper slope sediments of the Grand Banks continental slope based on heavy mineralogy and sand-surface textures.

HYDRAULIC EQUIVALENT RELATIONSHIPS

Mineralogical studies of mobile seabed sediments can, by their very nature, reveal certain hydraulic characteristics of an area (Slingerland, 1977). Heavy minerals will be located throughout a depositional area in a distribution which is related to both source areas and the modern prevailing superimposed hydraulic regime. These processes will be reflected by the concentrations, the individual mineral distributions and heavy and light mineral association patterns. The last relationship forms the basis of hydraulic equivalence, a concept first defined by Rubey (1933) and Rittenhouse (1943), as whatever hydrodynamic conditions prevailed allowing the deposition of quartz grains of a certain diameter, would also allow the deposition of heavy minerals (of a smaller size) that had the same settling velocity. It was found that the size of a heavy mineral is inversely proportional to a power of its density.

In order to examine the heavy mineral hydraulic equivalence relationships, size distribution of mineral separations were made every 1/2 phi interval over the 2.0 to 4.0 phi (0.25-0.063 mm) size range for individual samples. The size distributions of heavy and light minerals from vibrocore sediment samples were plotted on a similar axis of reference and the peak distributions or modes were compared. If the sediments are in hydraulic equilibrium, the mean grain size mode of the heavy minerals should fall in finer grain sizes than the mode of the light minerals, proportional to density differences betwen the two mineral species. In all samples analysed, both from surface

grabs and vibrocores, the sands appear to be in hydraulic equilibrium with the present environment based on texture and mineralogical analysis. This would be expected considering the mature nature of the sands.

OCEANOGRAPHY

The Labrador Current with surface current speeds of about 0.2 ms^{-1} (Petrie and Anderson, 1983), increasing greatly in the area of the continental slope, controls the circulation over the Newfoundland Shelf. A portion of the flow (up to 15%) can move into the Strait of Belle Isle as well as an outflow out of the Strait (Petrie and Anderson, 1983). The south-flowing Labrador current then splits into three parts between 48° and 49°N. The circulation of these branches (Fig. 22) over the Newfoundland Shelf and particularly the Grand Banks was first described by Smith et al. (1937) based on their work and earlier work by Matthews (1914).

An inshore branch flows through Avalon Channel (Fig.22) following the coastline to the west. At 55°W the flow turns eastward moving toward the stronger branch along the eastern shelf edge. Transport through Avalon Channel is about 0.6 x 10^6 m^3 s^{-1} (Petrie and Anderson, 1983). Only about 20% of the transport enters the Gulf of St. Lawrence through Laurentian Channel (Fig. 2).

The middle branch follows the eastern edge of the continental shelf through Flemish Pass (Fig. 22). The geostrophic transport of this Grand Banks slope branch averages

4.1×10^6 m^3 s^{-1} with mean currents of 0.2m to 0.6 ms^{-1} (Seaconsult, 1976; Petrie and Anderson, 1983) extending down some 250 to 300 m. Much of the current is directed eastwards under the influence of the North Atlantic Current but a portion of its flow has been observed to flow into the Gulf of St. Lawrence (Petrie and Anderson, 1983). The eastern branch flows north of Flemish Bank (Fig. 22) with a similar geostrophic transport rate as the middle branch. The flow from this branch then enters the North Atlantic Current system.

Flow over the broad flat-lying central Grand Banks was classified as weak by Smith et al. (1937) with a general southeastward drift. Flows of 0.02 - 0.1 ms^{-1} are predicted by Petrie and Anderson (1983) over the broad expanse with the possibility of an anticyclonic gyre in the southeastern area (Fig. 22).

Icebergs whose drift is controlled mainly by water flow (Dempster and Bruneau, 1975) drift with these same currents. An annual average of 400 bergs, though the deviation is great, drift primarily with the dominant middle branch around the eastern flank of Grand Bank while some drift north of Flemish Cap and others are carried by the western branch down the Avalon Channel close to the Island of Newfoundland (Murray, 1969; Dinsmore, 1972). Many bergs, however, deviate from these drift routes under the influence of variable currents and strong winds onto the bank itself (Blenkhorn and Knapp, 1969; Lewis and Benedict, 1981).

In the Hibernia area (Fig. 22), which falls just west of the middle branch of the Grand Banks slope branch, current meter measurements have been underway since 1980. Near mid-depth currents range about the 0.2 ms^{-1} mark with maximum currents reaching 0.95 ms^{-1} (Petrie, 1982). From current meter deployments 0.5 metres off the seafloor for eight months in 1980 and 1981, a mean current speed of approximately 0.05 ms^{-1} was determined. Maximum current speeds including the tidal component reached 0.45 ms^{-1} (Petrie, 1982). This velocity is exceeded less than 1% of the recording time, though it should be noted that during some of the most severe months of the year in 1980 (January through March and November) bottom sitting current metres were not deployed. Petrie (1982) suggests from a simple force balance equation that currents of 1.60 ms^{-1} at mid-depth and 1.50 ms^{-1} near the seabed can be predicted but the error of such predictions is great. Not included in the predictions is the effect the waves have on the current measurements. It is well known that current measurements taken by instruments with Savonius-type rotors (Aanderaa current meters were used for the Hibernia moorings) are severly affected by wave induced accelerations (Hammond and Collins, 1979b). These type of measuring devices are not suitable for use in a current field which includes high frequency oscillatory flows.

Current direction is predominantly from north to south based on geostrophic flow (Petrie and Anderson, 1983) and bottom current meter results from 1980-81 (MacLaren Plansearch, 1980; Petrie, 1982). Amos and Barrie (1980) also recorded a southerly

flow during station monitoring from **M.V. POLARIS V.** Petrie (1982) indicated the flow to 214°T was the mean flow at the seabed. It is interesting to note that current meters in the Hibernia area (Units D and E) recorded a preference for northerly flow from June 1980 to February in 1981 while current metres in the deeper Ben Nevis area (Units A and B), closer to the main core of the Labrador current, showed a constant southerly flow direction. The highest velocities recorded generally flow to the south.

Neu (1976; 1982) has examined the wave climate for the Canadian Atlantic shelf area including a detailed analysis of the Hibernia area wave regime. Mean wave height is quoted as Hsig which is the mean height of the highest one-third waves in a record (Wiegel, 1964; Ippen, 1966; Neu, 1976; Jardine, 1979). Wave period (Tsig) is approximately 0.9 of the peak period (Tp) (Goda, 1978).

The largest Hsig for Hibernia annually, in ten years and in 100 years is 9.0 m, 12.3 m and 15.6 m respectively (Neu, 1982). These correspond to maximum wave heights of 16.2 m, 22.2 m and 28.1 m for the same return period. Between 60-80% of the time waves exceed 1.5 m. Wave period, based on the largest 3% of the monthly waves, range between 11 to 14 sec (Neu, 1982). The spectra show more energy at the 11 sec period. During the winter months of January to March waves come primarily from NW and W. In June and July wave approach is equal from the W and from the SW. Throughout the year most storms come from NW with decreasing frequencies from W, SW, S and N.

As indicated, the general current over the northeastern Grand Banks is from north to south, though the near bottom currents are quite variable in direction. Extreme currents tend to come from the NW. The most severe conditions of storm surge then should also be from the NW.

SEDIMENT TRANSPORT

OSCILLATORY CURRENTS

The maximum Hsig for Hibernia (9.0 m) and maximum wave period Tsig (14 sec) expected every year demonstrate that the deep-water wave will be felt at the sea-bottom at approximately 300 m water depth. Wave base for periodic reworking of sediment is generally greater than 200 m in the Hibernia area of the northeastern Grand Banks. Using the total wave data set recorded in the Hibernia area from eight drilling locations during the period of November 25, 1979 to February 17, 1982, wave heights from Metoc Wave Data (MacLaren-Marex, 1980) and Airy wave theory (Inman, 1963), the frequency of bottom orbital velocities at various water depths have been determined (Fig. 23).

Sediment threshold under oscillatory water flow is expressed by use of the critical threshold equation:

$$\frac{\rho \quad u2m}{(\rho_s - \rho) g D} = 0.21 \ (do/D)^{1/2}$$

where ρ is the density of water and do is the orbital diameter of water motion (derived from Komar and Miller, 1974). In developing this equation, Komar and Miller (1973; 1974) used previously published flume (laboratory) data. Nevertheless, the

equation is regarded as 'conservative' in comparison to the situation which would be expected in the oceans (Komar and Miller, 1974). A computer program, utilizing the above equation has been presented by Komar and Miller (1975). In this, an input of grain diameter (D) and grain density (ρ_s) computes the period (T) and the orbital velocity (Um) needed for sediment movement. The orbital diameter of the grain motion is do. This section of the program is followed by one which combines wave height (H), wavelength (L) and water depth (h) into the equation, as orbital velocity (Um) depends on the combinations of these variables and period (T) in relation to the deep water linear Airy wave equation (Inman, 1963):

$$Um = \frac{\pi H}{T \sin h (2\pi h/L)}$$

Substituting the average of all mean grain sizes for the three sand grain size classifications (fine, medium, coarse) (Fig. 18) enables the conditions of threshold exceedence to be computed and compared with the wave period data recorded in the Hibernia area (as already described). The wave heights come from 10 years of Metoc Wave Data (MacLaren Marex, 1980) compiled for a monthly basis. The data set presents all the observed significant wave heights (Hsig) and their percent as occurrence. Figures 24a,b and c show the amount of time in terms of the month of the year in which threshold of initial transport for the particular sediment sizes are exceeded over the water depth range under study. The graph for medium sand (Fig. 24b) would be most

applicable above 110 m where medium sand is the dominant grain size.

These graphs demonstrate the control the average mean oscillatory energy has on the reworking of surficial sediments during the winter months above 100 m water depth. For example, in December, at a 70 m water depth, sediment is being reworked nearly 70% of the time, whereas in July there is no appreciable reworking of bottom sediment.

The equation used is similar to that used by Sternberg and Larsen (1975) which is based on field measurements on the Washington continental shelf. In both cases parameters generally make up analytical expressions for the onset of bedload transport under oscillatory flow; they are a parameter that closely resembles the Shields parameter and the ratio of a near-bottom horizontal excursion amplitude of the orbital motion to the mean diameter of the bottom sediment.

UNIDIRECTIONAL CURRENTS

The threshold of natural, non-cohesive sediment movement has been considered by most sedimentologists in relation to the empirical curves of Shields (1936) or the modified Shields graph (Madsen and Grant, 1976). These curves, together with others such as those of Hjulstrom and Inman have been summarized by Miller *et al.* (1977).

The limited near-bottom current meter data available for the Grand Banks give threshold exceedances, considering the mean grain size of the constituent sediment, of not more than 2%

during the periods of measurement, though this does not include any data for the months of January to April which, at present, do not exist. Regardless of this limitation, bedload transport attributable to uniform flow alone appears to be very low.

COMBINED OSCILLATORY AND UNIDIRECTIONAL FLOW

Sediment transport observed on the northeastern Grand Banks is a result of the combined action of the dominant waves and the residual current flow. The currents themselves vary and are driven by various forces including surface shear stresses due to wind, internal pressure field due to slopes of the sea surface or slopes of interface between water masses of different densities, or from tidal action. Oscillatory flow in the thin wave boundary layer and the varying unidirectional boundary layer interact in a non-linear fashion (Grant and Madsen, 1979). As a result, determining the value of shear stress acting on the sea bottom is extremely difficult. From flume observations, Hammond and Collins (1979a) state that thresholds of sediment transport tend to increase with increasing grain size or decreasing period. Smith's (1977) model, which is most appropriate for areas of the seabed dominated by unidirectional flows (unlike Hibernia), argues that the waves have the effect of increasing shear stress and, hence, sediment transport.

Grant and Madsen (1977; 1982) developed an analytical approach for the case of a wave dominated environment (similar to Hibernia). These analyses indicate that the magnitude of the mean shear stress acting on the bed is enhanced when there is a

large wave orbital speed with respect to that of the magnitude of the slowly moving current component. This is further enhanced by a greater apparent bottom roughness. The direction of the mean stresses within the wave orbital boundary layer tends to be turned in the direction of wave propagation so that it is not always parallel with the direction of the mean or slowly varying current.

Grant and Madsen (1982) have demonstrated that bed roughness (z_o) is a critical factor in the determination of sediment threshold. This conclusion was further reinforced by a study undertaken by Martec (1984) and Davidson and Amos (1985) where it was determined that bottom stress values can vary up to an order of magnitude when the roughness element is increased by Ø.1m.

Taking all these factors into account, it is very difficult to quantitatively determine sediment threshold exceedances for combined flows. Based on the work of Grant and Madsen (1979) and Hammond and Collins (1979a), it seems apparent that the threshold exceedance graphs (Fig. 24) will not alter significantly and, if anything, give a conservative measure of the exceedance of the initiation of bedload transport in the Hibernia area. The major directions for bedload transport then would be towards the south/southeast to south.

SEDIMENT TRANSPORT RESULTS

Of the many equations which have been developed for bedload transport, most relate to the fluvial environment. They are the 1) Bagnold (1966) 2) Yalin's (1963) and 3) Einstein/Brown (195Ø)

relationship. The Einstein/Brown approach was examined using various data sets for oscillatory flow by Madsen and Grant (1977). They found that the function works well when stress is calculated using the wave friction factors of Jonsson (1966). They propose the following equation for the total bedload sediment transport rate g(t):

$$g(t) = 40\ w d\ \psi^3\ \frac{\tau(t)}{\Delta\ pgD}$$

where w is fall velocity, D is the grain diameter, p is fluid density, g is the acceleration due to gravity, ψ is the Shields (1936) parameter at $\tau(t)$ instantaneous bed shear stress. The equations are directly a function of bed stress. The net sediment transport is obtained by integrating this equation over the time during which sediment transport exceeds threshold during the course of a wave cycle.

The mean and maximum current speeds and the mean current directions from the bottom current meter data, together with the mean wave chracteristics for the same period were used over a water depth range of 70-130 m, to get initial estimates of sediment transport rates. As mean values are used, due to lack of good simultaneous current and wave data, the resultant sediment transport rates have to be considered as only preliminary, considering that waves and currents interact in a non-linear fashion. The Einstein/Brown equation was used in a program developed by Martec (1984) and further evaluated by Davidson and Amos (1985). In their calculation of transport they separate bottom stress into skin friction and form drag components.

An initial calculation used the mean wave propagation direction (315°T), and the mean current direction (214°T). Sediment transport was used for near-bed current velocities of 0.1 ms^{-1} and 0.4 ms^{-1} using the same wave data in predicting oscillatory sediment thresholds. This combination of parameters was calculated for the following grain size ranges, coarse (0.63 mm) medium (0.32 mm) and fine (0.23 and 0.18 mm).

Results based on this sparse data set show that the mean sediment transport is in a southeasterly to southerly direction (150°-190°), 40 to 50% of the time with as much as 0.10 $m^3\ m^{-1}\ yr^{-1}$ of sand being transported at a 70 m water depth. Sediment transport becomes negligible at 110 m water depth, in accordance with the predictions of Barrie *et al.* (1984). The sediment transport rate at a current speed of 0.10 ms^{-1} has annual occurrence of 15% while at 0.40 ms^{-1} the occurrence is less than 2% of the time. The probability of an annual transport rate of 0.10 $m^3\ m^{-1}y^{-1}$ is very low, therefore. The sensitivity of the Einstein/Brown equation to bottom roughness very noticeable. If the roughness element is increased the annual transport rate also increases. The 0.03 m bedform height used was a calculated from BRUTIV photographs from a single survey line to the north of the study area (Simpkin, 1984). Further measurements of bed roughness are required to refine these sediment transport rates.

Lesht *et al.* (1980) have demonstrated that oscillatory motion at the seabed is the primary process for placing sediment in suspension. The sand sized fraction is suspended primarily by

bursts of turbulence related to peak waves (Clarke et al., 1983) and vortex shedding (Davis, 1983) off the ubiquitous ripples in the area. Suspended sediment transport in combined flows is complex value to calculate and requires knowledge of the vertical distribution of sediment concentration or eddy diffusivity together with the velocity profile data. Smith (1977) summarizes the methods of calculating suspended sediment transport. As no profiles of the boundary layer flows or sediment concentration exist for the Grand Banks, only bedload transport will be considered here.

SEDIMENTARY BEDFORMS AND SEDIMENT TRANSPORT

As can be seen from data presented here and the previous work of Barrie et al. (1984) sedimentary bedform migration is from north to south or northwest to southeast. Only in the Boundary Sand (Unit C) are there sand waves with north-south trending crests, indicating east-west migration, probably downslope to the east. Even the small ripples, which are only indicators of recent storm wave and current activity show a preferred orientation indicating possible movement to the south-southeast along the shelf edge.

From the previous section we calculated that net sediment transport was computed as being towards the south-southeast (150-190°), due to the preferred storm propagation direction and the main flow of the Labrador Current. Maximum unidirectional currents, for the eight months of measurement, only reach 0.45 ms^{-1} (Petrie, 1982). Megaripples form at unidirectional

velocities between Ø.5 - Ø.7 ms^{-1} and are independent of water depth (Dalrymple et al., 1978). Sand waves are generated by unidirectional currents in excess of Ø.4 ms^{-1} (Dalrymple et al., 1978). Megaripples can maintain the sediment supply to the sand waves by migrating up the sand wave stoss slopes. As can be seen the residual current velocities alone required to generate these bedforms are infrequent. The influence of a combination of strong oscillatory flow (Fig. 23) and residual current, which are often in the same direction, in the formation of sedimentary bedforms is not well understood.

DISCUSSION AND SUMMARY

The model for late-Pleistocene, early Holocene development of the northeastern Grand Banks of Newfoundland proposed by Barrie et al. (1984) has been verified based on recent data collection, particularly from vibrocores. The hydraulically mature sediments making up the Holocene section originate primarily from underlying Tertiary sands and from the island of Newfoundland and adjacent early Palaeozoic rocks, offshore. As the shelf deepens to the slope there is a progressive increase in iceberg rafted sediment following the middle branch of the Labrador current.

Vibrocores and boreholes above 9Ø m water depth give evidence of the nature of the early Holocene subaerial surface of the island of Grand Bank. Not only can the unconformable surface be recognized with fine resolution due to texture and

color change, it can also be mapped laterally based on mineralogy.

This old surface zone is distinctive in that the grain size distribution shows an increase in the amount of silt, and the heavy mineralogy is dominated by diagenetic iron-aluminum hydroxides as well as a large percentage of iron stained quartz. The upper contact zone of this unit is highly compact with a "soil-like" appearance. This unit was probably produced under subaerial exposure during the late-Pleistocene low sea level stand. At this time, iron rich surface waters circulated through the sediment precipitating hydroxides and staining the quartz. The leaching probably resulted in the removal of all organic material from the sediment as seen in boreholes. Ground-water circulation might then have precipitated cement which might account for the partially cemented hard contact zone seen in boreholes and vibrocore 5. Above this basal contact the cores in the sand ridge field (Unit E) show complex deposition in a dynamic environment during the mid to late Holocene with a general upward grain size coarsening trend.

Cores 14 and 15 (Fig. 3) taken in water depths greater than 90 m, further to the east in the Continuous Sand (Unit A) give evidence of a transgressive sequence. Starting with the earliest date of 22,780 B.P. the sediments exhibit a general fining upward trend. No evidence was seen of a subaerial surface. Mean grain size is finer than the core samples to the west. Cores in the Boundary Sand (Unit C) have a similar upward fining sequence but towards the base of this unit the depositional environment is

again a complex, higher energy environment which dates to the time of the Holocene transgression.

The sedimentology and few radiocarbon dates indicate that the lowest stand of sealevel was between 90 m and 100 m below present sea level. Transgression would have started sometime after 8,000 to 13,000 years B.P. These results reinforce the interpretations of Fader and King (1981) and Barrie et al. (1984). Samples from the P-15 sand ridge indicate, however, that the sand ridge may not be a relict feature as hypothesized by Barrie et al. (1984). The sand ridge shows a younger age towards the south and eastern flank indicating a south to southeast migration consistent with the smaller flow transverse bedforms. This slow migration fits the sand ridge classification of Amos and King (1984).

One other problem in the interpretation of Barrie et al. (1984) results from the analysis of the BRUTIV photographic transects. Sidescan reflectivity is very sensitive to complex patterns of small scale rippling as well as sediment texture, density and seabed morphology. The 500 kHz side scan is capable of resolving the small scale megarippling as sand-composed bedforms which are confirmed by BRUTIV photographs. This type of seabed is not as easily interpreted from the 100 kHz sonograms. In the northeastern portion of the study area, the Grand Banks gravel (Unit D) is not always a continuous lag gravel or pebble armour but predominantely a rippled sandy gravel or gravelly sand. This explains the deviations in the sand ridge boundaries from one survey to another. When the sand in the sand ridge

troughs has been rippled due to storm waves and currents and interference ripples form partially due to the seabed morphology, the sidescan sonograms show a high degree of backscatter which in some areas was interpreted previously as pebble armour. After a quiet period, ripples are quickly degraded and the sidescan sonograms show a lower amount of backscatter interpreted as sand.

As predicted by Barrie et al. (1984) initial analysis indicates sediment transport is south to southeast along the continental shelf edge, parallel to the orientation of the sediment facies. All the sedimentary bedforms observed (ripples, megaripples, sand waves, sand ribbons and sand ridges) appear to be in equilibrium with the modern hydrodynamic regime and intermittently moving towards the south-southeast based on initial analysis of the current regime. Though a preliminary value of sediment transport is given, a complete set of bottom current measurements and boundary layer current profiles are still required.

RECOMMENDATIONS

Fine microstructure within the vibrocores could not be detected during visual examination of cores. Continuous X-ray analysis is immediately needed on the archived halves of the eleven vibrocores to further benefit this study. In addition, further radiocarbon dates are needed to establish the stratigraphic time scale and possible depositional rates within each facies unit. Initial dates have shown the suitability of

using radiocarbon dating for sediments from the northeastern Grand Banks. The success of using these applied techniques to understand the depositional history of the area amplifies the need for additional cores to be taken across the sediment facies of the Hibernia study area.

The principal conclusion from the theoretical sediment transport models is that there is a need for further current meter and preferably current profile data with photography over the winter months. Research to quantify and calibrate the models, such as a tracer sand studies should be initiated along with the boundary layer current measurements.

REFERENCES

Akenhead, S.A., Petrie, B.D., Ross, C.K. and Ware, D.M., 1981. Ocean climate and the marine fisheries of Atlantic Canada: An assessment. Bedford Institute of Oceanography Report Series, 81-8, 121p.

Alam, M. and Piper, D.J.W., 1981. Detrital mineralogy and petrology of deep-water continental margin sediments off Newfoundland. Canadian Journal of Earth Sciences, 18, 1336-1345.

Amos, C.L. and Barrie, J.V., 1980. Hibernia and Ben Nevis seabed study - **Polaris V** cruise report, June 1980. C-CORE Data Report 80-17, 40p.

Amos, C.L. and King, E.L., 1984. Bedforms of the Canadian Eastern seaboard: A comparison with global occurrences. Marine Geology, 57, 167-208.

Andrews, J.T., Mears, A., Miller, G.H. and Pheasant, D.R., 1972. Holocene late glacial maximum and marine transgression in the eastern Canadian Arctic. Nature, 239, 147-149.

Arthur, K.R., Cole, D.R., Henderson, G.G.L. and Kushner, D.W., 1982. Geology of the Hibernia Discovery. AAPG Memoir, 32, 181-195.

Bagnold, R.A., 1966. An approach to the sediment transport problem from general physics. U.S. Geol. Surv., Prof. Pap. 422-I, 37pp.

Bailey, W.B., 1961. Annual variations of temperature and salinity in the Grand Banks region. Fish Res. Board of Canada, Manuscript Rep. Ser. No. 74, 30p.

Barrie, J.V., Lewis, C.F.M., Fader, G.B. and King, L.H., 1984. Seabed processes on the northeastern Grand Banks of Newfoundland; Modern reworking of relict sediments. Marine Geology, 57, 209-227.

Bartlett, G.A. and Smith, L., 1971. Mesozoic and Cenozic history of the Grand Banks of Newfoundland. Canadian Journal of Earth Sciences, 8, 65-84.

Blenkhorn, K.A. and Knapp, A.E., 1969. Ice conditions on the Grand Banks. CIM Special Volume 10, The Ice Seminar, 61-72.

Briggs, L.I., 1965. Heavy mineral correlations and provenances. Journal of Sedimentary Petrology, 35, 939-955.

Brown, C.B., 1950. Sediment Transportation. In: Engineering Hydraulics, Rouse, H. (ed.), John Wiley and Sons, Inc., N.Y., 1039pp.

Carter, L., 1979. Significance of unstained and stained gravel on the Newfoundland continental slope and rise. Journal of Sedimentary Petrology, 49, 1147-1158.

Carter, L., Schafer, C.T. and Rashid, M.A., 1979. Observations on depositional environments and benthos of the continental slope and rise, east of Newfoundland. Canadian Journal of Earth Sciences, 16, 831-846.

Carver, R.E., 1971. Procedures in Sedimentary Petrology. Wiley-Interscience, New York, 653pp.

Clarke, T.L., Swift, D.J.P. and Young, R.A., 1983. A stochastic modelling approach to the fine sediment budget of the New York Bight. Journal of Geophysical Research, 88, 9653-9660.

Dalrymple, R.W., Knight, R.J. and Lambiasae, J.J., 1978. Bedforms and their hydraulic stability relationship in a tidal environment, Bay of Fundy, Canada. Nature, 275, 100-104.

Davidson, S. and Amos, C.L., 1985. A re-evaluation of SED1D and SED2D: Sediment transport models for the continental shelf. Contract report submitted to the Geological Survey of Canada, 44pp.

Davis, A.G., 1983. Wave interactions with rippled sand beds. In: Physical Oceanography of Coastal and Shelf seas, Johns, B. (ed.); Elsevier Science Publishing Co., Amsterdam, 1-65.

Dempster, R.T. and Bruneau, A.A., 1975. Dangers presented by icebergs and protection against them. Contributions du Centre d'Etudes Arctiques, 12, 348-362.

Dinsmore, R.P., 1972. Ice and its drift into the North Atlantic Ocean. International commission for the Northwest Atlantic Fisheries Special Publication No. 8, 89-127.

Fader, G.B. and King, L.H., 1981. A reconnaissance study of the surficial geology of the Grand Banks of Newfoundland. Current Research Part A, Geological Survey of Canada, Paper 81-A, 45-81.

Folk, R.L., 1974. Petrology of Sedimentary Rocks. Hemphills, Austin, Texas, 168pp.

Foulkes, T.J., 1984. The development of a Bottom-Referencing Underwater Towed Instrument Vehicle, BRUTIV, for Fisheries Research 1973-1979. In: P.F. Smith, Underwater Photography Scientific and Engineering Applications. Van Nostrand Reinhold Company, New York, 95-107.

Galehouse, J.S., 1971. Point counting. In: Procedures in Sedimentary Petrology, Carver, R.E. (ed.); John Wiley, New York, 653pp.

Geocon, 1980a. Marine geotechnical investigation Hibernia O-35 step out well. Contract report to Mobil Oil Canada Ltd.

Geocon, 1980b. Marine geotechnical investigation Hibernia B-08 step out well. Contract report to Mobil Oil Canada Ltd.

Geocon, 1980c. Marine geotechnical investigation Ben Nevis I-45 step out well. Contract report to Mobil Oil Canada Ltd.

Gillespie, R.T. and Rendell, C.M., 1985. Centre for Cold Ocean Resources Engineering Sedimentation Tube - User Manual. C-CORE Technical Report 85-6, 41pp.

Goda, Y., 1978. The observed joint distribution of periods and heights of sea waves. Proceedings of the 16th Coastal Engineering Conference, Hamburg.

Grant, W.D. and Madsen, O.S., 1979. Combined wave and current interaction with a rough bottom. Journal of Geophysical Research, 84, 1797-1808.

Grant, W.D. and Madsen, O.S., 1982. Moveable bed roughness in unsteady oscillatory flow. Journal of Geophysical Research V. 87, 469-481.

Hammond, T.M. and Collins, M.B., 1979a. On the threshold of transport of sand-sized sediment under the combined influence of unidirectional and oscillatory flow. Sedimentology, 26, 795-812.

Hammond, T.M. and Collins, M.B., 1979b. Flume studies of the response of various current meter rotor/propellors to combinations of unidirectional and oscillatory flow. Deutsche Hydrographische Zeit.

Hubert, J.F., 1962. A zircon-tourmaline-rutile maturity index and the interdependance of the composition of heavy mineral assemblages with the gross composition and texture of sandstones. Journal of Sedimentary Petrology, 32, 440-450.

Inman, D.L., 1963. Sediments: Physical properties and mechanics of sedimentation. In: Submarine Geology, Shepard, F.P. (ed.), N.Y.; Harper & Row, 2nd. Ed., 101-151.

Ippen, A.T., 1966 (ed.). Estuary and coastline hydrodynamics Chapter 3 by Bretschneider, C.L.; McGraw-Hill, New York.

James, N.P. and Stanley, D.J., 1967. Sediment transport on Sable Island, Nova Scotia. Smithsonian Miscellaneous Paper 4727, V. 152, 33p.

James, N.P. and Stanely, D.J., 1968. Sable Island Bank of Nova Scotia: Sediment dispersal and recent history. Am. Ass. Petr. Geol. Bull., 52, 2208-2230.

Jansa, L.F. and Wade, J.A., 1974. Geology of the continental margin off Nova Scotia and Newfoundland. Offshore Geology of Eastern Canada, Geological Survey of Canada, Paper 74-30, V.2, 51-105.

Jardine, T.P., 1979. The reliability of visually observed wave heights. Coastal Engineering, 3.

Johnson, G.L., Campsie, J., Rasmussen, M. and Dittmer, F., 1972. Mesozoic rocks from the Labrador Sea. Nature, 236, 86-87.

Jonsson, I.G., 1966. Wave boundary layers and friction factors. In: Proc. 10th Conf. Coastal Eng., Tokyo, ASCE, 1, 127-148.

Judd, J.B., Smith, W.C. and Pilkey, O.H., 1970. The environmental significance of iron stained quartz grains on the southeastern United States Atlantic Shelf. Marine Geology, 8, 355-362.

King, L.H., Fader, G.B., Jenkins, A. and King, E., 1986. Occurrence and regional setting of lower Paleozoic Sediments on the Grand Banks of Newfoundland. Canadian Journal of Earth Science, 23, 504-526.

Komar, P.D. and Miller, M.C., 1973. The threshold of sediment movement under oscillatory water waves. Journal of Sedimentary Petrology, 43, 1101-1110.

Komar, P.D. and Miller, M.C., 1974. Sediment threshold under oscillatory waves. In: Proceedings of the 14th Coastal Engineering Conference. Copenhagen, Denmark, 756-775.

Krinsley, D.H. and Doornkamp, J.C., 1973. Atlas of Quartz Sand Surface Textures. Cambridge University Press. Cambridge, England, 91pp.

Lewis, C.F.M., 1983. Sediment Stability; Coring on Grand Bank. In: Cruise Report for **Hudson** 83-017. Atlantic Geoscience Centre, Bedford Institute of Oceanography.

Lewis, C.F.M. and Barrie, J.V., 1981. Geological evidence of iceberg groundings and related seafloor processes in the Hibernia discovery area of Grand Bank, Newfoundland. In: Symposium on Production and Transportation Systems for the Hibernia Discovery, St. John's, Newfoundland, 146-177.

Lewis, J. and Benedict, C.P., 1981. Icebergs on the Grand Banks: Oil and gas considerations. World Oil, January, 1981.

Lesht, B.M., Clarke, T.L., Freeland, L.L., Swift, D.J.P. and Young, R.A., 1980. An empirical relationship between the concentration of suspended sediment and near bottom wave-orbital velocity. Geophysical Research Letters, 2, 1049-1052.

MacLaren Marex, 1980. Metoc wave chart analysis, Grand Banks and Sable Island 1970-1979. Contract Report submitted to Mobil Oil Canada Ltd.

MacLaren Plansearch, 1980-81. Data analysis from bottom current meters on the Grand Banks, April 19 to June 2, 1980; June 4 to July 23, 1980; July 27 to October 1, 1980; December 6 to February 2, 1981. Contract Reports submitted to Mobil Oil Canada Ltd.

Madsen, O.S. and Grant, W.D., 1975. The threshold of sediment movement under oscillatory water waves: A discussion. Journal of Sedimentary Petrology, 45, 360-361.

Madsen, O.S. and Grant, W.D., 1976. Sediment transport in the coastal environment. Ralph M. Parsons Lab. (MIT), Rep. #209, 105pp.

Madsen, O.S. and Grant, W.D., 1977. Quantitative description of sediment transport by waves. Proc. 15th Conf. Coastal Eng., Honohulu, Hawaii, ASCE, 2, 1093-1112.

Martec, 1984. SED1D: A sediment transport model for the continental shelf. Contract Report submitted to the Geological Survey of Canada, 63pp.

Matthews, D.J., 1914. Report on the work carried out by the **SS Scotia**, 1913. Ice observation, meteorology and oceanography in the North Atlantic Ocean. Darling and Son Publ., London.

McIver, N.L., 1972. Cenozoic and Mesozoic stratigraphy of the Nova Scotia Shelf. Canadian Journal of Earth Sciences, 9, 54-70.

Miller, M.C., McCave, I.N. and Komar, P.D., 1977. Threshold of sediment motion under unidirectional currents. Sedimentology, 24, 507-527.

Murray, J.F., 1969. The drift, deterioration and distribution of icebergs in the North Atlantic Ocean. CIMM Special Vol.10, The Ice Seminar, 3-18.

Neu, H.J.A., 1976. Wave climate of the North Atlantic, 1970. Atlantic Oceanographic Laboratories, Bedford Institute of Oceanography, Report Series BI-R-76-10, 37pp.

Neu, H.J.A., 1982. 11-year deep-water wave climate of Canadian Atlantic waters. Canadian Technical Report of Hydrography and Ocean Sciences, #13, 41pp.

Parrott, D.R., Dodds, D.J., King, L.H. and Simpkin, P.G., 1980. Measurements and evaluation of the acoustic reflectivity of the sea floor. Canadian Journal of Earth Sciences, 17, 722-737.

Petrie, B., 1982. Aspects of the circulation on the Newfoundland continental shelf. Canadian Report of Hydrography and Ocean Sciences, #11, 78pp.

Petrie, B. and Anderson, C., 1983. Circulation on the Newfoundland continental shelf. Atmosphere-Ocean, 21, 207-226.

Powers, M., 1953. A new roundness scale for sedimentary particles. Journal of Sedimentary Petrology, 23, 117-119.

Rine, J.M. and Tillman, R.W., 1983. Lithologic comparison of two linear sand ridges from nearshore and middle portions of the New Jersey Continental Shelf, U.S.A. AAPG Bull., V. 67, 540-541.

Rittenhouse, G., 1943. Transportation and deposition of heavy minerals. Geological Society of American Bulletin, 54, 1725-1780.

Rubey, W.W., 1933. The size distribution of heavy minerals within a water-laid sandstone. Journal of Sedimentary Petrology, 3, 3-29.

Seaconsult, 1976. Analysis of ocean currents, Flemish Pass. Contract Report submitted to Imperial Oil Ltd.

Simpkin, P.G., 1984. Effects of small scale seafloor roughness on acoustic reflectivity measurements on the Newfoundland Shelf. Contract Report submitted to Geological Survey of Canada, 168pp.

Shields, A., 1936. Anwendung der Ahnlichkeitsmechanik und der Turbulenzforschung auf die Geschiebebewegnung. Mitteilungen der Preuss. Versuchsanst. fur Wasser, Erd. und Schiffbau, Berlin, 26, 26pp.

Slatt, R.M., 1974. Continental shelf sediments off eastern Newfoundland: A preliminary investigation. Canadian Journal of Earth Science, 11, 362-368.

Slatt, R.M., 1977. Late Quaternary terrigenous and carbonate sedimentation on Grand Bank of Newfoundland. Geological Society of American Bulletin, 88, 1357-1367.

Slingerland, R.L., 1977. The effects of entrainment on the hydraulic equivalence relationships of light and heavy minerals in sands. Journal of Sedimentary Petrology, 47, 753-770.

Smith, J.D., 1977. Modelling of sediment transport on continental shelves. In: The Sea, Vol. 6, E.D. Goldberg, I.N. McCave, J.J. O'Brien and Q.Q. Steele (Eds.); N.Y., Wiley-Interscience.

Smith, E.H., Soule, F.M. and Mosby, D., 1937. The Marion and General Greene expeditions to Davis Strait and Labrador Sea. Bulletin of the U.S. Coast Guard, #13, 259pp.

Sternberg, R.W. and Larson, L.H., 1975. Threshold of sediment movement by open ocean waves: Observations. Deep Sea Research, 22, 299-309.

Stubblefield, W.L., Kersey, D.G. and McGrail, D.W., 1983. Development of middle continental shelf sand ridges: New Jersey, AAPG Bull. 67, 817-830.

Syvitski, J.P.M., Fader, G.B., Josenhans, H.W., MacLean, B. and Piper, D.J.W., 1983. Seabed investigations of the Canadian east coast and Arctic using **Pisces IV.** Geoscience Canada, 10, 59-68.

Thorsteinsson, R. and Tozer, E.T., 1969. Geology of the Arctic Archipelago. In: Geology and Economic Minerals of Canada, Douglas, R.J.W. (ed.), Geological Survey of Canada, Economic Geology Report, 1, 547-590.

Vilks, G., 1984. **Hudson** 83-033 Cruise Report. Bedford Institute of Oceanography.

Wiegel, R.L., 1964. Oceanographical Engineering. Prentice-Hall, Inc., Eaglewood Cliffs, N.J.

Williams, G.L., 1974. Dinoflagellate and spore stratigraphy of the Mesozoic-Cenozoic, Offshore Eastern Canada. In: Offshore of Eastern Canada, Geological Survey of Canada Paper 74-30, 2, 107-161.

Williams, G.L. and Brideaux, W.W., 1975. Palynological analysis of late Mesozoic-Cenozoic rocks of the Grand Banks of Newfoundland. Geological Survey of Canada Bulletin #236, 163pp.

Yalin, M.S., 1963. An expression for bedload transportation. ASCE, J. Hydraul. Div., 89(HY3), 221-250.

APPENDIX 1

ANALYSIS OF SURFICIAL SEDIMENTS AND BEDFORMS

CSS HUDSON 83-033 CRUISE

INTRODUCTION

The following interpretations of the surficial sediments within the Hibernia-Ben Nevis region are based on seismic and continuous photographic data obtained during the **CSS HUDSON 83-033** cruise (see map sheet of track plot in folder). This cruise, which took place from October 26 to November 7, 1983, was a joint scientific study undertaken by the Atlantic Geoscience Centre in Dartmouth, Nova Scotia and C-CORE, St. John's, Newfoundland.

The nine lines analysed in this report covered a total distance of approximately 236 km. Of this, 30 km were surveyed with the Klein 500 kHz side scan and 52 km with the BRUTIV photographic unit (Approximately 180 km of data were collected with the Klein 100 kHz sidescan and Huntec DTS). An additional 30 km (Line 21) were surveyed; however, unfavourable weather conditions caused considerable heave of the Huntec DTS and sidescan fish. The BRUTIV photographs were the only reliable data obtained along this line.

METHODOLOGY

In analysing the data from this cruise, bedforms have been described in such a way as to best compensate for the inherent limitations of the shallow seismic recording systems.

Thus, wavelengths of sand waves have been determined by measuring the distance between troughs on the sidescan record rather than from crest to crest. While this is not the conventional method of determining bedform wavelength, it resolves the difficulty of determining the absolute crests of the

features from the sonogram. Huntec DTS records are not reliable for this type of analysis as it is difficult to determine at what angle to the bedform the record has been shot. A shot at anything other than at right angles to the bedform would make the distance between bedform crests appear wider than that which actually exists. This discrepancy could vary from a few centimeters error to the scale of meters, depending on the angle of the fish to the feature. Where the widths of features cannot be resolved on the sidescan records and have to be derived from Huntec profiles, the change is noted in the text.

The BRUTIV photographic unit was towed approximately 3 metres above the seafloor at some distance behind the Huntec DTS fish. Because of the varying ship's speed and change in time between frames, the exact lag time of the photographs with respect to the Huntec DTS profiles is difficult to determine except at obvious contacts.

Line 11 HUNTEC DTS/100 KHZ Sidescan: An Interpretation

Line 11 which is approximately 80 km long was surveyed during the **CSS Hudson** cruise 83-033 using the HUNTEC DTS and 100 kHz sidescan. Although it originates further north, analysis consists of that portion of the line south of 47°00N for the purpose of this report. Because the BRUTIV photographic unit was not deployed, it is impossible to define conclusively units where controversy may arise with respect to a seabed consisting of pebble/gravel armour versus a highly rippled surface. Where this discrepancy exists, interpretation is based on lines for which seismic data and BRUTIV photographs have been obtained as well as previously analysed grab samples.

A sand ridge extends along Line 11 for approximately 4.8 km from 307/0450 to 307/0528. The HUNTEC DTS profile reveals this ridge to have a maximum thickness of 1.1 m. From 307/0455 to 307/0459 the ridge thins to less than 0.4 m and is composed of highly rippled sand which appears as a slightly irregular morphology. On the HUNTEC profile, large scale ripples (megaripples) or raised features have wavelengths from 10 to 21 m. The irregular seabed surface is also in part due to small pits and boulders which abound in the area.

A sand wave field is found at the southern edge of the sand ridge from 307/0507 to 307/0528 with a 200 m wide, northeast-southwest trending sand wave trough as the most noticeable feature. From this point to the gravel contact at 307/0528, sand waves form a very thin unit on the substrate with wavelengths averaging 50 m and amplitudes of 0.4 m. From 307/0506 to

307/0515 the sonogram shows a well defined contact between the eastern sand wave field and what is assumed to be a western gravel armour unit. Small scale megarippling occurs at the contact.

This region falls within the northernmost sector of the Boundary Sand unit described by Barrie, et al. (1984) and is followed by a tract of pebble/gravel armour with thin, narrow sand stringers to 307/0538. From 307/0538 to 307/0548 sand less than 0.4 m thick with the majority of wavelengths averaging from 12 to 36 m on the Huntec DTS profile and amplitudes of 0.4 m appears at the surface.

A sand body approximately 4 km long varying in thickness from 1.4 to 1.8 m extends southward to 307/0611. The slightly irregular seabed surface is a function of megaripple crests and troughs. The well-defined troughs have depths of 1.1 m. Wavelengths range from 25 to 50 m. The troughs are shown on the sonograms as east northeast to west southwest trending linear patches. Pockets which are interpreted to be shell beds occur throughout the area. From 307/0611 to 307/0618 the sand becomes very thin and in places is replaced by gravel at the surface.

From 307/0618 to 307/0707 R_1 values ranging from 45 to 65% indicate the presence of some gravel; however, northeast-southwest trending linear patches with a high degree of backscatter snow a buildup of sand along their northern edges. This type of feature is more indicative of a medium to coarse grained sand and gravel substrate than a true gravel. Shell beds occur within depressions throughout the region.

A northwest-southeast trending degraded iceberg scour infilled by sand and showing traces of megarippling is found from 307/0638 to 307/0640 on the sonogram. The Huntec DTS profile shows the scour to have a surface width of 20 m and depth of 0.7 m.

From 307/0653 to 307/0657 a sand ribbon with a trough or scour 1.1 m deep crosses the area. The irregular seabed record originating at 307/0653 and extending to 307/0707 is in part due to an irregular morphology, intermittent gravelly texture, and the presence of boulders giving variable R_1 and R_2 profiles.

Four unusual features which have the appearance of segmented scours on the sonogram and are also seen on the Huntec DTS profile occur at 307/0705, 307/0710, 307/0714 and 307/0718 (Figure 25a,b,c). In each case the features trend east-west and at 307/0714 a large boulder occurs just to the south of the scour. The scour shown at 307/0718 could be an extension from 307/0710 to 307/0714. A highly pitted surface typical of that found within regions of grounding icebergs is found to the southwest with one large pit surrounded by raised features measuring 15 m in diameter. The Huntec DTS profile shows the scour at 307/0705 to be 43 m wide and 1.1 m deep. At 307/0711 the scour is 76 m wide at the surface, 8 m wide at the base and 2.5 m deep. A depression, pit or possible scour which is 76 m wide and 1.1 m deep exists at 307/0712. The southernmost scour within this cluster has surface and base widths of 84 and 29 m, respectively and a depth of 1.8 m.

From 307/0722 to 307/0744 the seabed is composed of very thin to 2.5 m thick sand bodies migrating over a pebble/gravel armour. At 307/0722 the Huntec profile shows a possible feature (buried channel) which was once 2.9 m deep and 79 m wide, but is now completely infilled with sand (Fig. 26). R_1 and R_2 values over this feature are 60% and 3%, respectively. The sonogram shows this to be a part of what is interpreted as an east-west trending, highly degraded scour which could extend to 307/0727. Similar features are observed from 307/0733 to 397/0735 and 307/0738 to 307/0742 on the sonogram but are not resolved by the Huntec DTS. Large scale bedforms within the region consist of north-south trending sand wave troughs, megarippling and possible shell beds.

North northeast to south southwest trending sand bodies less than 1.4 m thick with well defined eastern contacts and poorly defined western contacts occur from 307/0743 to 307/0815. Sand wave troughs trend north-south. Two questionable features which are possibly northwest-southeast and east-west trending degraded scours are found from 307/0744 to 307/0746 and 307/0754 to 307/0822, respectively. These features are not prominent enough to be resolved by the Huntec DTS. From 307/0808 the sand body is undisturbed by large scale morphological or erosional features and has extensive small scale megarippling.

Highly variable R_1 and R_2 median profiles characterize the seabed from 307/0815 to 307/0820. A feature which could be a northeast-southwest trending highly degraded iceberg scour occurs at 307/0817. A more obvious east-west oriented degraded scour

crosses the region from 307/0817 to 307/0819. This scour is resolved to be 181 m wide at the surface, 101 m wide at the base and 2.3 m deep on the Huntec DTS profile (Fig. 27). This is one of the deepest scours surveyed on the Grand Banks to date.

A dissected sand body similar to that previously mentioned exists to 307/0837 and is terminated at what has been classified by Barrie et al. (1984) as a lag gravel unit with sand ribbons. An iceberg scour arcing from 307/0900 to 307/0912 was surveyed extensively on the **CSS Hudson** 83-033 cruise (Fig. 28a,b,c). It is parabolic in shape with the facing direction to the southwest and appears at 307/0900, 307/0912 and 307/0931 where orientations show the segments to be part of the same feature. Boulders are found within the area enclosed by the scour. The scour itself is resolved by the Huntec DTS to range from less than 0.4 m in depth in the southeast to 1.3 m in the northwest. This difference in scour depth is not bathymetrically controlled and could indicate the iceberg's grounding or scouring pattern. Given the orientation of the scours it is possible that the iceberg moved across the present survey site from the northeast and was deflected to the southeast and eventually north where it is only tentatively discernible on the seismic records. As it circled the region (the inner distance between the scour traces is approximately 1.8 km) it gradually lost energy with an accompanying shallowing of the trough.

A highly degraded north-south trending iceberg scour is found within a mobile sand ribbon from 307/0938 to 307/0941. It is not known if this scour bears any relationship to the

previously mentioned feature. There is no evidence of cross-cutting of scours within the area.

A sand body approximately 1.1 m thick with north-south trending sand wave troughs and numerous gas showings in the subsurface occurs at 307/1000.

The sonogram is thought to give the most accurate description of the seabed for the remainder of Line 11. In many cases the surficial sand layer is so thin it is not resolved by the Huntec DTS system and is apparent only on the sidescan record. Very thin sand, thickening into a small ribbon, is found from 307/1038 to 307/1101. North northeast to south southwest trending ripples characterize the thin sand. Small scale rippling is also apparent on the thicker unit; however, the orientations cannot be resolved. A north-south trending iceberg scour which has been infilled by sand, crosses the sonogram from 307/1046 to 307/1048. This is followed by what may also be a scour at 307/1053:30, trending northwest-southeast. Neither feature is obvious on the Huntec profile. Gas pockets occur in the substrate.

To the southwest the sonogram depicts a unit of medium reflectivity which could be a very thin coverage of pebbles and shells on sand. Small raised features are possibly sand mounds. Northwest-southeast oriented sand ribbons with northeast-southwest trending megaripples cross the seabed from 307/1112 to 307/1140. Sand wave troughs trend north-south and north-northeast to south-southwest.

At 307/1122 the sonogram depicts a very faint scour trace. It has been partially infilled by sand which is possibly fretted

by small scale megaripples in the trough and larger scale megaripples on the flanks.

An interesting highly degraded iceberg scour occurs from 307/1124 to 307/1126 and from 307/1128 to 307/1130 (Figure 29). This scour trends north northeast to south southwest and appears only in thicker sand at the northeastern and southwestern portions of the sonogram. From the linearity and consistent nature of the scour it can be assumed that it once crossed the entire area and is now obliterated in the region between the two less reflective sand bodies. The seabed for that portion of the scour which is assumed to have been obliterated is shown as a medium reflectivity on the sonogram. Comparing this reflectivity with sonograms and BRUTIV photographs from Lines 17 and 18, it is possible that the central area on which the scour does not appear is predominantly overlain by sand consisting of small scale ripples. The less reflective sand patches where the scour trace has been maintained, are probably composed of larger scale ripples.

A thick shell bed occurs on the northern flank of a small rise at the edge of a sand ridge which extends from 307/1144 to 307/1214. The sand ridge has a maximum thickness of 1.8 m with what are possibly Tertiary unconformity reflectors shallowing from 9 m at 307/1144 to 3.6 m at 307/1151 (Fig. 12). The sand ridge itself appears to be controlled to some degree by the Tertiary unconformity. From 307/1151 to 307/1155 the seabed becomes irregular with numerous raised and erosional features and possibly a highly degraded north-south trending scour.

Northwest-southeast oriented 2-D megaripples are found on the sand ridge from 307/1208 to 307/1214.

From this point to 307/1220 the sonogram shows the seabed to have a medium reflectance which is dotted by numerous small pits and boulders. The Huntec DTS profile indicates the region is probably covered by a thin layer of pebble/gravel armour with bedrock very close to or possibly outcropping locally at the surface.

The seabed becomes more irregular from 307/1240 to 307/1250 and it is likely that gravel predominates with bedrock possibly outcropping at the surface. A highly rippled seabed exists from 307/1250 to the end of Line 11 at 307/1345, passing over the Rankin wellsite. Here, megaripples trend west northwest to east southeast.

Lines 12 and 13 Huntec DTS kHz/100 Side Scan: An Interpretation

Lines 12 and 13 have been surveyed using the 100 kHz Klein side scan. Because of their relatively short coverage and similarity of bedforms they have been analysed together.

From 307/1345 to 307/1652 the seabed is composed of highly rippled sand, with the probability of pebbles and shells occupying the troughs to some degree. Very large scale features which cannot be resolved with present seismic coverage result in irregularities within the seabed from 307/1438 to 307/1442.

The morphology of the seabed becomes very complex from 307/1652 to 307/1704. Boulders and pits dot a pebble/gravel armour. East-west trending megaripples have formed in depressions. In this region the sonogram depicts similar elongated, segmented features to those which are identified as scours from 307/0702 to 307/0715, occurring in a northwest-southeast orientation.

A sand ridge with 45 m wide arcuate shaped troughs facing northwest and trending northeast-southwest, characterizes the seafloor from 307/1704 to 307/1740. Narrower troughs having a higher degree of backscatter are oriented in an east-west direction. Thick, lunate sand patches, arcuate sand waves and highly rippled sand are found from 307/1740 to 307/1814, terminated by reflective gravel armour with northeast-southwest trending 2-D megarippled sand stringers.

Line 14 Huntec DTS/100 kHz Side Scan: An Interpretation

Line 14 which is approximately 17 km long has been analysed using Huntec DTS and 100 kHz side scan shallow seismic instrumentation procedures. Although the BRUTIV unit was not deployed along this line, inferences have been drawn with respect to a seabed comprised of pebble/gravel armour versus intensive small-scale rippling. This was accomplished on the basis of reflective contacts, depth of Huntec DTS penetration and comparison of similar seismic signatures from lines in which all three descriptive methods were used.

From 307/1920 to 307/1928 the seabed appears as a sand/sand wave cover with small scale megarippling. Maximum trough depth is approximately 1 m.

This unit extends northward to 307/1938 where a sand ridge with thicknesses ranging from 1.8 to 3.0 m occurs. Northeast-southwest trending sand waves range from 0.6 to 1.0 m in amplitude. As the spread between the 20th and 80th percentiles is relatively constant and the range of distribution in R_1 and R_2 values is fairly uniform, we can assume the infill material is predominantly sand characterized by small-scale rippling. 307/1938 to 307/1957 is an area of higher backscatter and an irregular expression of the seabed surface. Troughs or pits of 0.7 and 0.4 m occur at 307/1942:30 and 307/1944:40, respectively, with possible sand stringers exhibiting larger scale rippling from 307/1942 to 307/1952. These sand bodies have been deduced primarily from R_1 and R_2 values and appear only faintly on the sonogram. A sand ribbon which marks the southern extremity of

the succeeding sand ridge crosses the unit from 307/1953 to 307/1955. Fresh 2-D, north-south trending megaripples occur at the contacts of the sand ribbon with the predominant seabed facies on either side.

A very thin sand body 1.5 km long extends from 307/1957 to 307/2010. What appears to be extensive small scale megarippling on the sonogram probably coincides with troughs averaging 1 m in depth. These features grade into a series of crests and troughs with slight asymmetry possibly occurring on the northern or stoss sides. East-west trending troughs with north-south trending 2-D and 3-D megaripples are found from 307/2002 to 307/2008.

HU-83-033 data supports the earlier interpretation of a pebble/gravel armoured seabed over much of the region bounded by 307/2012 and 307/2028. Numerous and locally extensive shell beds occur in troughs or depressions, ranging in thickness from surficial cover to approximately 3.5 m.

It is interesting to note that the sonogram records the same intensity of reflectivity over the previously mentioned gravel unit and over shells which are found in troughs from 307/2029 to 307/2134. Distinguishing characteristics are found in the grey level Huntec profiles and R_1 and R_2 values which show increased backscatter and indicate the presence of shells. This unit forms the southern and thin leading edge of a sand ridge which extends to 307/2138. Shell beds averaging 1 m in thickness occupy the northeast-southwest trending sand wave troughs which shift to a north northeast to south southwest orientation from 307/2110 to 307/2138. R_1 values of 40% to 60% are found from 307/2110 to

30//2113. Bathymetric control within the area shows a level seabed on which the sand ridge is 1.8 m thick.

Troughs of sand waves trending north northeast to south southwest, probably containing concentrations of shells up to 1.1 m thick, characterize the region from 307/2126 to 307/2129. At 307/2129 a shell bed occurs on a very gentle south-west slope.

A very thin sand veneer with a maximum thickness of 0.4 m exists over lag gravel at the western edge of the sand ridge from 307/2128 to 307/2135. The uniformity of the R_1 median profile decreases to the west with an accompanying increase in the spread of distribution about the median; and is probably caused by the progressively thinning sand over gravel. The spread of distribution about the R_2 median profile is relatively constant at ±5%. Tertiary unconformity reflectors are picked up from depths of 8.7 m at 307/2134 to 3.6 m at 307/2139.

Line 15 Huntec DTS/100 kHz Side Scan: An Interpretation

The 100 kHz side scan and Huntec DTS were used to seismically determine the surficial sediments along Line 15 which extends for approximately 23 km.

The initial portion of the line traverses a section of a sand ridge for 7 km. This sand ridge was also identified on Line 17. At the beginning of Line 15 the ridge is 3.6 m thick, thinning to less than 0.4 m at 307/2134. Sand wave troughs are oriented in a northeast-southwest fashion or are arcuate-shaped and contain megarippling. Large scale 2-D megaripples occur from 307/2135 to 307/2142 at what has been determined by Barrie et al., (1984) as a contact between the eastern sand and a western lag gravel patch. Where BRUTIV, side scan, and Huntec DTS data exist for Lines 17 and 18, similar 2-D megaripples as that which are seen on the Line 15 sonogram occur at contacts between thick and thin sand units as well as between sand and gravel.

From 307/2142 to 307/2148, the high degree of backscatter on the sonogram is shown to be gravelly sand and shells with megaripples trending northwest-southeast. This morphology occurs on the northern edge of a thick sand ridge. The dense occurrence of shells on the flank of the sand ridge is a common feature throughout the study region.

From 307/2158 to 307/2229 the Huntec record becomes slightly more irregular in terms of R_1 and R_2 profiles and the grey level indicates a substantial thinning of sand to less than 0.4 m. On the sonogram this appears as well defined northern and southern contacts with 2-D megaripples enclosing a unit of greater

backscatter. Sporadic occurrences of boulders are found in this region as are trawl marks. What is possibly a north-south trending degraded iceberg scour is seen at 307/2212 but this feature is not detectable on the Huntec DTS profile.

At 307/2225 the sonogram depicts the leading edge of a northeast-southwest trending moderately reflective sand ridge which is 1.1 m thick. This ridge extends to 307/2242. North-south trending depressions or troughs occur at the western edge of the sand ridge at 307/2238 and extend into the next unit of thin sand to 307/2246. As well, the sonogram shows numerous trawl marks to the west of the ridge which seem to skirt along its base.

From 307/2246 to 307/2308 the seabed is irregular and covered by depressions in the very thin sand. Several large boulders and numerous cross-cutting trawl marks occur throughout the area. Two mobile(?) sand bodies exhibiting megarippling are also present. At 307/2308 the concentration of boulders on the seabed increases considerably as do raised features approximately 35 m in diameter. The thin sand is replaced by lag gravel from 307/2308 to 307/2320; however, gas pockets in the substrate indicate the lag itself is very thin. A north northwest to south southeast trending iceberg scour is tentatively identified at 307/2315. This scour is cut by a trawl mark and features a boulder at its western side.

Very thin sand, probably containing some pebbles and gravel as well as a high proportion of shelly material, forms the seabed from 307/2321 to 307/2326. R_1 values are consistent at 50%;

however, R_2 values vary widely from 15 to 35%. The remainder of the line is characterized by a sand ridge with extensive megarippling.

Line 17 BRUTIV TOW#4/HUNTEC DTS/100kHz Side Scan: A comparison

Line 17 from 308/0240 to 308/0410 has been surveyed using the Huntec Deep Tow shallow seismic system, 100 kHz side scan and BRUTIV photographic techniques and from 308/0410 to 308/0505 using Huntec DTS and 100 kHz side scan.

The entire line, which is approximately 16.2 km long, is characterized by a sand ridge of variable thickness which extends to the west and the east.

The Huntec DTS profile shows the ridge to be at its thickest from 308/0240 to 308/0258 where it is roughly bounded by the 80 m bathymetric contour (Fig. 13). Here the ridge attains thicknesses ranging from 2.8 to 3.7 m. Interpretation of the sonogram records indicates the sand is predominantly featureless with minor rippling. Sand wave troughs trend east-west and northeast-southwest or are arcuate in shape. This region is afforded greater resolution by photographs recovered from BRUTIV which allow analysis of small-scale bedforms. Class B ripples with wavelengths of approximately 35 cm, trending northeast-southwest and north northeast to south southwest, shelter smaller northeast-southwest trending ripples within their troughs. These ripples are thought to be wave generated because of their symmetric nature. Clam burrows (?)exist on the flanks of sand ripples.

The sand ridge forming the remainder of Line 17 is shown to thin to less than 1 m over a relatively flat, smooth seabed. Medium reflectivity on the sonogram from 308/0300 to 308/0416 was initially interpreted as a pebble/gravel armour; however, uniform

R_1 values of 50% obtained from Huntec DTS profiles combined with BRUTIV photographs show the seabed to be part of the western sand ridge. This ridge has been intensely fretted by Class A ripples within the northeast to southwest trending Class B ripples. These small scale features, which cannot be resolved on the sidescan sonogram, would produce a greater amount of backscatter than is seen for smoother sand surfaces.

While BRUTIV data do not exist for the line east of 308/0410, combined sonogram and Huntec profiles indicate only a very thin surficial covering of sand from 308/0425 to 308/0432 with northwest-southeast trending 2-D megarippling and exposed shells and gravel from 308/0427 to 308/0432. Sand wave troughs up to 0.5 m deep punctuate a thicker portion of the sand ridge from 308/0432 to 308/0448 with at least one of the troughs extending to the base of the sand unit. The eastern edge of this small sand ridge is flanked by a gravel patch, containing a small proportion of shells which extends to 308/0454. Shell contents cannot be confirmed definitely without photographs; however, R_1 and R_2 values derived from the Huntec DTS profile indicate their presence.

A well derined contact with the gravel patch characterized by east-west trending 2-D megarippling leads into the following sand ridge wnich extends into Line 18. It is generally less than 1.9 m thick and broken by northeast-southwest trending sandwave troughs which do not extend to the base of the sand.

Line 18 BRUTIV TOW #5/HUNTEC DTS/100 kHz Side Scan: A Comparison

Line 18 from 308/0505 to 308/0526 has been surveyed using the Huntec Deep Tow shallow seismic system, 100 kHz side scan and BRUTIV photographic techniques; from 308/0626 to 308/0720 Huntec DTS and 100 kHz side scan were used.

Line 18 which is approximately 15 km long crosses a relatively smooth seabed comprised of sand ridges broken by narrow gravel patches at the surface. Huntec DTS profiles show the sand ridge which continues from Line 17 to be 1 m thick at the beginning of the line and thinning at 308/0512 into a gravel patch which extends from 308/0521 to 308/0527.

This sand ridge, as shown by the sidescan sonogram, is cut by northwest-southeast trending sand wave troughs and trawl marks. BRUTIV data show that the initial, thicker portion of the ridge is typified by sand which has formed Class A and B ripples trending northwest-southeast and northeast-southwest, respectively. The eastern portion of the ridge is interrupted for a short distance by north northeast-south southwest trending Class C ripples, the troughs of which are infilled by shells and shell hash. Where the sand ridge begins to thin at 308/0512, sinuous crested, bifurcating north northeast-south southwest trending Class C degraded ripples, with wavelengths of approximately 50 cm, appear outlined by shell hash and minor shells. East-west to northwest-southeast trending Class A ripples are found in the troughs.

As the ridge continues to thin eastward, a high predominance of northwest-southeast trending Class A ripples dominate the

photographs with only occasional scattered shells and pebbles. This intensely rippled sand appears as a medium reflectant on the sonogram. When the BRUTIV photographs are incorporated with the sonogram records, it appears that these ripples have formed in the troughs of the larger scale northwest-southeast trending sand waves.

The previously mentioned gravel patch extending from 308/0521 to 308/0527 is cut by trawl marks and east-west trending megaripples. BRUTIV, Huntec DTS and side scan data correlate very well over this short distance. North-south and northwest-southeast migratory sand stringers from the sand ridge cross the gravel patch. East-west trending 2-D megarippling occurs on the sand to the north of the gravel patch. The contact between the western sand ridge and eastern gravel patch is marked by north northeast-south southwest oriented degraded ripples as shown by BRUTIV (Figure 30a,b,c). A sharp uneven contact distinguished by east-west trending 2-D megaripples marks the change between sand and gravel facies. Low amplitude northwest-southeast trending Class A ripples and north northeast-south southwest trending Class B ripples with minor to moderate shell cover occur on the thin leading edge of the next sand ridge for approximately 1.3 km (Figure 30a,e). The ridge thickens between 308/0538 and 308/0546 as well as between 308/0548 and 308/0602. Because the exact lag time for BRUTIV is unknown, the positioning of smaller scale features within the parameters of those indicated by sidescan and Huntec is open to some question. Bedforms have been correlated as closely as possible using all three diagnostic techniques and

are thought to be related to the thickness or position of the sand within the ridge.

The sonogram shows that from 308/0527 to 308/0538 the sand ridge is very thin (i.e. less than 0.5 m thick) and highly indented by the troughs of northwest-southeast trending 2-D megaripples; these are also apparent on Huntec DTS profiles. These slightly irregular profiles are probably a function of morphology rather than composition. BRUTIV photographs indicate that this sand contains minor shells and shell hash. The large scale sandwaves and megaripples have been further modified by low amplitude sinuous Class A and B ripples which are oriented northwest-southeast and north northeast to south southwest respectively.

As the ridge attains its maximum thickness (1.4 m) for the area from 308/0540 to 308/0601, several changes occur among the small scale bedforms:

1. increased sinuosity of Class A ripples,
2. more pronounced Class B ripples, and
3. appearance of north northeast-south southwest trending Class C ripples with large quantities of shell hash in their troughs.

The larger Class C ripples seem to be associated in this region with only the thickest portions of the sand ridge.

A marked descrease in sand thickness from 308/0601 to 308/0610 is seen in the seabed profiles as a high surface scatter. This is confirmed by BRUTIV to be the result of two sets of ripples contained within one another:

1. northeast to southwest trending degraded Class C ripples heavily marked by shells, shell hash and pebbles, and

2. northwest-southeast trending Class B ripples within the troughs of 1.

This sequence of thickening and thinning sand facies is continued to the end of the line, marked in each instance by the characteristic small scale bedforms.

Line 19 BRUTIV TOW #6/HUNTEC DTS/500 KHz Sidescan: A Comparison

Line 19, which is approximately 30 km long, roughly follows the 98 m bathymetric contour. Lying as it does on the edge of the lower terrace, this line is very complex hydrodynamically. Sediment transport in the region is very active with thin sand migrating and forming ribbons locally on a lag gravel substrate. Where the source of sand is not sufficient to form a veneer on the seabed or has been removed by currents and/or waves, gravel, pebbles and shells are seen to outcrop with persistence and regularity.

The 500 kHz side scan is capable of revealing the small scale megarippling as sand-composed bedforms. These bedforms are confirmed by BRUTIV photographs. On the 100 kHz sonograms these highly fretted surfaces could be interpreted as a gravel armour. It is, however, more limited in horizontal range (100 m swath width compared with 250 m on the 100 kHz sonogram) giving a less general view of the overall gross characteristics of the region.

The entire line from 308/0720 to 308/1310 is composed of alternating patches of sand and gravel primarily formed by sand stringers or sand waves migrating across gravel. This interpretation is drawn from features displayed on the 500 kHz sonogram.

This interpretation is further clarified by BRUTIV photographs. Areas on either side of a pebble/gravel seabed show the pebble/gravel armour grading outwards from the dense inner core to a region where pebble/gravel cover is only slight, stabilizing the underlying sand. This gradational contact

possibly indicates that in some localities at least, a unit of sand underlies the dense pebble/gravel armour. This would produce a "sandwich" effect with sand overlying the Tertiary unconformity and in turn being overlain by a coating of the pebble/gravel armour.

The sonogram shows that the seabed is composed of highly reflective sand from 308/0720 to 308/0742, probably containing a large amount of intermixed shells. Small scale megarippling exists in patches and trawl marks cross the area.

From 308/0720 a thin layer of sand extending for approximately 192 m to the southeast is indented by northwest-southeast trending troughs of small scale megaripples and trawl marks. Smaller bedforms as shown by BRUTIV consist of two classes of ripples:

1. northeast-southwest trending bifurcating, wave generated Class B ripples cut obliquely by
2. smaller scale (Class A and B) north northeast to south southwest trending ripples (Fig. 5).

Cobbles of approximately 16 cm in diameter appear in troughs of less than 0.4 m which are filled with copious shell hash. On the Huntec DTS profile, this more irregular surface occurs for approximately 83 m on the northern edge of a very gentle rise, the crown of which is covered by predominantly clean sand. Northeast-southwest trending low amplitude megaripples of approximately 1 m wavelength increase in sinuosity to the southern slope of the sand where they become increasingly infilled by pebbles and shells.

A shallow trough comprised of seismically impenetrable pebble/gravel lag extends along Line 19 for the next 600 m. The sonogram displays what is likely a highly degraded iceberg scour cutting through the area with an east northeast-west southwest orientation. This is not easily discernible on the Huntec DTS profile as it crosses an area covered by gravel and is probably very shallow. From 308/0738 to 308/0749 the Huntec DTS and BRUTIV photographs show a thin layer of sand approximately 1.2 km long (sand ribbon) grading into a pebble/gravel lag. Class 'A' northeast-southwest oriented, bifurcating ripples with shells and minor shell hash in the troughs are the predominant bedform.

308/0749 to 308/0751 features a pebble/gravel lag with minor small scale ripples surrounded by lag extending for 100 m (Fig. 7b). This is followed by a 200 m tract of sand with northeast-southwest trending, large scale ripples with shells and gravel in their troughs.

300 m of pebble/gravel lag with fresh and degraded megaripples at the outer margins covers the seabed from 308/0752 to 308/0757. The sonogram shows what could be a parabolic-shaped depression.

From 308/0757 to 308/0815 the seabed is predominantly gravel with narrow areas of pebbles and gravel on sand. Numerous clusters of boulders approximately 0.35 m in diameter appear on BRUTIV photographs and sidescan records. The minor sand bodies which occur are probably very thin stringers or patches of mobile sand which appear to trend east-west or northeast-southwest. The side scan record shows extensive small scale northeast-southwest

oriented rippling in the sandier areas. This is confirmed by BRUTIV.

A very thin sand ribbon approximately 1 km long with maximum R_1 values for that facies extends from 308/0820 to 308/0826. The area depicted by BRUTIV photographs is covered with alternating patches of gravel/shell armour (Fig. 7a) and northeast-southwest trending small scale bifurcating ripples with minor to moderate gravel and shells (Fig. 7b). Each of these units extends for approximately 50 m. The sonogram shows the outer margins of the ribbon to be fretted by extensive megarippling. The gravel patches, which are shown to be sand wave troughs are oriented in a north-south manner with northwest-southeast trending ripples.

The sand ribbon is terminated by a gravel/shell patch with minor rippling from 308/0828 to 308/0830. Both Huntec DTS and side scan records show an abrupt northern contact and gradational southern contact for the feature which is difficult to distinguish in the BRUTIV photographs. The minor rippling is shown to be east-west trending sand ripples within the gravel/shell armour.

Alternating pebble/gravel lag with northwest-southeast trending ripples at its outer margins and sand bodies with features similar to those of 308/0830 to 308/0833 typify the seabed to 308/0900.

Huntec DTS profiles show major gas pockets beneath a sand ribbon which thickens to the south from 308/0910 to 308/0952. Slight irregularities in R_1 and R_2 profiles as well as the

relatively high R_1 values for sand indicate some proportion of shells and pebbles within the sand.

From 308/0958 to 308/1008 the seabed is characterized by a very thin unit of sand probably containing shells and pebbles. Small scale bifurcating megaripples trend northwest-southeast in isolated patches and trawl marks cross the region. An interesting erosional (?) feature is found at 308/1000. What seems to be a triangular-shaped depression with the tip pointing to the northeast is flanked on either side from apex to base by ripples radiating outwards almost perpendicularly. It has been cut across the base by a trawl mark. Boulders of approximately 0.5 m in diameter are found in clusters throughout the region.

A sand ribbon with maximum thicknesses of 0.8 m appears to extend to the end of Line 19. Gas pockets occur in the subsurface throughout the remainder of the line.

Line 21 BRUTIV Tows #8 and #9: An Interpretation

Line 21 which extends for approximately 28.5 km across the southern portion of the study area was surveyed using 100 kHz side scan, Huntec DTS and BRUTIV photography. Unfavorable weather conditions caused considerable heave of both Huntec DTS and side scan fish degrading the quality of the records and thus making interpretation highly unreliable. Only very general facies boundaries could be determined from the sonogram. These have been refined using BRUTIV photographs. The descriptions for Line 21, therefore, pertain predominantly to small scale features and it is impossible to relate their positioning to larger bedform morphologies.

BRUTIV photographs show Line 21 to be surficially composed of sand with pebbles/shells, sand, and gravel in order of decreasing abundance. Comparing the photographs with those of lines in which all three interpretive methods were used, it is probable that the line is dominated by sand waves. Pebbles and shells would then occur on the flanks of sand wave troughs with gravel occupying the trough bases.

The most extensive gravel armour tracts which occur for approximately 5,000 1,000, and 300 m along Line 21 are encountered at 309/2345, 310/0037, and 310/0058, respectively. The positions for these gravel patches were taken from the Huntec DTS record and are therefore not precise due to lag time between the Huntec fish and BRUTIV tow. The initial portion of Tow 8 from 309/2135 to 309/2145 is composed of sand waves with shells and gravel in the troughs. The sand itself, contains a small

proportion of shells and pebbles. A gravelly area with north-south oriented degraded ripples precedes a unit of sand which is overlain by moderate to heavy shell armour from 309/2145 to 309/2150.

From 309/2150 to 309/2155 the seabed is characterized by sand overlain by a sparse to very dense gravel armour. A greater percentage of small boulders occurs toward the eastern portion of this region. This is followed by sand containing only minor pebbles and shells to 309/2208. Previous research conducted by Barrie et al., 1984, shows this narrow tract of predominantly sand to be part of a sand ridge field. The BRUTIV photographs depicting a sand substrate do not appear to have the necessary seabed coverage (i.e. > 1 km) for the region to qualify as a sand ridge. This is possibly due to a change (decrease) in the time lapse between photographs which would make the feature appear to have less width than actually exists or more likely to the narrowing of the sand ridge from north to south. Without complementary Huntec DTS or sidescan data, the presence of a sand ridge at this location is difficult to confirm.

Vibrocore samples taken in 1983 (Figure 2) indicate the presence of a narrow sand body which is probably the southern continuation of a sand ridge field. The coarse sand extends to a depth of 2.03 m, which is thought to be the contact with the Tertiary unconformity.

Alternating gravel and sand patches occur on the seabed from 309/2208 to 309/2300. North northeast to south southwest

trending degraded ripples are seen in sandier areas along with fresh Class A and B wave generated ripples.

The remainder of Tow 8 is predominantly composed of sand waves. It is assumed that the frames showing sand with small rippling occur on the crests of sand waves with pebbles, shells and gravel increasing in abundance towards the bases of the troughs.

At 309/2340, the seabed is composed of sand ripples of low amplitude which increase in magnitude to the west. Shell hash occupies the troughs of east-west trending Class A ripples and northeast-southwest trending Class B and C ripples.

From approximately 309/2345 to 310/0030 a gravel/shell armour predominates with very narrow patches of sand occurring sporadically. Where the sand does appear, contacts with the overlying gravel lag are gradational and in places degraded northeast-southwest trending Class C ripples are found. Alternating moderate gravel/shell cover over sand, and sand and gravel armour are found from 309/0030 to 309/0115. Sand with elongate northeast-soutwest trending Class B ripples and east-west trending Class A ripples occurs in the remainder of the Tow 9 frames.

A side scan record taken on the **CSS HUDSON** cruise 80-010 just to the north of Line 21 correlates fairly well with the basic boundaries determined by BRUTIV photographs. This record, as well, was of very poor quality and is only useful for identifying major facies boundaries.

APPENDIX II

Logs for vibrocores taken on

CSS HUDSON cruise 83-017

Sample 83017-4

Location 46°35.32'N 48°47.96'W

Length 230 cm

Water Depth 66.7 m

Log (cm)

0-119.5

Sand, Buff to 33 cm, light grey to 119.5 cm except for dark grey interval 59 cm to 76 cm. Shell fragments, Laminations 39 to 59 cm, Shell laminations 76 to 119.5 cm. Sharp bottom contact.

119.5 - 180

Sand, Pebbles, Light grey, Shell fragments, Yellow stain 56 cm - 60 cm, 173 to 180 cm. Gradational bottom contact.

180 - 205

Sand, Pebbles, Light grey, Shell fragments (some large pieces), Yellow stain 180 to 184 cm. Gradational bottom contact.

205 - 230

Sand, Pebbles, Trace of mud, Buff, Shell fragments.

Sample 83017-5

Location 46°35.40'N 48° 47.65'W

Length 283 cm

Water Depth 67.7 m

Log (cm)

0 - 113

Sand, Pebbles, Trace of mud, Pale yellow, Pebbles and large shell fragments 44 - 73 cm, Sharp bottom contact with shell fragments aligned parallel to bedding.

113 - 174

Sand, Pale yellow, Shells and shellbeds 140.5 - 141.5 cm and 151 - 153 cm, Laminations, Gradational bottom contact.

174 - 203

Sand, Silt, Pebbles, Light grey shell fragments with some whole shells. Contact zone at 202 - 203 cm consists of Grey sand, Sharp bottom contact.

203 - 273

Sand, Mud, Olive brown, Trace shell fragments, Densely packed. At 203 - 208 cm very dark grey soil-like appearance.

Sample 83017-6

Location 46°44.93'N 48°45.78'W

Length 133.5 cm

Water depth 75.0 m

Log (cm)

0 - 17

Sand, Pebbles, Buff, Shell fragments, Graditional bottom contact.

17 - 37.5

Sand, Trace of mud, Light grey, Shell fragments, Abundance of heavy minerals, Sharp bottom contact.

37.5 - 44

Sand, Pebbles, Light grey, Shell fragments and one whole gastropod, Distinct lamination at 42 cm. Gradational bottom contact.

44 - 66

Sand, Trace of mud, Medium grey, Shell fragments, Sharp bottom contact.

66 - 121

Sand, Pebbles, Medium grey, Shell fragments, Laminations of coarser and finer grained sediment.

121 - 133.5

Sand, Pebbles, Medium grey, Shell fragments.

Sample	83017-7
Location	46°44.91'N 48°45.84'W
Length	112.5 cm
Water depth	75.0 m

Log (cm)

0 - 10.5

Sand, pebbles (higher conc. at top), Buff, Shell fragments with whole shell at 9 cm.

10.5 - 40

Sand, Pebbles, Buff, Shell fragments, Gradational bottom contact.

40 - 57.5

Sand, Light grey, Shell fragments, Sharp bottom contact

57.5 - 80

Sand, Light grey, Shell fragments, Coaser sediment 72 - 80 cm. Sharp bottom contact.

80 - 104.5

Sand, Pebbles, Light grey, Shell fragments, Laminations, Densely packed, Very sharp bottom contact.

104.5 - 112.5

Sand, Pebbles, Light medium grey, Shell fragments with some whole shells.

Sample 83017-8

Location 46°45.29'N 48°46.32'W

Length 103 cm

Water depth 74.0 m

Log (cm)

0 - 27

Sand, Pebbles, Buff, Shell fragments with whole Bivalves and Echinoderms, Gradational contact.

27 - 52.5

Sand, Pebbles, Light grey, Shells, Sharp bottom contact at 35° angle to core length.

52.5 - 88

Sand, Light grey to buff, Shell fragments, Laminations 2 mm thick and 2 cm spacing.

88 - 103

Sand, Pebbles, Light grey, Shell fragments.

Sample	83017-9
Location	46°45.26'N 48°45.81'W
Length	155.5 cm
Water depth	73.2 m

Log (cm)

0 - 11.5

Sand, Pebbles, Buff, Shell fragments, Sediment is loosely packed.

11.5 - 104

Sand, Pebbles (conc. near top), Buff to 50 cm and then light grey, Shell fragments, Laminations of coarser sediment, Gradational bottom contact.

104 - 155.5

Sand, Light grey, Shell fragments.

Sample	83017-10
Location	46037.22'N 48035.63'W
Length	90.5 cm
Water depth	78.6 m

Log (cm)

0 - 53.5

Sand, Pebbles at 38 - 41 cm, Light grey, Shell fragments, Sharp bottom contact.

53.5 - 81.0

Sand, Light grey, Shell fragments, Gradational bottom contact.

81.0 - 90.5

Sand, Dark grey, Shell fragments aligned parallel to bedding.

Sample	83017-11
Location	46°37.37'N 48°34.39'W
Length	102 cm
Water depth	85.0 m

Log (cm)

0 - 53

Sand, light grey, Trace of shell fragments.

53 - 61

Top of unit is a lag surface, Sand, Light grey, Shell fragments, Gradational bottom contact.

61 - 102

Sand, medium grey, shell fragments.

Sample	83017-14
Location	46°39.31'N 47°50.74'W
Length	152 cm
Water depth	125.0 m

Log (cm)

0 - 143

Sand, Trace of mud 67 - 71 cm, Olive yellow to 19 cm, light grey to 143 cm, except medium grey at 61 - 71 cm, Shell fragments, Laminations at 102 - 104 cm, Gradational bottom contact.

143 - 153

Sand, Cobbles of limestone and siltstone, light grey, shells.

Sample	83017-15
Location	46°39.25'N 47°50.90'
Length	181 cm
Water depth	124.0 m

Log (cm)

0 - 181

Sand, Pebbles including a large quartz grain, Olive yellow to 18 cm light grey to 181 cm. Shell fragments increasing down core, Layer of coarser sediment 43 - 52 cm.

Sample	83017-16
Location	46°37.14'N 48°32.94'W
Length	200 cm
Water depth	85 m

Log (cm)

0 - 127

Sand, Pebbles including carbonate fragment, Pale yellow to 55 cm and grey to 127 cm. Shell fragments, Sharp bottom contact.

127 - 142

Sand, Light grey, Shell fragments, Sharp bottom contact.

142 - 167

Sand, Medium grey, Shell fragments, Lamination of coarse sediment 1 cm thick and evenly spaced at 2 cm. Sharp bottom contact.

167 - 200

Sand, Grey, Shell fragments, Lamination at 183 - 185 cm.

APPENDIX III

PEBBLE LITHOLOGIES OF VIBROCORE SAMPLES;

CSS HUDSON CRUISE 83-017

Sample # 83-017-5 Size : ≥ 4 mm Depth: 53-56 cm

Rock Classification	Point Count %	Weight %	Weight (g)	Rock Type Grain Type	Color	Size (cm)	Roundness	Features, Notes
			0.06	shell fragments	white	.8 x .3	subrounded	- medium thickness
Sedimentary (carbonate) (1)	5.26	0.50	0.06	limestone or calcareous sandstone	greyish	.5 x .4	subrounded to subangular	- medium crystalline - large proportion of quartz
Sedimentary (siliciclastic) (7)	36.84	18.37	0.55	siltstone (2)	banded greyish and orange (1)	.8 x .6	subrounded	- smoothed
					green/black (1)	.6 x .5	subrounded	- smoothed
			1.45	sandstone (4)	buff to reddish (3)	1.3 x .8	subrounded	- fine to medium-grained - well sorted - minor calcite cement
					greyish (1)	1 x .4		
			0.19	arkose (1)	white/grey/light orange/black (1)	.4 x .6	subrounded to subangular	- calcite cement & secondary calcite mineralization - medium grained - equigranular except for larger angular mafics fragments
Igneous (10)	52.63	79.95	9.53	granite (10)	orange/black/white (5)	2.5 x1.3-.3 x .3	subangular to subrounded	- large fragment: approx. 70% quartz & 2 feldspars; 30% mafic - medium crystalline

...CON'D

Sample #83-017-5 Con'd Size : ≥ 4 mm Depth: 53-56 cm

Rock Classification	Point Count %	Weight %	Weight (g)	Rock Type Grain Type	Color	Size (cm)	Roundness	Features, Notes
					orange/black/white (2)	1.2 x .6 .5 x .4	subangular to subrounded	- minor foliation - augen-like mafic features
					white and grey (3)	.5 x .3 .3 x .3 1 x .5	subrounded to subangular	- plagioclase phenocrysts - Fe-oxide encrustations - clay-like coating in fractures
Metamorphic (1)	5.26	1.17	0.14	quartzite (1)	greyish	.4 x .4	subrounded to sub-angular	- granoblastic texture - massive - minor feldspar & biotite (?)
Total	99.99	99.99	11.98					

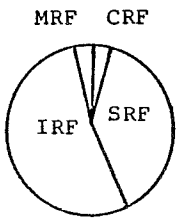

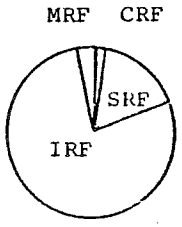

Total weight of sample before seiving (g)	76.58
Weight of shells removed for dating (g)	0.72
Weight of shells ≥ 4 mm (g)	0.06
Total weight % of shells in sample	>1.02

Sample # 83-017-5 Size : ≥ 4 mm Depth: 142-145 cm

Rock Classification	Point Count %	Weight %	Weight (g)	Rock Type Grain Type	Color	Size (cm)	Roundness	Features, Notes
			0.11	shell fragments (2)	grey	.3 x 1.4 .5 x .5	angular	- medium thickness
Sedimentary (carbonate) (1)	50.00	6.93	0.94	limestone (1)	whitish	.4 x .3	rounded	- sugary - finely crystalline - 2 large solution cavities
Igneous (1)	50.00	93.07	1.01	basalt (1)	grey/brown	1 x 1	subangular	- heavily Fe-oxide stained - secondary quartz crystallization in pitted surface
Total	100.00	100.00	2.06					

Total weight of sample before seiving (g)	111.47
Weight of shells removed for dating (g)	1.27
Weight of shells ≥ 4 mm (g)	0.11
Total weight % of shells in sample	>1.24

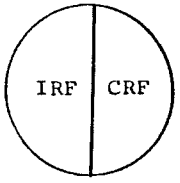

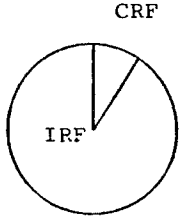

Sample # 83-017-5 Size : ≥ 4 mm Depth: 189-192 cm

Rock Classification	Point Count %	Weight %	Weight (g)	Rock Type Grain Type	Color	Size (cm)	Roundness	Features, Notes
			0.08	shell fragments(3)	grey (1)	1 x .5	sub-angular	- medium thickness
			0.22		white (2)	.5 x .5	sub-angular	- medium thickness
Sedimentary (2) (carbonate)	66.6	80.72	0.67	limestone (2)	buff (1)	1 x .7	sub-rounded	- buff weathering - smoothed - minor denritic Cu-encrustation
					grey (1)	.5 x .4		
Metamorphic (1)	33.3	19.28	0.16	quartzite (1)	mottled grey	.8 x .4	sub-angular	
Total	99.99	100.00	1.13					

Total weight of sample before seiving (g)	95.05
Weight of shells removed for dating (g)	2.49
Weight of shells ≥ 4 mm (g)	0.30
Total weight % of shells in sample	>2.94

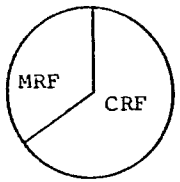

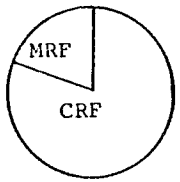

Sample # 83-017-6 Size : ≥4 mm Depth: 55-58 cm

Rock Classification	Point Count %	Weight %	Weight (g)	Rock Type Grain Type	Color	Size (cm)	Roundness	Features, Notes
			2.69	shell fragments (20)	white (18) grey (2)	≥4 mm	angular	- thin to medium thickness
Sedimentary (carbonate) (2)	40.00	3.10	0.35	limestone (3)	white to dark grey	.5 x .3	angular	- solution cavities in two lighter fragments
Sedimentary (siliciclastic) (2)	40.00	2.30	0.26	siltstone (2)	dark grey/green dark grey	.3 x .3 .6 x .3	angular	
Igneous (1)	20.00	94.60	10.69	granite (1)	grey/white	2.8 x 2	subrounded to subangular	- coarse-grained
Total	100.00	100.00	13.99					

Total weight of sample before seiving (g)	115.24
Weight of shells removed for dating (g)	15.46
Weight of shells ≥ 4 mm (g)	2.69
Total weight % of shells in sample	15.75

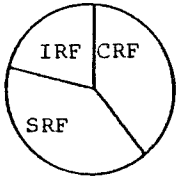

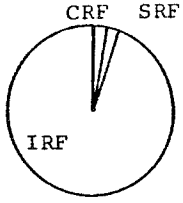

Sample # 83-017-6 Size : ≥ 4 mm Depth: 132-134 cm

Rock Classification	Point Count %	Weight %	Weight (g)	Rock Type Grain Type	Color	Size (cm)	Roundness	Features, Notes
			0.28	shell fragments	white	.8 x .5 .4 x .4	subangular to angular	- medium to very thick
Sedimentary (carbonate) (6)	50.00	76.08	2.99	limestone (6)	grey	1.1 x .8 .1 x .2	subangular to subrounded	
Sedimentary (siliciclastic) (4)	33.33	15.52	0.25	sandstone (2)	light greenish/grey	1 x 1 .3 x .3	subangular to angular	- fine to medium grained - 1 fragment has concentrated alignment of biotite (?) flakes
			0.36	shale (2)	dark grey	1.1 x .7 1 x .5	angular	
Igneous (2)	16.67	8.40	0.33	granite (2)	grey (1) grey/white/black (1)	.7 x .5 .6 x .4	subrounded subangular	
			0.29	quartz (2)	greenish (1) whitish/orange (1)	.5 x .4 .4 x .4	subangular subrounded	- translucent
Total	100.01	99.99	4.50					

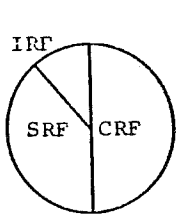

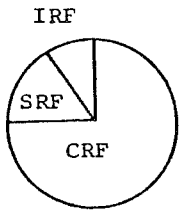

Total weight of sample before seiving (g)	87.29
Weight of shells removed for dating (g)	4.10
Weight of shells ≥ 4 mm (g)	0.28
Total weight % of shells in sample	>5.02

Sample # 83-017-7 Size : ≥ 4 mm Depth: 0-5 cm

Rock Classification	Point Count %	Weight %	Weight (g)	Rock Type Grain Type	Color	Size (cm)	Roundness	Features, Notes
Sedimentary (carbonate) (3)	12.50	2.88	1.52	limestone (3)	light grey to grey	.3 x .4	subrounded	
Sedimentary (siliciclastic) (12)	50.00	59.53	3.41	sandstone (4)	light grey to buff	.2 x .2 1.8 x 1.7 .5 x .4 1.2 x .6	subrounded to subangular	- calcite cement - calcite veining across fragment
			1.46	shale (2)	dark grey	.3 x .4 1.1 x .6	subrounded	
			0.46	conglomerate (3)	brown	.5 x .5 1.8 x .8	subrounded	-
			26.06	chert (3)	red-brown	1.2 x 1 1.7 x 1 5 x 3.5	subangular	- pitted surface; clay-like coatings within pits
Igneous (7)	29.17	31.69	13.10	granite (6)	white/light orange/grey/ black	2.8 x 2.2 to .3 x .3	subangular to subrounded	- coarse to very coarse-grained - 70% quartz and feldspar - Fe-oxide staining of quartz & feldspar
			3.61	diorite (1)	black and white	.9 x .4	subangular	
Metamorphic (2)	8.33	5.90	2.97	hornblende-biotite schist (1)	black/grey schistose	2.2 x 1.2	subangular	- coarse-grained - moderately developed schistosity
			0.14	quartzite (1)	reddish-pink	1.3 x 1	subrounded	
Total	100.00	100.00	52.73					

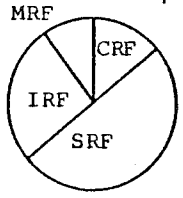

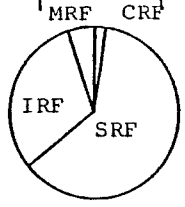

Total weight of sample before seiving (g)	134.83
Weight of shells removed for dating (g)	4.02
Weight of shells ≥ 4 mm (g)	0
Total weight % of shells in sample	>2.98

Sample # 83-017-7 Size : ≥ 4 mm Depth: 50-52 cm

Rock Classification	Point Count %	Weight %	Weight (g)	Rock Type Grain Type	Color	Size (cm)	Roundness	Features, Notes
			0.27 0.06	shell fragments (4)	white (3) grey (1)	.7 x .4- .4 x .4	angular	- medium thickness
Sedimentary (siliciclastic) (5)	62.5	86.46	1.24	shale (2)	greyish	1 x .8 .6 x .4	subangular to subrounded	
Igneous (2)	25	9.61	0.62	siltstone (2)	grey	.6 x .4 .5 x .3	subangular rounded to subrounded	- minor calcite crystallization & encrustation - very minor Cu-mineralization on surface - Fe-oxide staining/ weathering on surface
			0.12	chert (1)	grey	.5 x .5	subrounded	
			0.22	granite (2)	greyish/white/light orange	.3 x .4 .5 x .3	subangular to subrounded	- approx. 50% quartz & feldspar; 50% mafic constituents - coarse-grained, inclusions of hornblende (?)
Metamorphic (1)	12.5	3.93	0.09	quartzite (1)	light greenish	1 x .4	subrounded	
Total	100.00	100.00	2.62					

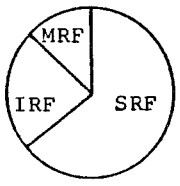

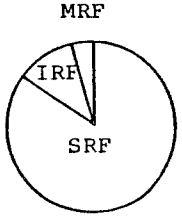

Total weight of sample before seiving (g)	108.33
Weight of shells removed for dating (g)	3.99
Weight of shells ≥ 4 mm (g)	0.33
Total weight % of shells in sample	>3.99

Sample # 83-017-7 Size : ≥ 4 mm Depth: 110-112.5 cm

Rock Classification	Point Count %	Weight %	Weight (g)	Rock Type Grain Type	Color	Size (cm)	Roundness	Features, Notes
			0.20	shell fragments	grey (2)	1.3 x .8 .7 x .3	angular	- thick
			0.22		white (3)	1.2 x .6 .4 x .4	angular	- thin
Igneous (4)	50.00	45.95	0.13	granodiorite (?) (1)	speckled black and white	.6 x .3	subrounded to subangular	
			0.27	granite (2)	light orange/white/ greyish	.6 x .3	subrounded	- larger fragment has center banding of translucent reddish quartz (?) and mafic minerals
			0.28	basalt (1)	dark grey	.6 x .5	subrounded	- heavily Fe-oxide stained - minor vessicular features
Metamorphic (4)	50.00	54.05	0.35	quartzite (1)	grey	.9 x .5	subrounded	- coarsely crystal line
			0.45	calc-silicate (marble?) (3)	greenish (1) buff (1) grey (1)	.4 x .4 .6 x .6 .5 x .3	subrounded to subangular	- easily scratched - medium crystalline - does not react with HCl (aq)
			0.61	quartz (2)	milky white to yellowish	.7 x .5	subangular to subrounded	- translucent
Total	100.00	100.00	2.51					

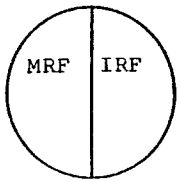

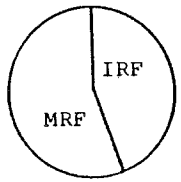

Total weight of sample before seiving (g)	125.34
Weight of shells removed for dating (g)	4.36
Weight of shells ≥ 4 mm (g)	0.42
Total weight % of shells in sample	>3.81

Sample # 83-017-8 Size : ≥ 4 mm Depth: 0-5 cm

Rock Classification	Point Count %	Weight %	Weight (g)	Rock Type Grain Type	Color	Size (cm)	Roundness	Features, Notes
			0.37 0.22	shell fragments	white (4) grey (1)	.9 x .6	angular	- thin - thick
Sedimentary (siliciclastic) (18)	39.13	40.72	1.12	shale (5)	green (4) black (1)	.5 x .3 .4 x .4	subangular to subrounded subrounded	- smoothed - minor, very thin black banding
			2.23	siltstone (8)	light brown	1 x 1 to .3 x .3	subrounded to subangular	- smoothed
			1.35	sandstone (2)	grey	.6 x .4 .3 x .3	subrounded	- well sorted - smoothed - medium-grained
			0.51	conglomerate (1)	variable	1 x .9	subangular	- dark grey to black, fine-grained matrix - fragments: feldspar, quartz, siltstone
			1.79	chert (2)	red-brown	.5 x .5 1.2 x .8	subangular	
Igneous (28)	60.87	59.28	0.50	unidentified (2) (possibly basalt)	dark grey	1 x .5 .5 x .5	rounded to subrounded	- smoothed - fine grained matrix; quartz phenocrysts
			0.44	diabase (?) (2)	dark grey	.8 x .6 .6 x .5	subangular	- fine to medium grained - minor, very small plagioclase phenocrysts

...CON'D

Sample # 83-017-8 Size : ≥ 4 mm Depth: 0-5 cm

Rock Classification	Point Count %	Weight %	Weight (g)	Rock Type Grain Type	Color	Size (cm)	Roundness	Features, Notes
			9.25	granite (24)	orange/light grey/white (16)	.3 x .2 1 x .9	subrounded to subangular	- coarse grained >55% quartz and plagioclase, 20% orthoclase, 10% mafic minerals
					orange/black/white (5)	.6 x .3	subangular	- protruding crystals with smoothed corners - milky quartz
					light orange/white/black (3)	.5 x .3 1.7 x .5	subangular to subrounded	- very smoothed, internally highly fractured - tiny black pyroxene (?) laths - some translucent quartz
			0.77	quartz (4)	clear translucent to light milky orange (3)	.4 x .4 .7 x .6	subrounded to rounded	- minor inclusions of mafic minerals
					milky to light greenish (1)	.5 x .3	subangular	- mafic constituents on one side; - fragments indicate the greenish coloration could be due to hornblende
Total	100.00	100.00	18.55					

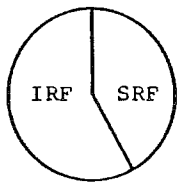

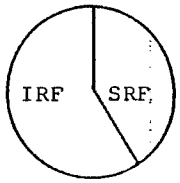

Total weight of sample before seiving (g)	152.93
Weight of shells removed for dating (g)	5.73
Weight of shells ≥ 4 mm (g)	0.35
Total weight % of shells in sample	>3.98

Sample #83-017-8 Size : ≥ 4 mm Depth: 36-39 cm

Rock Classification	Point Count %	Weight %	Weight (g)	Rock Type Grain Type	Color	Size (cm)	Roundness	Features, Notes
			0.65	shell fragments	white	.3 x .5	subrounded to subangular	- thick
Sedimentary (carbonate) (2)	11.76	2.59	0.59	limestone (2)	very light grey medium grey	1 x .5 .6 x .5	subrounded to subangular	- all edges and corners smoothed
Sedimentary (siliciclastic (8)	47.06	74.10	0.29	shale (1)	dark grey	.5 x .4	subrounded to subangular	- light grey laminations
			16.27	siltstone (3)	light grey (1) medium grey (2)	.4 x .4 .9 x .5 2.5 x 3.0	subrounded angular subrounded	- quarts growths in fractures - calcite cement and crystallization
			0.16	sandstone (1)	reddish brown	.4 x .8	subangular	
			0.13	arkose (1)	white and grey	.4 x .4	subrounded	- heavily Fe-oxide stained - Fe-oxide cement
Igneous (5)	29.41	21.72	4.94	granite (5)	brown/black/white (2)	.3 x .6 .4 x .4	subangular subrounded	- minor clay particles in fractures
					grey/white (1)	.5 x .4	subangular	- perthetic-like structure on extremely thin feldspar crystal
					pink/white (1)	1.7 x 1.3	subangular to angular	- elongate mafic laths
					pink/light grey/white/black	.3 x .7	subangular to angular	- graphitic-like nature of quartz or feldspar

...CON'D

Sample # 83-017-8 Con'd Size : ≥ 4 mm Depth: 36-39 cm

Rock Classification	Point Count %	Weight %	Weight (g)	Rock Type Grain Type	Color	Size (cm)	Roundness	Features, Notes
Metamorphic (2)	11.76	1.58	0.36	quartzite (2)	very light grey light grey	.9 x .3 .3 x .3	subangular	- edges & corners smoothed - very minor calcite in fractures
			0.49	quartz (3)	milky quartz (2)	.3 x .5 .6 x .4	subrounded to subangular	- highly fractured - tiny (approx. 0.03 cm) pyrite or Cu rounded bleb
					yellow translucent quartz (1)	.4 x .5	subangular	- minor black impurities along fractures
Total	99.99	99.99	24.39				-	

Total weight of sample before seiving (g)	151.45
Weight of shells removed for dating (g)	9.13
Weight of shells ≥ 4 mm (g)	0.62
Total weight % of shells in sample	>6.44

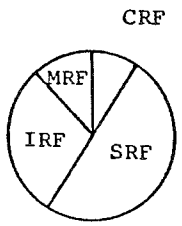

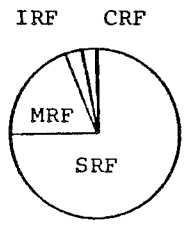

Sample # 83-017-10 Size : ≥ 4 mm Depth: 87.5 - 90 cm

Rock Classification	Point Count %	Weight %	Weight (g)	Rock Type Grain Type	Color	Size (cm)	Roundness	Features, Notes
			0.71	shell fragments (7)	white	1 x .8 to .5 x .5	angular	- thin to medium thickness
Sedimentary (carbonate) (1)	50.00	67.86	0.19	limestone (1)	light grey with buff weathering	.8 x .3	subangular	- finely crystalline
Metamorphic (1)	50.00	32.14	0.09	quartzite (1)	grey	.6 x .5	subrounded	- coarse grained - minor layerings of biotite (?)
Totals	100.00	100.00	0.99					

Total weight of sample before seiving (g)	76.58
Weight of shells removed for dating (g)	0.72
Weight of shells ≥ 4 mm (g)	0.06
Total weight of shells in sample	>1.02

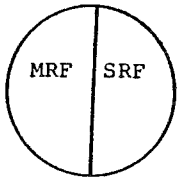

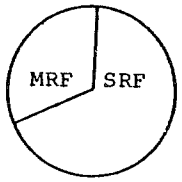

Sample # 83-017-11 Size · ≥ 4 mm Depth: 55-59 cm

Rock Classification	Point Count %	Weight %	Weight (g)	Rock Type Grain Type	Color	Size (cm)	Roundness	Features, Notes
Sedimentary (siliciclastic)	36.36	18.58	0.29	shale (1)	black	.6 x .4	subangular	- Fe-oxide/clayey encrustations
			0.33	siltstone (2)	green (1) grey (1)	.5 x .4	subangular	- quartz over-growths
			2.31	chert (1)	light reddish	1.5 x 1	subrounded	- massive
Igneous (5)	45.45	78.31	12.35	diorite (?) (5)	black and white (1) grey (4)	2 x 3 .3x.4(4)	subangular	- coarse grained, equigranular - minor accessory garnet (?) and Cu/Fe- oxide encrustations
Metamorphic (2)	18.18	3.11	0.49	quartzite (2)	light grey	.6 x .7 .6 x .5	subangular to subrounded	- minor tiny mafic fragments on surface
			0.59	quartz (4)	milky	.7 x .5	subangular to subrounded	- minor tiny inclusions of mafic minerals - some dark impurities along fracture lines
Total	99.99	100.00	16.36					

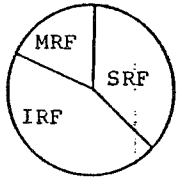

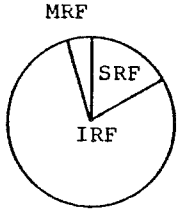

Total weight of sample before seiving (g)	52.52
Weight of shells removed for dating (g)	7.27
Weight of shells ≥ 4 mm (g)	0
Total weight % of shells in sample	>13.84

Sample # 83-017-14 Size : ≥ 4 mm Depth: 148-153 cm

Rock Classification	Point Count %	Weight %	Weight (g)	Rock Type Grain Type	Color	Size (cm)	Roundness	Features, Notes
Sedimentary (siliciclastic) (7)	70.00	59.08	3.55	shale (1)	dark grey	2 x 1	subangular	- minor Fe-oxide encrustations, especially along fractures - several fractures extend through rock
			2.34	siltstone with calcite (3)	light to dark grey	.7 x .5	subangular	- minor amounts of calcite forming cement as well as infilling fracture - one chip also has Fe-oxide encrustation
				siltstone with calcite cement only (2)	dark grey	.7 x .5 1 x 1.2	subangular	- medium grained - calcite cement - 1x1.2 has calcite overgrowth of crystals over entire fragment
				siltstone with quartz or feldspar (1)	dark grey	.7 x .5	subangular	- quartz (or k-spar as small rounded "spherulites" as well as infilling fractures - minor Cu-encrustation (probably bornite)

...CON'D

Sample # 83-017-14 Con'd Size : ≥ 4 mm Depth: 148-153 cm

Rock Classification	Point Count %	Weight %	Weight (g)	Rock Type Grain Type	Color	Size (cm)	Roundness	Features, Notes
Igneous (2)	20.00	5.62	0.56	granite (2)	white/black/pink	1 x 1.2 .5 x .7	subrounded	- approximately 20% each quartz, k-spar, hornblend 40% Na-spar
Metamorphic (1)	10.00	35.31	3.52	quartzite (1)	light grey	1.7 x 1.5	subangular	- calcite cement
Total	100.00	100.01	9.97					

Total weight of sample before seiving (g)	142.57
Weight of shells removed for dating (g)	5.55
Weight of shells ≥ 4 mm (g)	0
Total weight % of shells in sample	>3.89

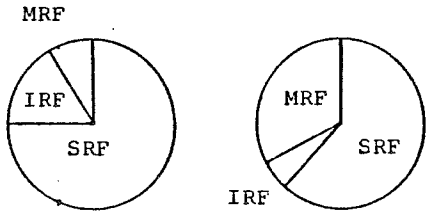

Sample #83-017-15 Size : ≥ 4 mm Depth: 114 cm

Rock Classification	Point Count %	Weight %	Weight (g)	Rock Type Grain Type	Color	Size (cm)	Roundness	Features, Notes
			1.01	quartz (1)	milky white	1.2 x 1.2	subangular	- translucent
Total	0	0	1.01					

Sample # 83-017-15 Size : ≥ 4 mm Depth: 176-180 cm

Rock Classification	Point Count %	Weight %	Weight (g)	Rock Type Grain Type	Color	Size (cm)	Roundness	Features, Notes
Sedimentary (carbonate) (5)	26.32	22.82	1.23	limestone (5)	buff to grey	1 x .8 to .2 x .2	angular to subangular	
Sedimentary (siliciclastic) (9)	47.37	46.20	0.97	shale (2)	dark grey	1.1 x .8 .8 x .4	subangular to subrounded	
			0.77	siltstone (4)	grey	1 x .6	subangular to angular	
			0.23	sandstone (1)	grey	.5 x .4	subangular	- medium grained - medium sorted
			0.52	chert (2)	grey/buff	.4 x .6 .4 x .5	angular	
Igneous (4)	21.05	25.42	1.37	granite (4)	white/grey/black (4)	1 x .5 to .8 x .4	subangular	- larger crystals of feldspar
Metamorphic (1)	5.26	5.57	0.30	quartzite (1)	light grey	.6 x .6	subangular	
!			0.12	quartz (1)	milky	.5 x .4	subangular	- translucent to opaque
Total	100.00	100.01	5.51					

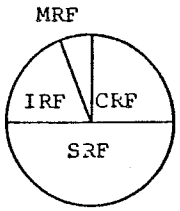

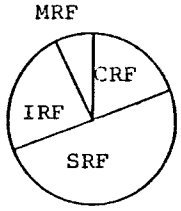

Total weight of sample before seiving (g)	99.83
Weight of shells removed for dating (g)	7.01
Weight of shells ≥ 4 mm (g)	0
Total weight % of shells in sample	>7.02

Sample # 83-017-16 Size : ≥ 4 mm Depth: 114-117 cm

Rock Classification	Point Count %	Weight %	Weight (g)	Rock Type Grain Type	Color	Size (cm)	Roundness	Features, Notes
			0.10 0.10	shell fragments (2)	white (1) grey (1)	.5 x .5 .9 x .5	angular	- medium thickness
Sedimentary (carbonate) (2)	33.33	27.30	1.54	limestone (2)	light grey (1) buff (1)	.5 x .6 1.3 x .8	subrounded to rounded	- very finely crystalline
Sedimentary (siliciclastic) (1)	16.67	57.62	3.25	shale (1)	dark grey	2.5 x 1	subrounded to subangular	- micaceous intervals at partings
Igneous (2)	33.33	8.33	0.47	granite (2)	light grey/white	.8 x .5	angular to subangular	- hornblend inclusions - coarsely crystalline
Metamorphic (1)	16.67	6.74	0.38	quartzite (1)	grey	.7 x .4	subangular	
			0.29	quartz (1)	milky	.5 x .5	subrounded	
Totals	100.00	99.99	6.13					

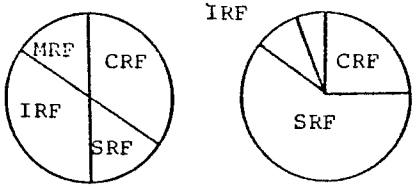

Total weight of sample before seiving (g)	93.35
Weight of shells removed for dating (g)	8.76
Weight of shells ≥ 4 mm (g)	0.20
Total weight % of shells in sample	>9.60

Sample # 83-017-16 Size : ≥ 4 mm Depth: 198-200 cm

Rock Classification	Point Count %	Weight %	Weight (g)	Rock Type Grain Type	Color	Size (cm)	Roundness	Features, Notes
Sedimentary (siliciclastic) (1)	100.00	100.00	1.33	shale (1)	dark grey	1.5 x 1	subangular to subrounded	- fine bands of lighter colored more highly resistant silt-stone
Total	100.00	100.00	1.33					

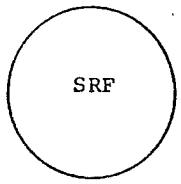

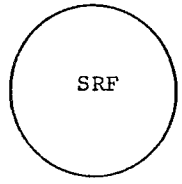

Total weight of sample before seiving (g)	84.85
Weight of shells removed for dating (g)	5.52
Weight of shells ≥ 4 mm (g)	0
Total weight % of shells in sample	>6.51

APPENDIX IV

HEAVY MINERALS IN SURFACE GRABS AND VIBROCORES

SURFACE GRAB SAMPLES

HEAVY MINERALS	142	123	112	82 Ø 3.5	82 Ø 3	82 Ø 2.5	82 Ø 2	64	51	30	21 Ø 3.5	21 Ø 3	21 Ø 2.5	21 Ø 2	4
OPAQUES	51	29	25	25	14	20	18	25	24	44	60	54	22	44	38
GARNET	27	42	33	52	58	56	45	39	46	23	21	35	40	8	33
ZIRCON	8	13	8	5	6	3	5	13	7	11	8	3	4	4	18
AMPHIBOLE	5	7	3	4	5	4	11	7	6	8	4	3	9	14	2
RUTILE	2	4	8	5	5	6	3	5	1	2	1	1	7	5	2
SPHENE	3	4	7	4	6	3	2	3	6	2	2	2	6	4	3
ANDALUSITE	-	-	2	-	-	-	-	-	-	-	-	-	-	-	-
KYANITE	-	-	2	-	-	-	-	1	-	-	-	-	-	-	-
EPIDOTE	-	-	-	1	2	3	4	2	-	4	-	-	5	15	-
CLINOPYROXENE	-	-	-	-	-	-	-	-	-	-	-	-	-	-	-
ORTHOPYROXENE	-	-	-	-	-	-	-	-	-	-	-	-	-	-	-
APATITE	-	-	-	-	-	-	-	-	-	-	-	-	3	-	-
STAUORLITE	-	-	5	1	-	-	-	-	1	1	-	-	3	-	-
OTHERS	5	2	2	-	5	5	11	5	9	4	4	2	6	22	3

*Tr = Trace Amount

VIBROCORES

HEAVY MINERALS	5 (88-91cm)	5 (189-192cm)	5 (267-270cm)	6 (42-43cm)	6 (132-134cm)	7 (110-112cm)	8 (71-74cm)	10 (87.5-90cm)	14 (66-70cm)	14 (148-153cm)	16 (158-160cm)	16 (198-200cm)
OPAQUES	48	36	90	22	14	38	31	33	9	24	30	46
GARNET	32	32	5	27	46	23	36	35	47	44	40	28
ZIRCON	6	7	3	5	3	4	4	3	9	7	5	4
AMPHIBOLE	2	3	1	5	1	3	4	Tr	Tr	3	4	4
RUTILE	3	5	-	7	4	5	8	9	7	6	5	3
SPHENE	Tr	Tr	-	2	-	Tr	Tr	-	2	3	1	2
ANDALUSITE	Tr	3	-	3	2	3	4	Tr	2	Tr	2	1
KYANITE	-	-	-	2	-	1	-	-	-	Tr	-	Tr
EPIDOTE	4	3	1	3	6	5	4	3	6	6	4	1
CLINOPYROXENE	Tr	2	-	2	-	Tr	Tr	Tr	Tr	Tr	Tr	-
ORTHOPYROXENE	Tr	2	-	2	3	3	Tr	Tr	3	3	2	2
APATITE	-	-	-	2	-	Tr	Tr	-	-	Tr	-	-
STAUORLITE	2	2	-	3	1	3	2	-	2	Tr	2	Tr
OTHERS	2	5	-	12	19	10	5	5	12	5	5	6

*Tr = Trace Amount

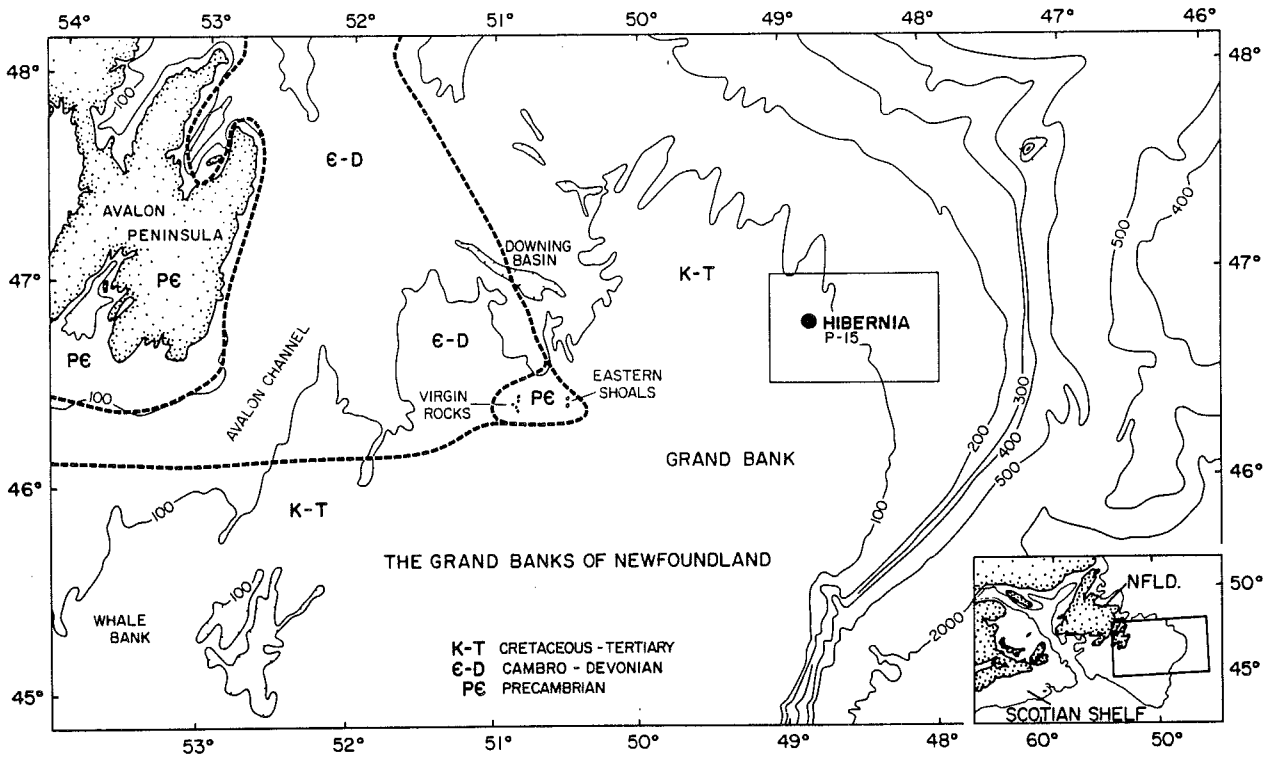
54°
53°
52°
51°
50°
49°
48°
47°
46°
48°
47°
46°
45°
Є-D
AVALON
PENINSULA
PЄ
PЄ
100
AVALON CHANNEL
DOWNING
BASIN
Є-D
VIRGIN
ROCKS
PЄ
EASTERN
SHOALS
K-T
HIBERNIA
P-15
GRAND BANK
100
200
300
400
500
400
500
K-T
THE GRAND BANKS OF NEWFOUNDLAND
100
100
WHALE
BANK
2000
K-T CRETACEOUS - TERTIARY
Є-D CAMBRO - DEVONIAN
PЄ PRECAMBRIAN
NFLD.
SCOTIAN SHELF
60°
50°
53°
52°
51°
50°
49°
48°

Figure 1

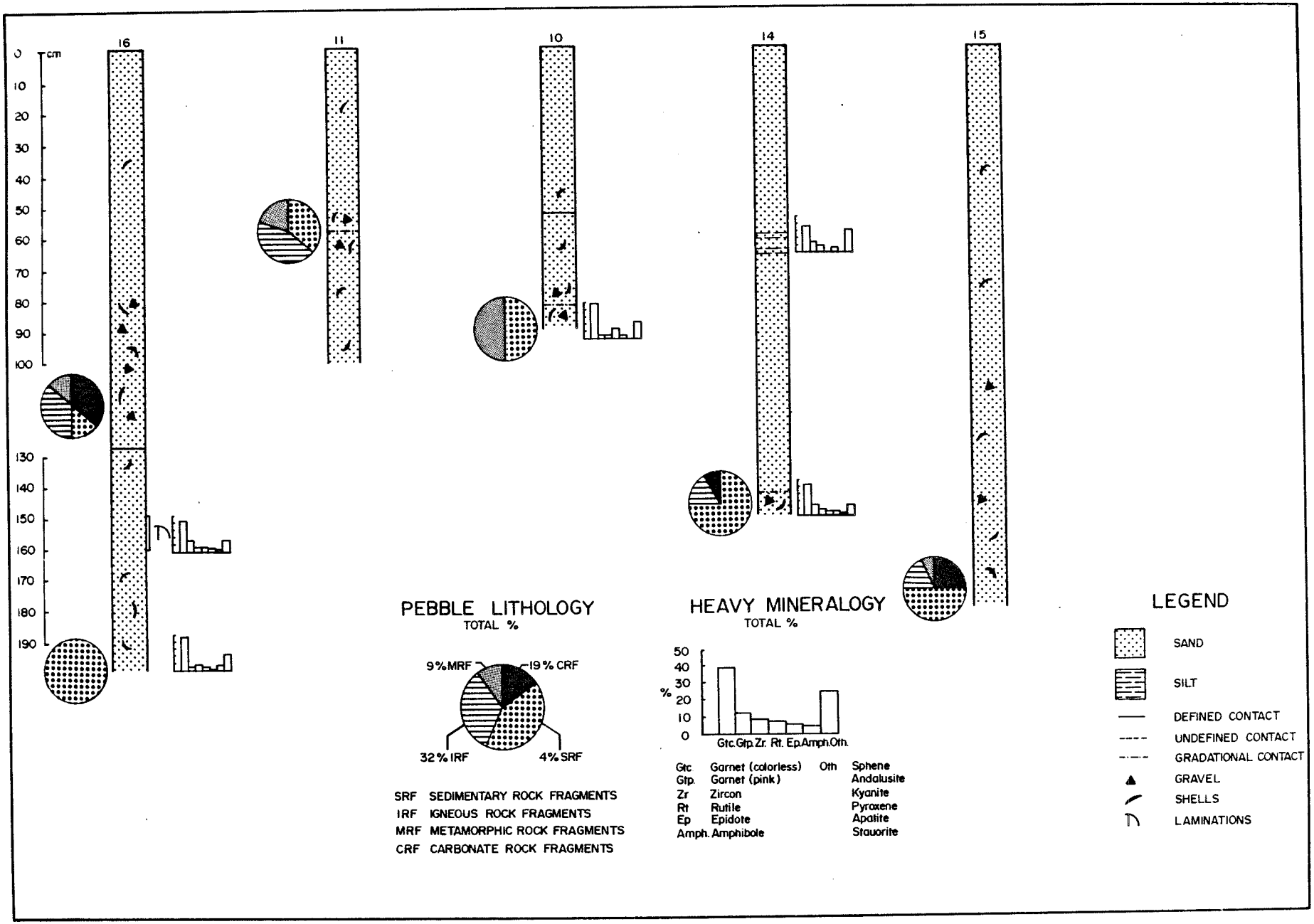
16
11
10
14
15
0 cm
10
20
30
40
50
60
70
80
90
100
130
140
150
160
170
180
190
PEBBLE LITHOLOGY
TOTAL %
9% MRF
19% CRF
32% IRF
4% SRF
SRF SEDIMENTARY ROCK FRAGMENTS
IRF IGNEOUS ROCK FRAGMENTS
MRF METAMORPHIC ROCK FRAGMENTS
CRF CARBONATE ROCK FRAGMENTS
HEAVY MINERALOGY
TOTAL %
50
40
30
20
10
0
%
Gtc Gtp Zr Rt Ep Amph Oth
Gtc Garnet (colorless)
Gtp Garnet (pink)
Zr Zircon
Rt Rutile
Ep Epidote
Amph Amphibole
Oth Sphene
Andalusite
Kyanite
Pyroxene
Apatite
Staurorite
LEGEND
SAND
SILT
DEFINED CONTACT
UNDEFINED CONTACT
GRADATIONAL CONTACT
GRAVEL
SHELLS
LAMINATIONS

Figure 2

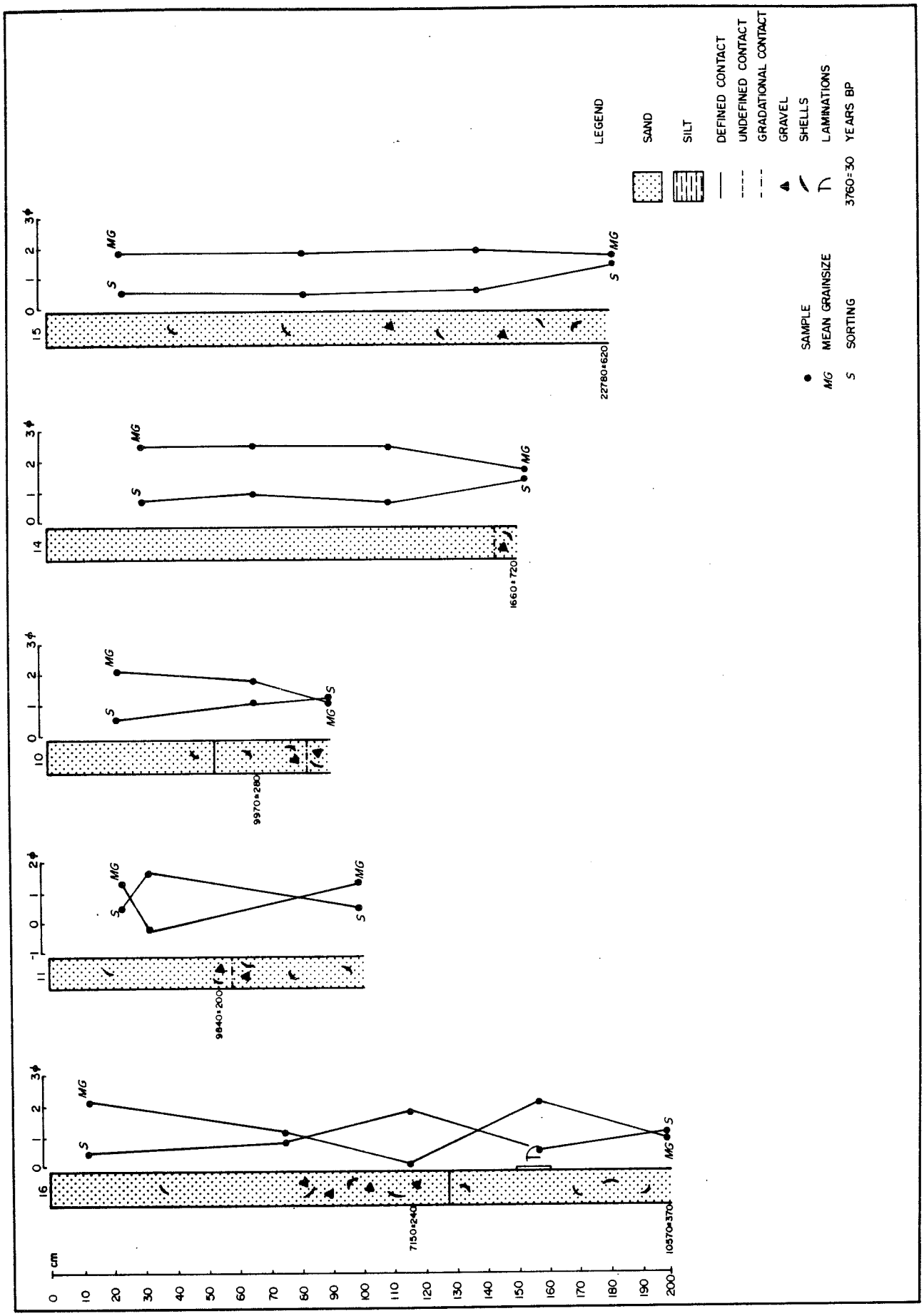
LEGEND
SAND
SILT
DEFINED CONTACT
UNDEFINED CONTACT
GRADATIONAL CONTACT
GRAVEL
SHELLS
LAMINATIONS
YEARS BP
SAMPLE
MEAN GRAINSIZE
SORTING
3760±30
22780±620
16600±720
9970±280
9840±200
7150±240
10570±370
cm

Figure 3

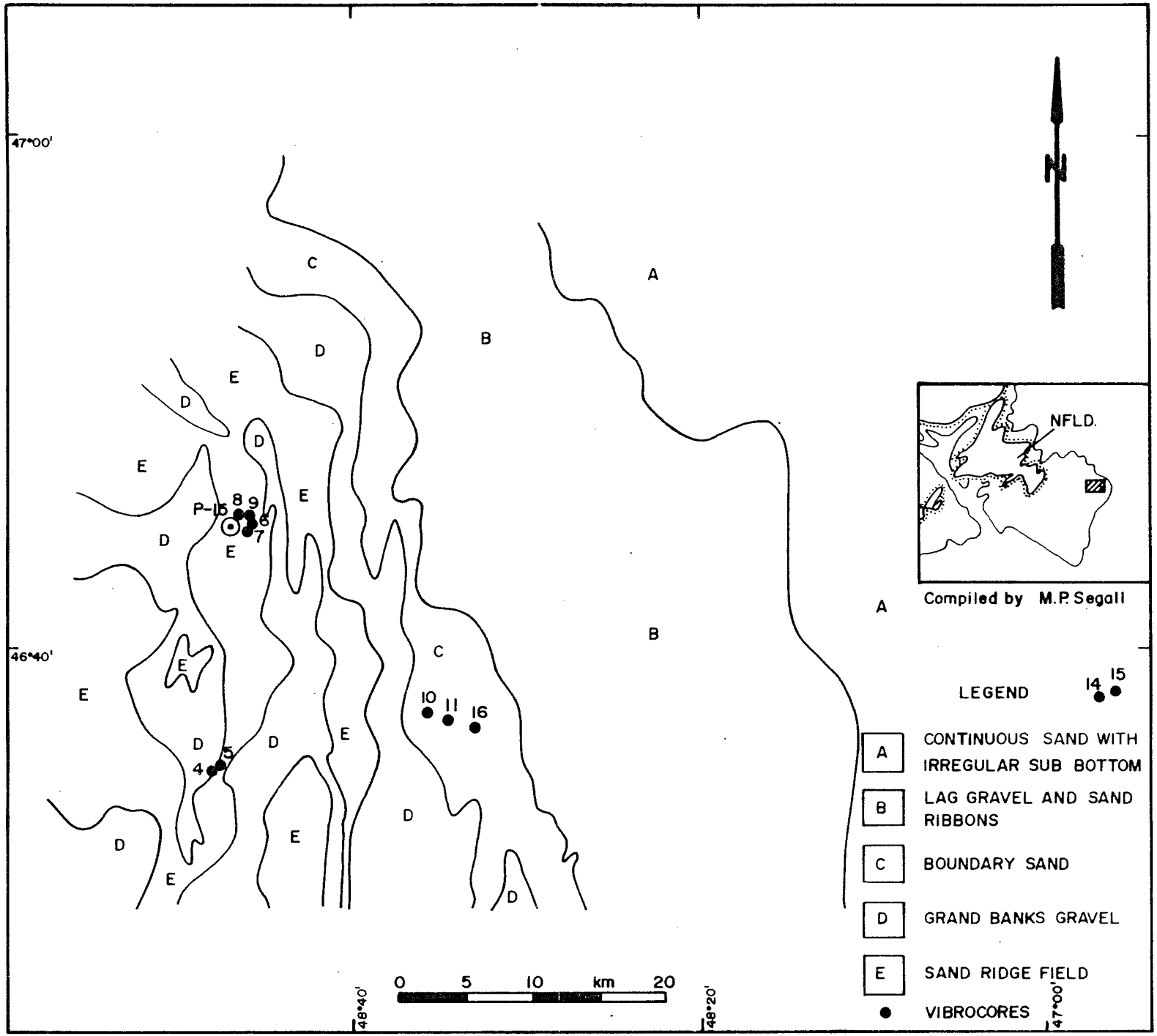
47°00'
46°40'
48°40'
48°20'
A
B
C
D
E
P-15
8
9
6
7
10
11
16
5
4
0 5 10 km 20
NFLD.
Compiled by M.P. Segall
LEGEND
14
15
A CONTINUOUS SAND WITH IRREGULAR SUB BOTTOM
B LAG GRAVEL AND SAND RIBBONS
C BOUNDARY SAND
D GRAND BANKS GRAVEL
E SAND RIDGE FIELD
VIBROCORES

Figure 4

(a)

0 100 (cm)

APPROXIMATE SCALE

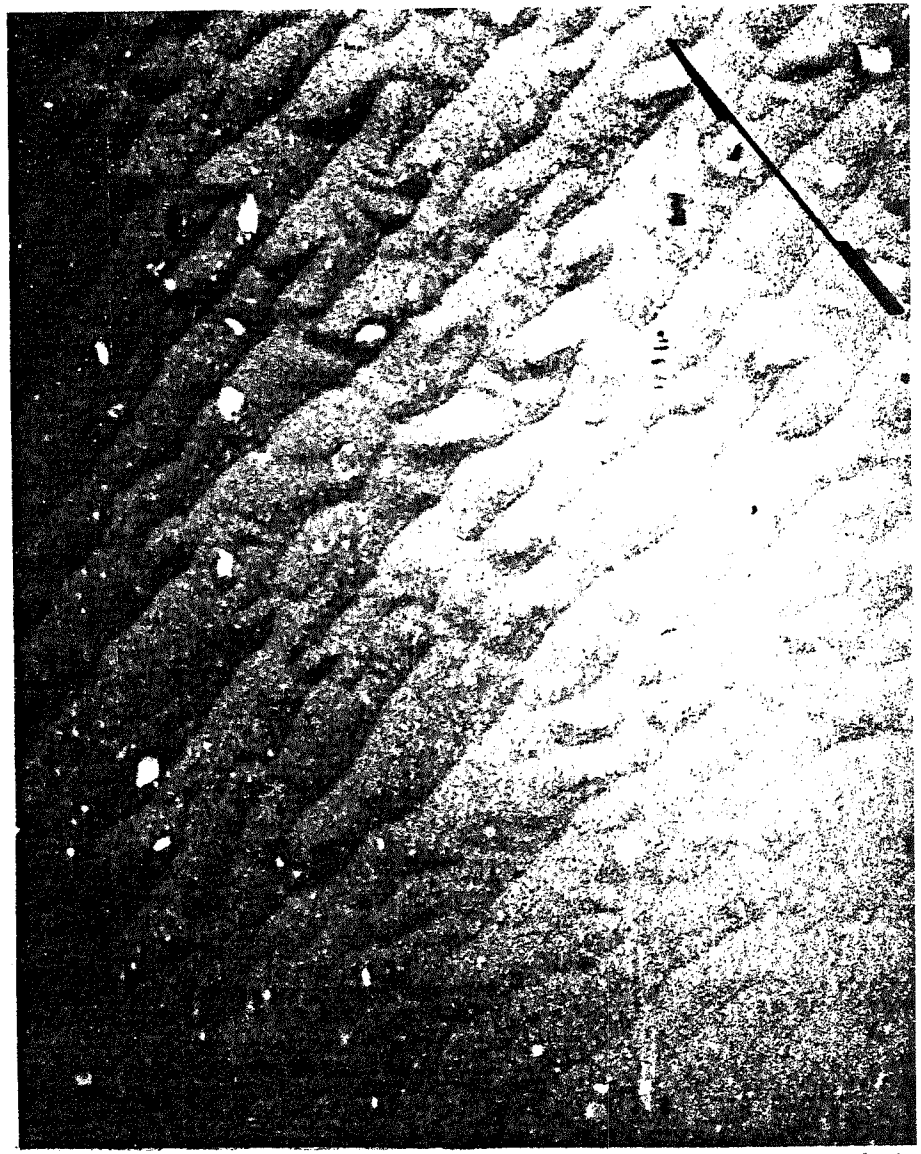

(b)

0 100 (cm)

APPROXIMATE SCALE

Figure 5

Figure 6

0 100 (cm)

APPROXIMATE SCALE

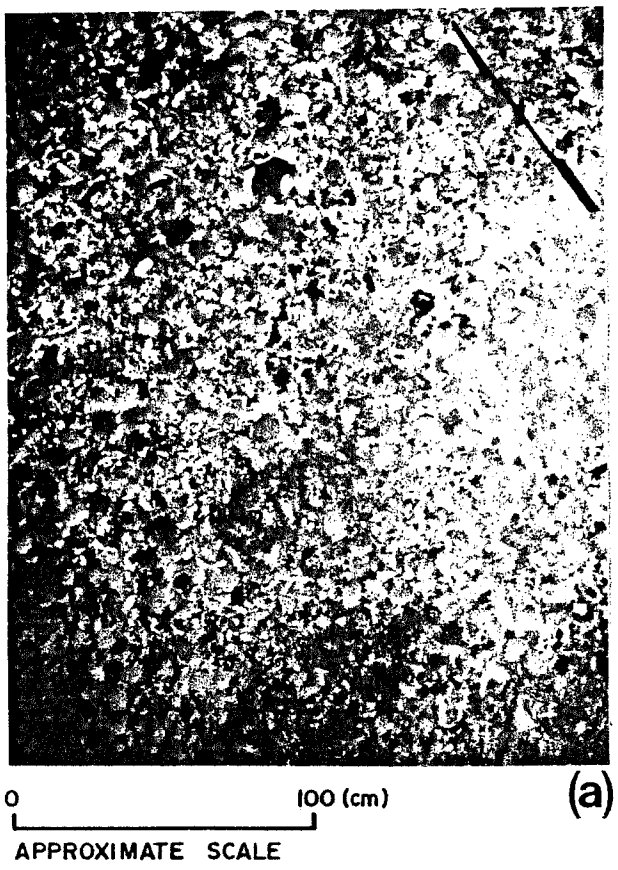
0
100 (cm)
APPROXIMATE SCALE
(a)


0
100 (cm)
APPROXIMATE SCALE
(b)


0
100 (cm)
APPROXIMATE SCALE
(c)

Figure 7

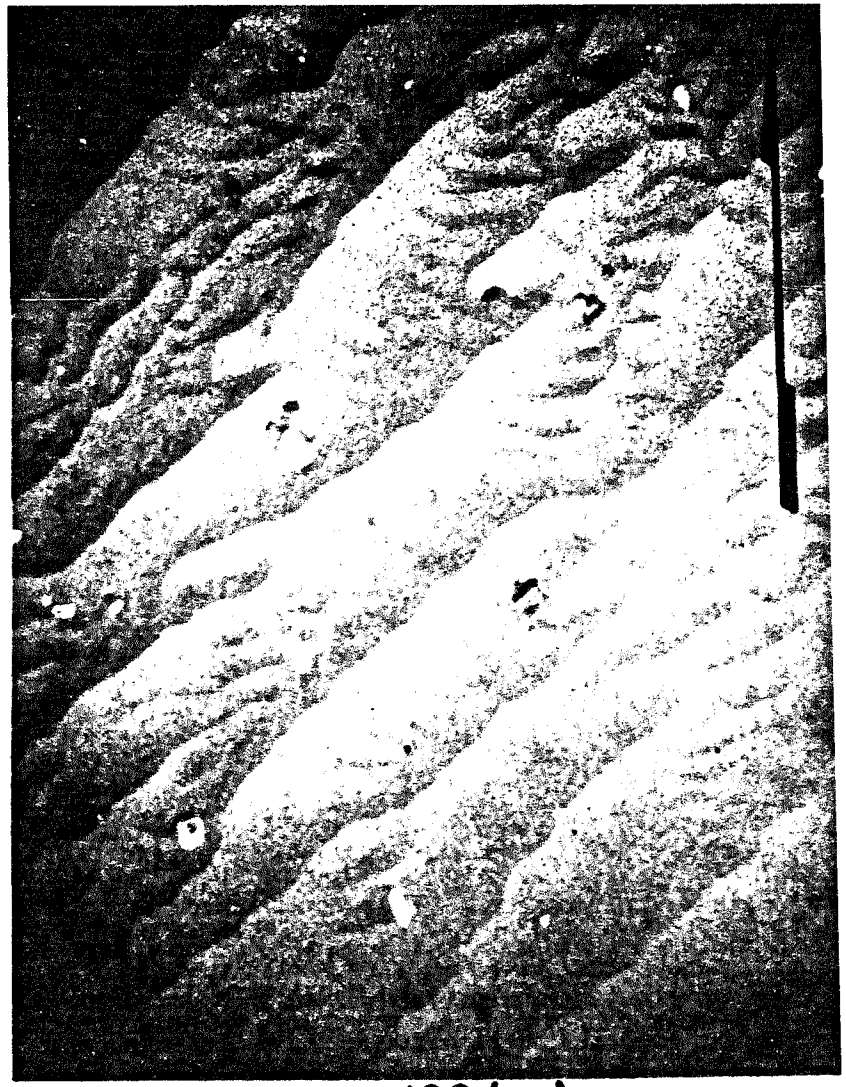

Figure 8

Figure 9

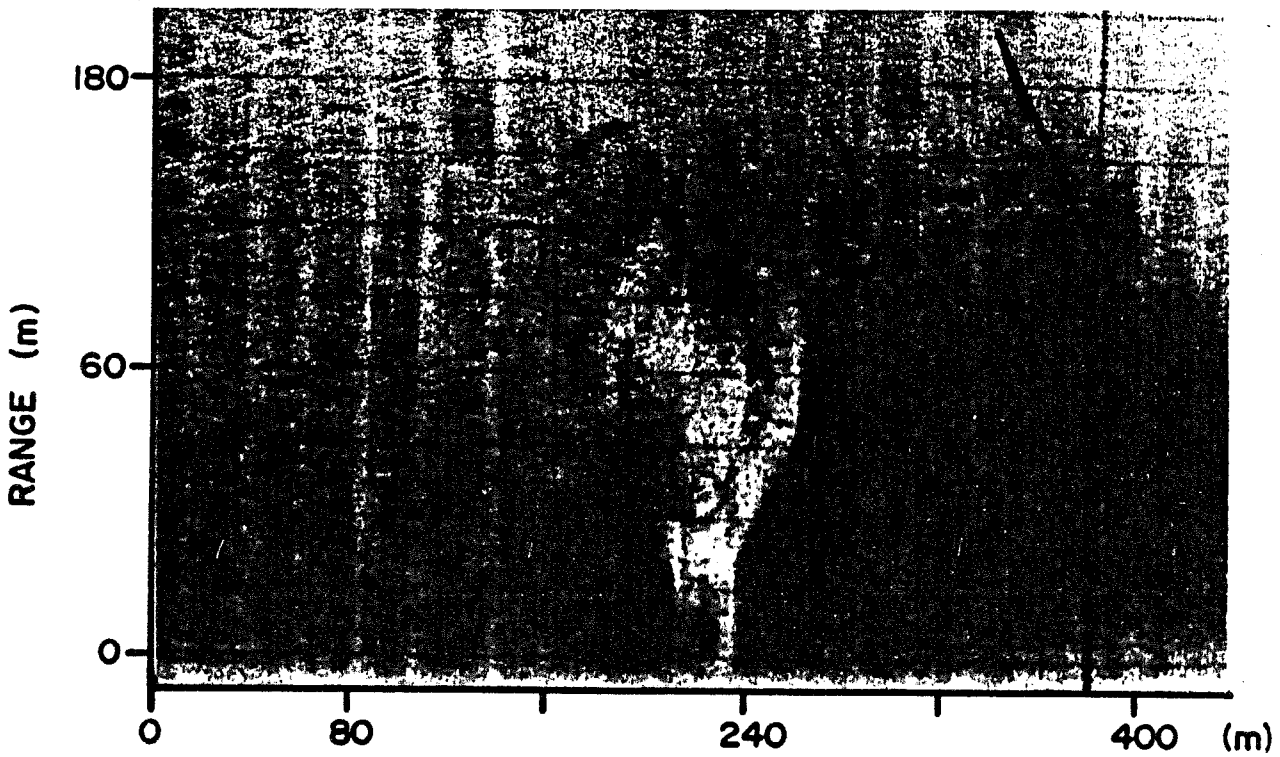

Figure 10

Figure 11

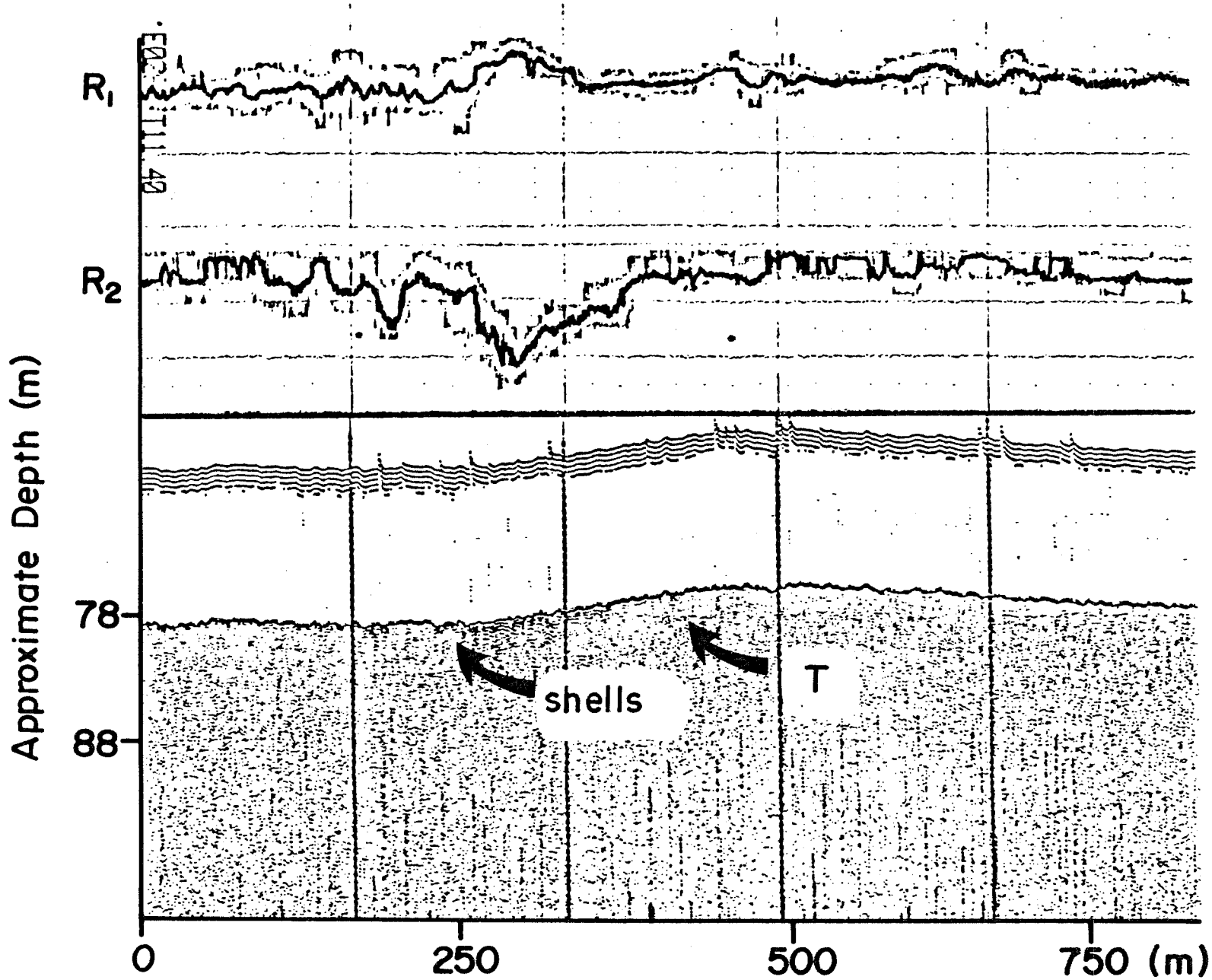
R1
R2
Approximate Depth (m)
78
88
shells
T
0
250
500
750 (m)
T= Tertiary unconformty

Figure 12

Figure 13

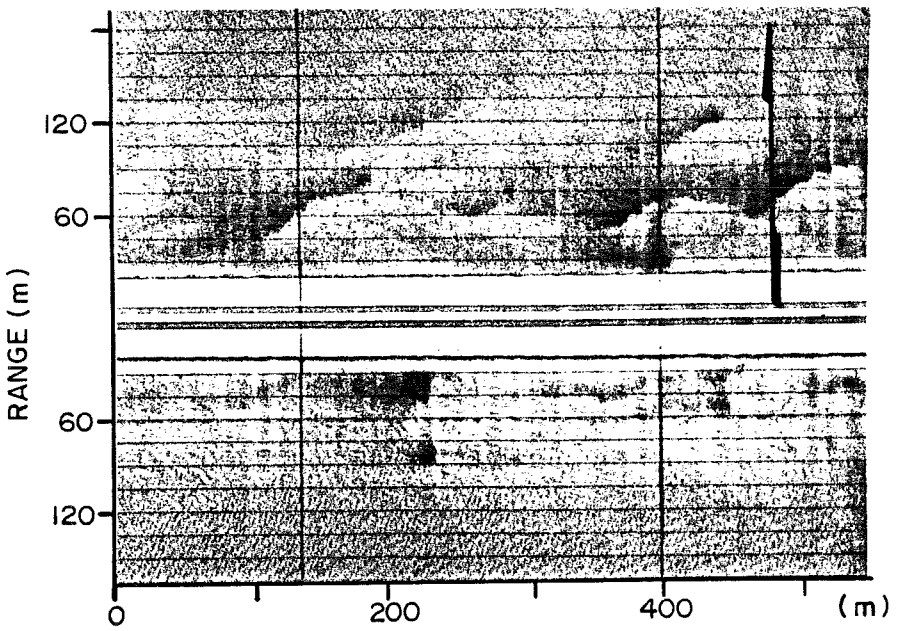

Figure 14

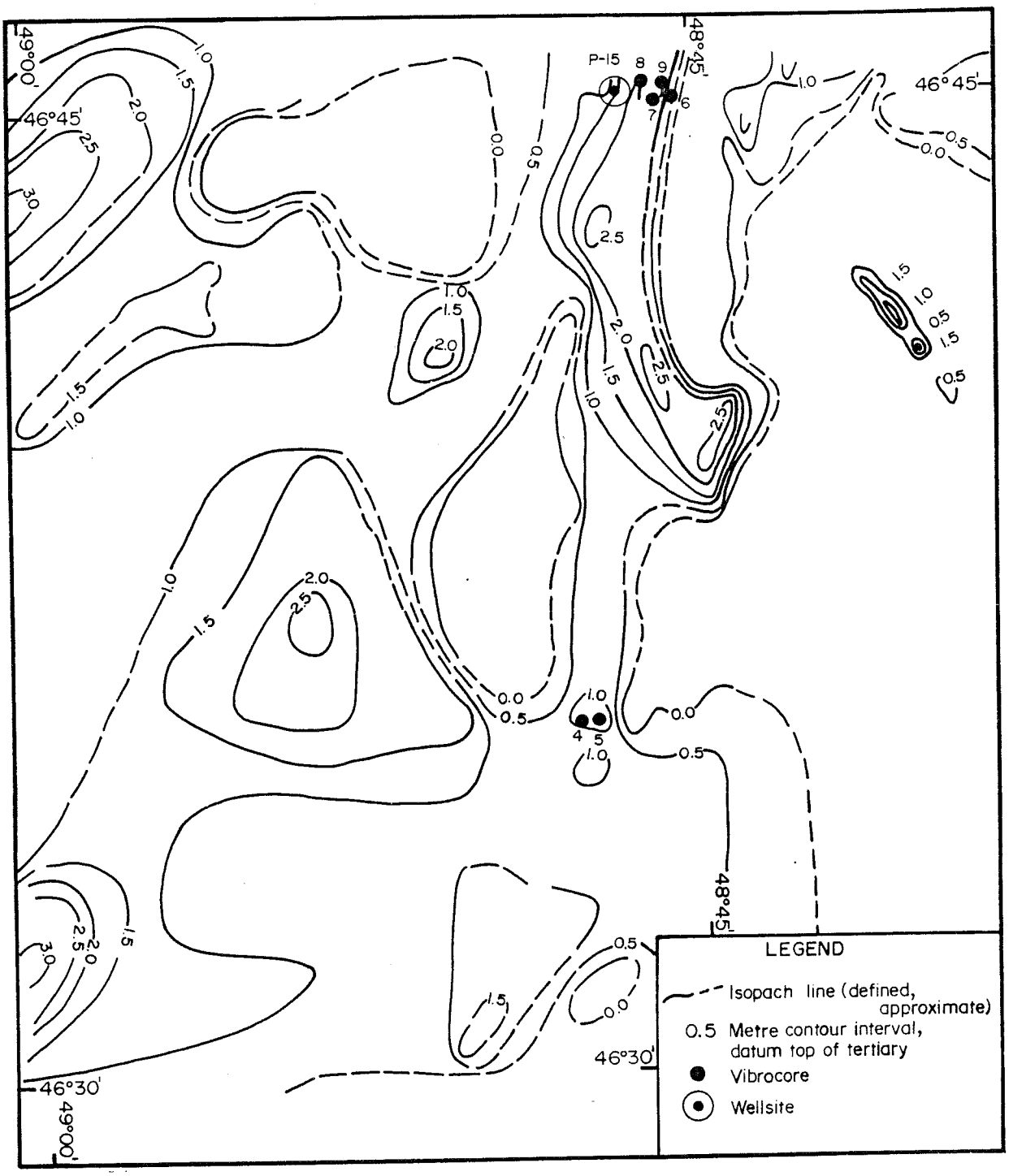
49°00'
46°45'
46°30'
48°45'
P-15
8
9
7
6
4
5
LEGEND
Isopach line (defined, approximate)
0.5 Metre contour interval, datum top of tertiary
Vibrocore
Wellsite

Figure 15

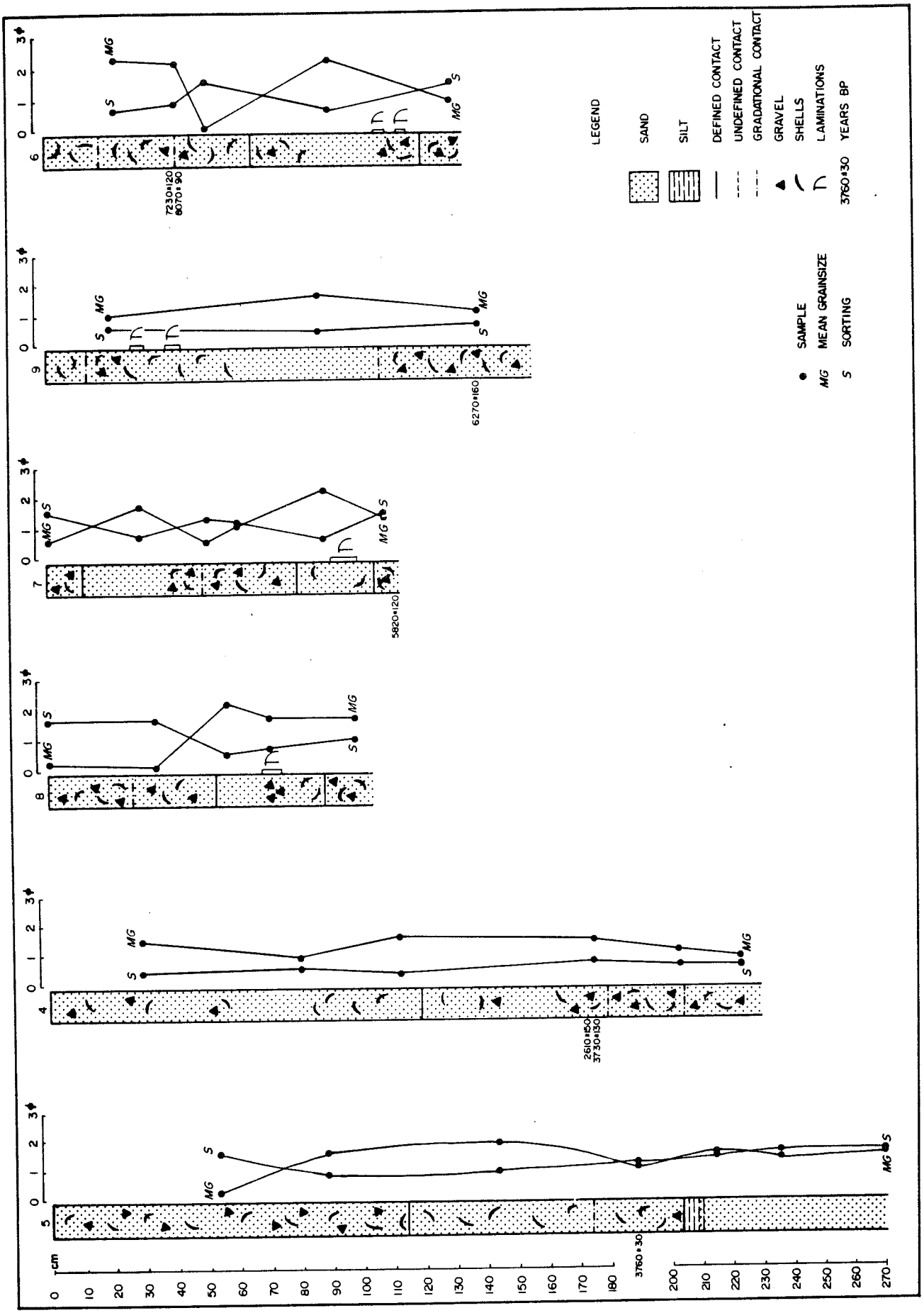
LEGEND
SAND
SILT
DEFINED CONTACT
UNDEFINED CONTACT
GRADATIONAL CONTACT
GRAVEL
SHELLS
LAMINATIONS
3760±30 YEARS BP
SAMPLE
MG MEAN GRAINSIZE
S SORTING
cm
0 10 20 30 40 50 60 70 80 90 100 110 120 130 140 150 160 170 180 200 210 220 230 240 250 260 270
5
4
8
7
9
6
3760±30
2610±50
3730±30
5820±120
6270±160
7230±120
8070±90

Figure 16

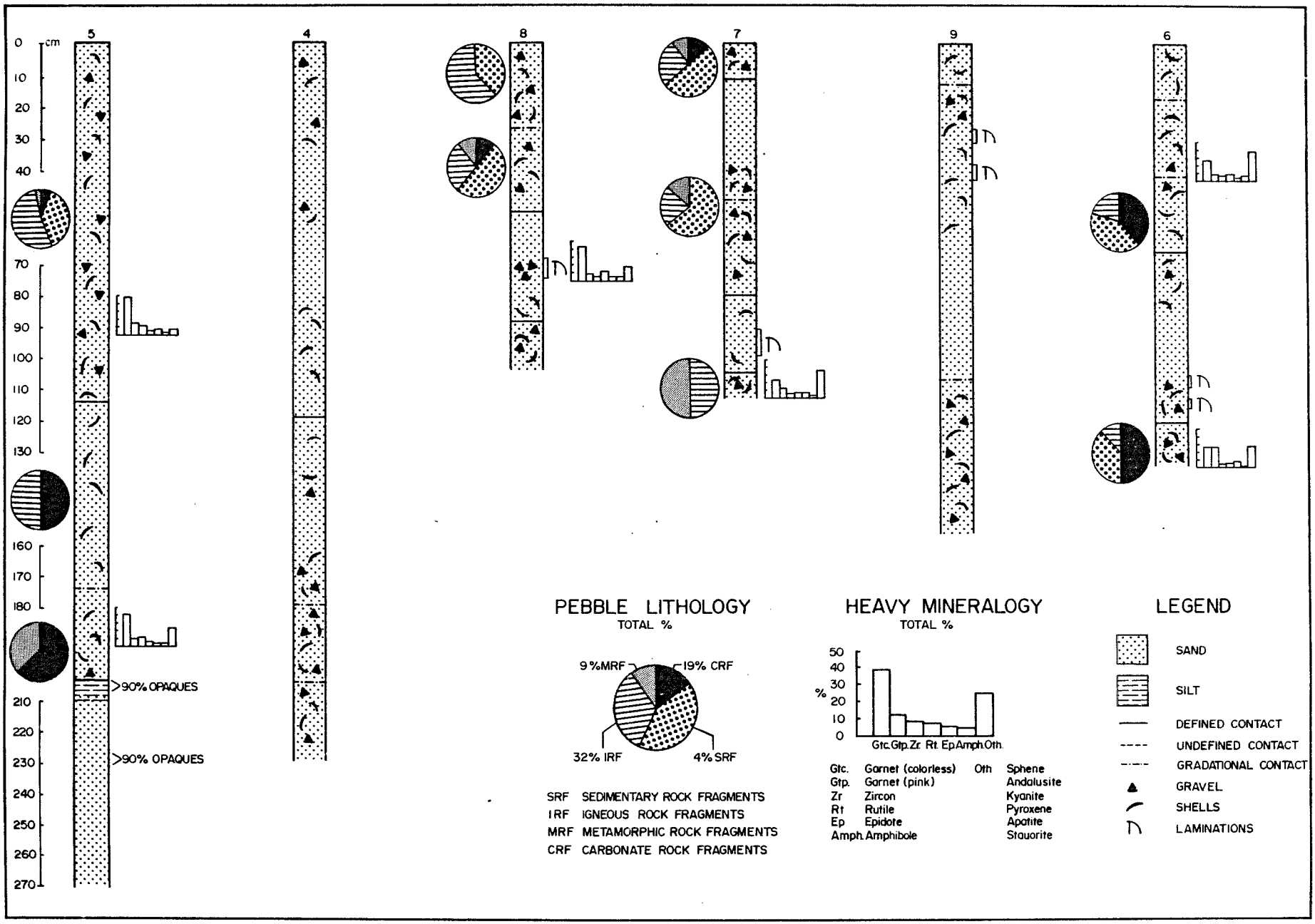
0 cm
10
20
30
40
70
80
90
100
110
120
130
160
170
180
210
220
230
240
250
260
270
5
4
8
7
9
6
>90% OPAQUES
>90% OPAQUES
PEBBLE LITHOLOGY
TOTAL %
9 %MRF
19% CRF
32% IRF
4% SRF
SRF SEDIMENTARY ROCK FRAGMENTS
IRF IGNEOUS ROCK FRAGMENTS
MRF METAMORPHIC ROCK FRAGMENTS
CRF CARBONATE ROCK FRAGMENTS
HEAVY MINERALOGY
TOTAL %
%
50
40
30
20
10
0
Gtc. Gtp. Zr. Rt. Ep. Amph. Oth.
Gtc. Garnet (colorless)
Gtp. Garnet (pink)
Zr Zircon
Rt Rutile
Ep Epidote
Amph. Amphibole
Oth Sphene
Andalusite
Kyanite
Pyroxene
Apatite
Staurolite
LEGEND
SAND
SILT
DEFINED CONTACT
UNDEFINED CONTACT
GRADATIONAL CONTACT
GRAVEL
SHELLS
LAMINATIONS

Figure 17

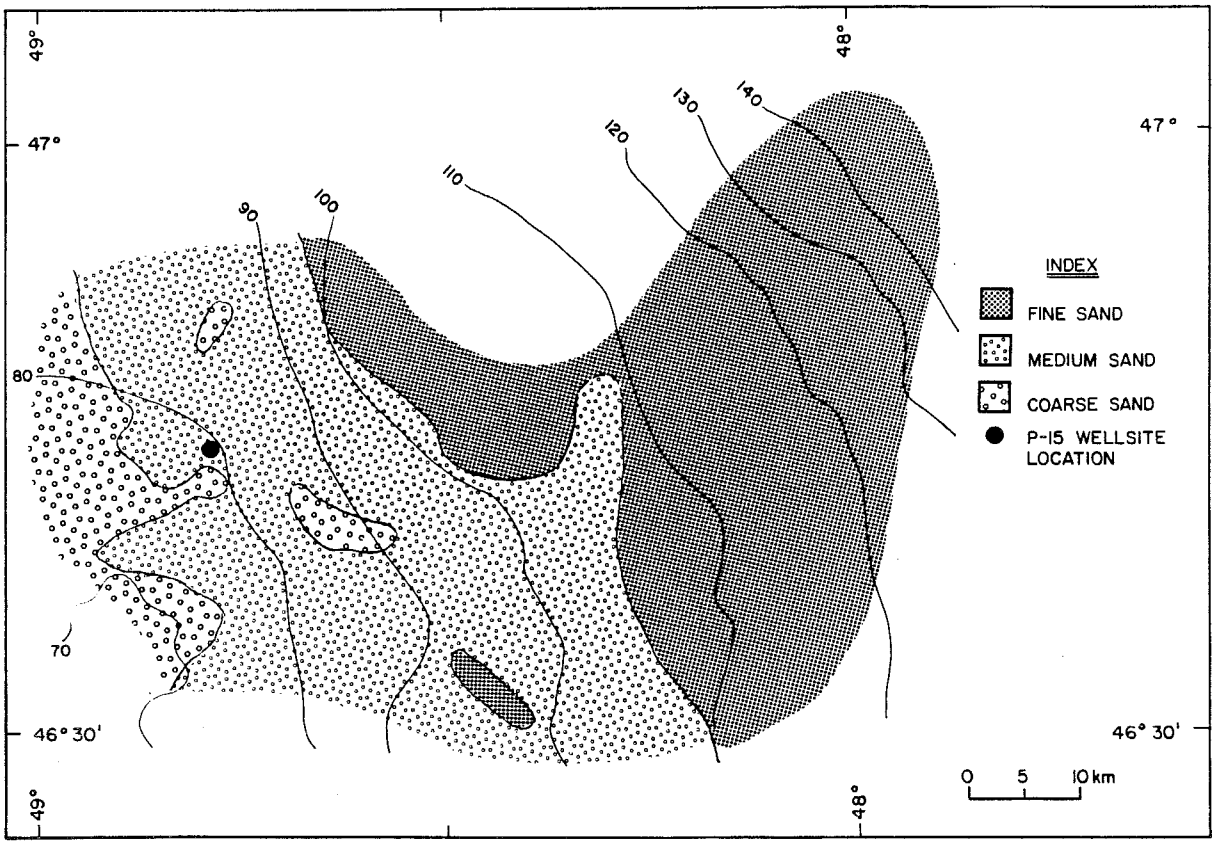
49°
48°
47°
47°
130
140
120
110
100
90
80°
70
46° 30'
46° 30'
49°
48°
INDEX
FINE SAND
MEDIUM SAND
COARSE SAND
P-15 WELLSITE LOCATION
0 5 10 km

Figure 18

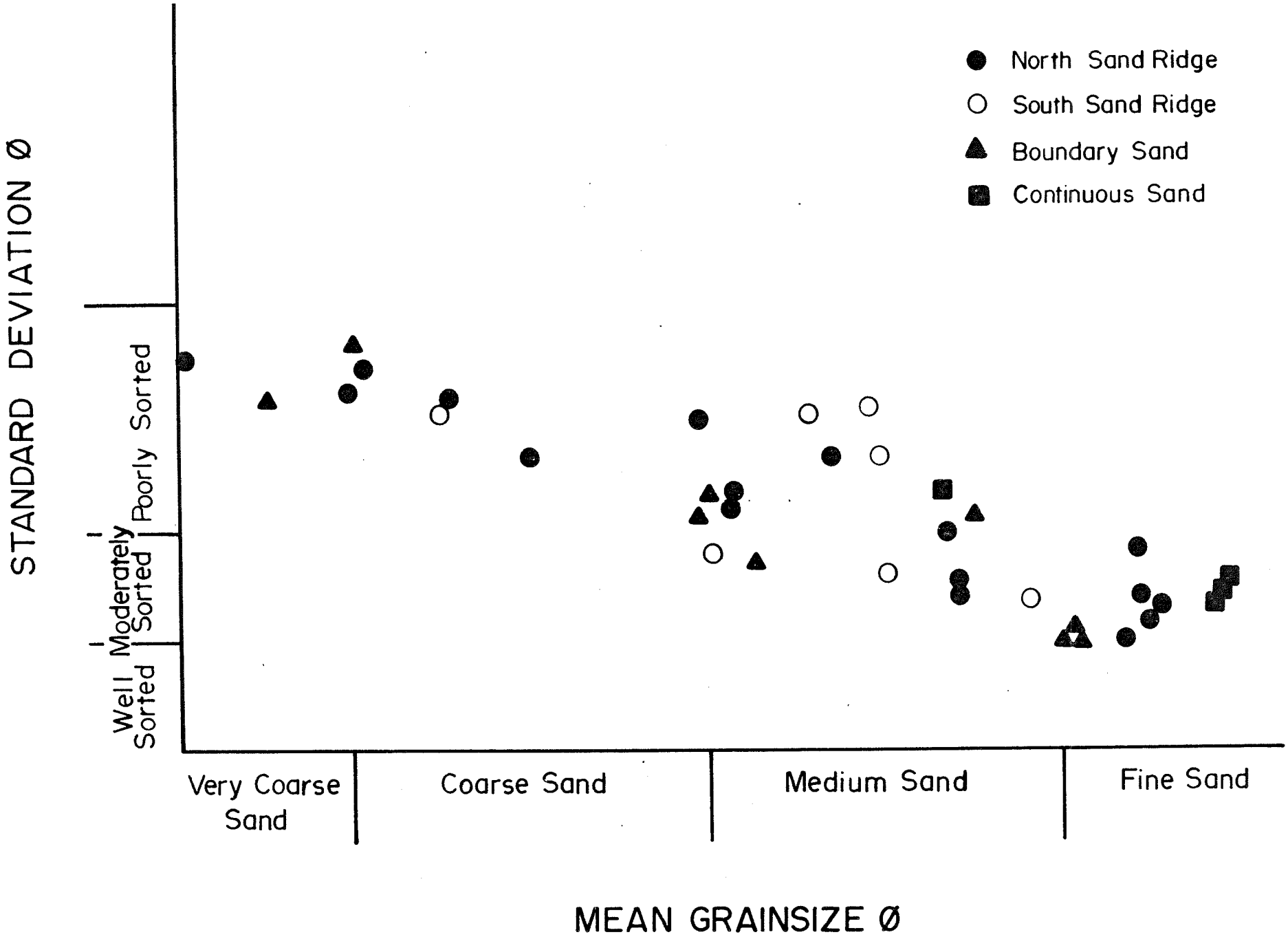
North Sand Ridge
South Sand Ridge
Boundary Sand
Continuous Sand
STANDARD DEVIATION Ø
Poorly Sorted
Moderately Sorted
Well Sorted
Very Coarse Sand
Coarse Sand
Medium Sand
Fine Sand
MEAN GRAINSIZE Ø

Figure 19

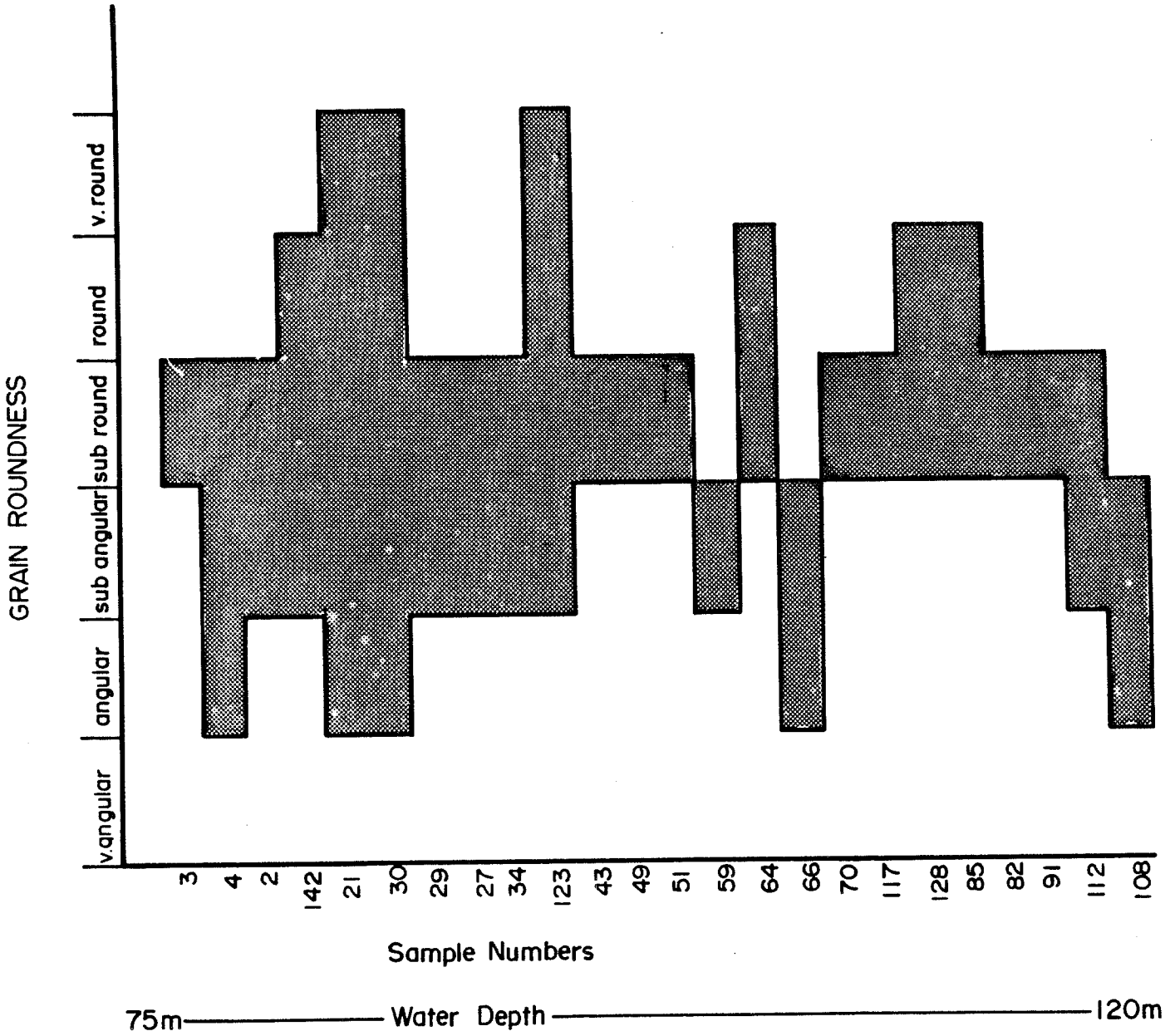
GRAIN ROUNDNESS
v.angular
angular
sub angular
sub round
round
v.round
3
4
2
142
21
30
29
27
34
123
43
49
51
59
64
66
70
117
128
85
82
91
112
108
Sample Numbers
75m
Water Depth
120m

Figure 20

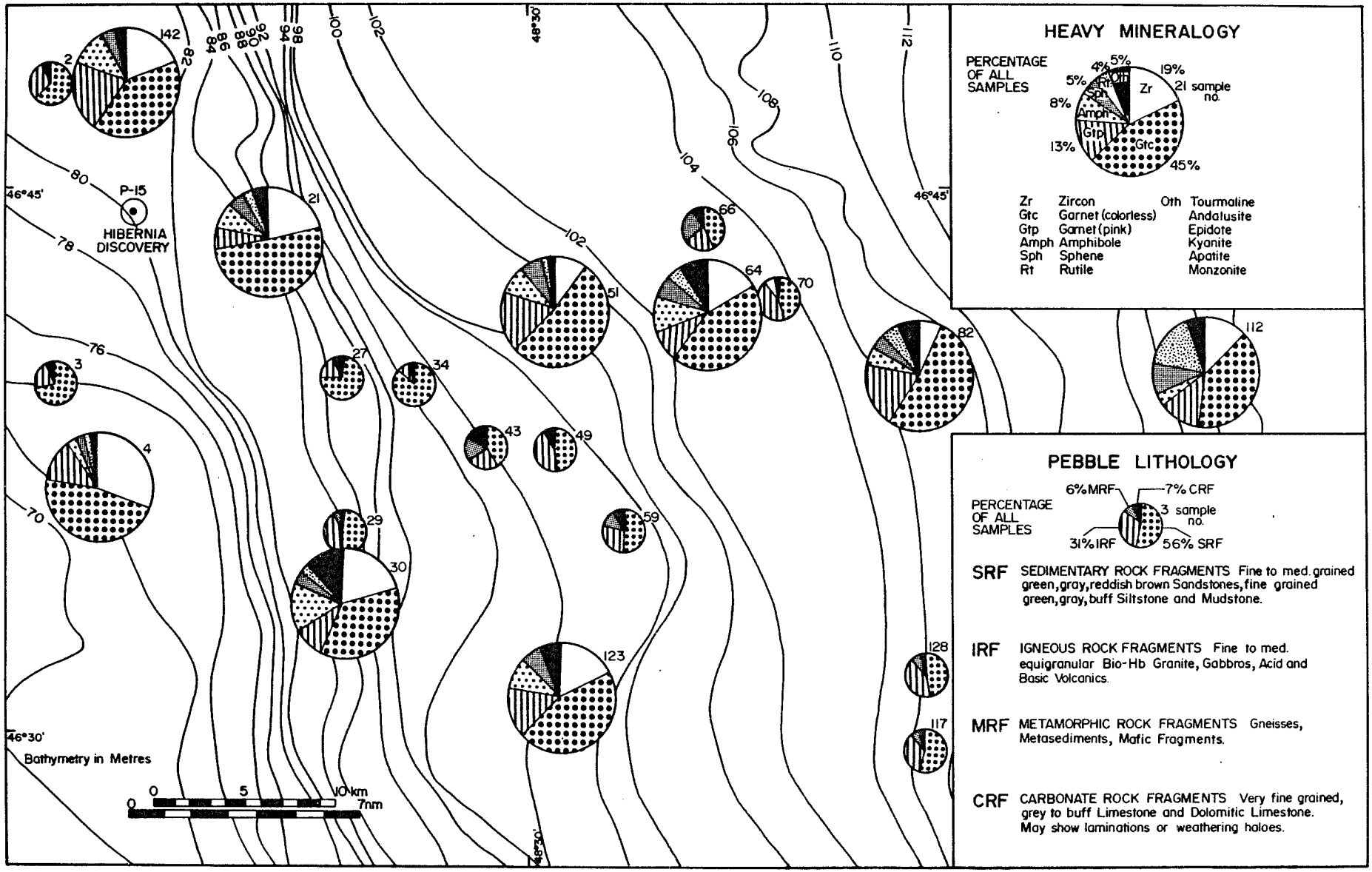
HEAVY MINERALOGY
PERCENTAGE OF ALL SAMPLES
19%
5%
4%
5%
8%
13%
45%
Zr
Oth
Rt
Sph
Amph
Gtp
Gtc
21 sample no.
Zr Zircon
Gtc Garnet (colorless)
Gtp Garnet (pink)
Amph Amphibole
Sph Sphene
Rt Rutile
Oth Tourmaline
Andalusite
Epidote
Kyanite
Apatite
Monzonite
PEBBLE LITHOLOGY
PERCENTAGE OF ALL SAMPLES
6% MRF
7% CRF
31% IRF
56% SRF
3 sample no.
SRF SEDIMENTARY ROCK FRAGMENTS Fine to med. grained green, gray, reddish brown Sandstones, fine grained green, gray, buff Siltstone and Mudstone.
IRF IGNEOUS ROCK FRAGMENTS Fine to med. equigranular Bio-Hb Granite, Gabbros, Acid and Basic Volcanics.
MRF METAMORPHIC ROCK FRAGMENTS Gneisses, Metasediments, Mafic Fragments.
CRF CARBONATE ROCK FRAGMENTS Very fine grained, grey to buff Limestone and Dolomitic Limestone. May show laminations or weathering haloes.
P-15
HIBERNIA DISCOVERY
46°45'
46°30'
48°30'
Bathymetry in Metres
0 5 10 km
0 7nm
80
78
76
70
84
86
88
90
92
94
96
98
100
102
104
106
108
110
112
142
2
21
3
4
27
34
43
49
51
66
64
70
82
112
29
30
59
123
128
117

Figure 21

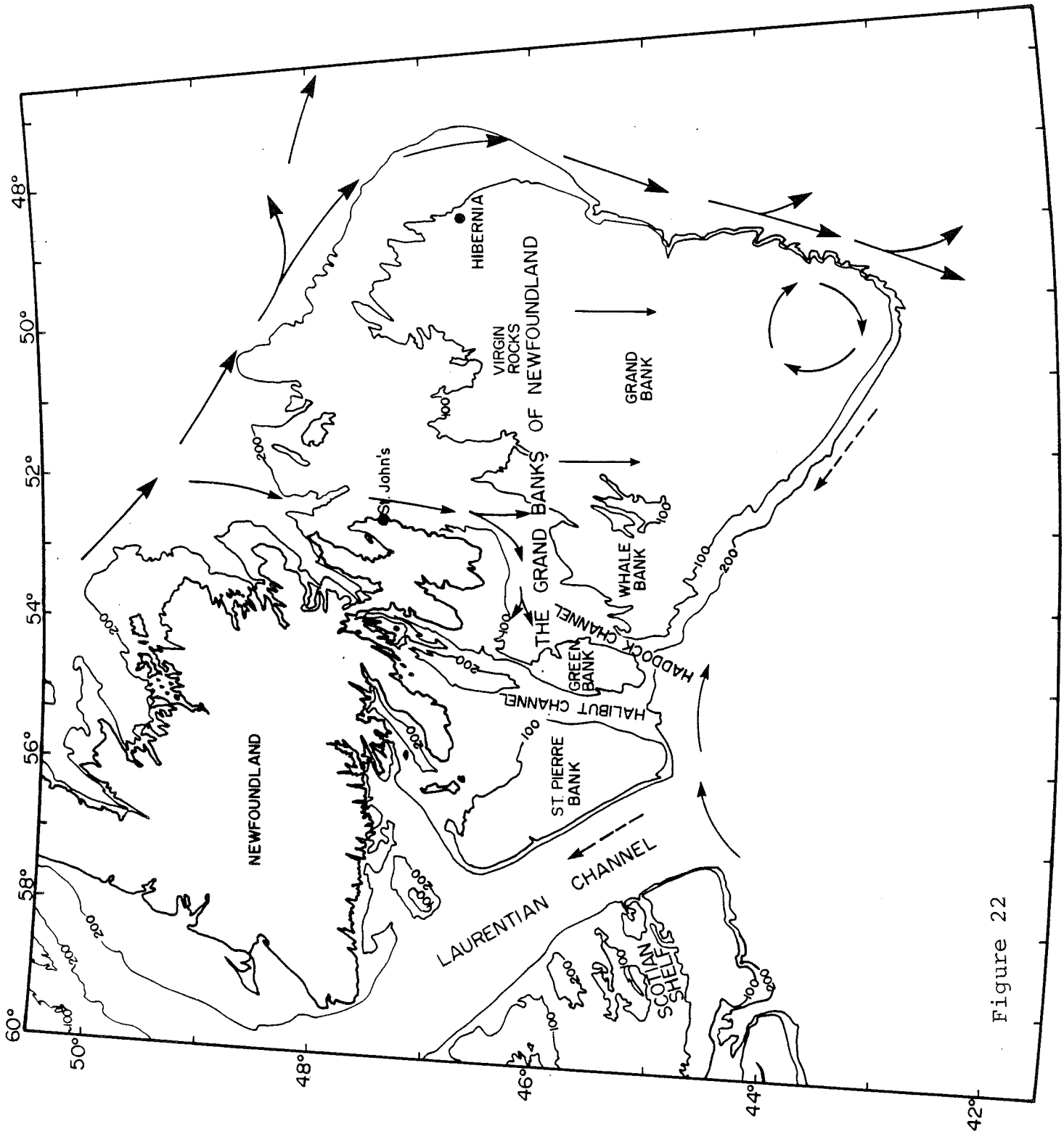
HIBERNIA
VIRGIN ROCKS
OF NEWFOUNDLAND
GRAND BANK
St. John's
THE GRAND BANKS
WHALE BANK
HADDOCK CHANNEL
GREEN BANK
HALIBUT CHANNEL
ST. PIERRE BANK
NEWFOUNDLAND
LAURENTIAN CHANNEL
SCOTIAN SHELF
48°
50°
52°
54°
56°
58°
60°
50°
48°
46°
44°
42°

Figure 22

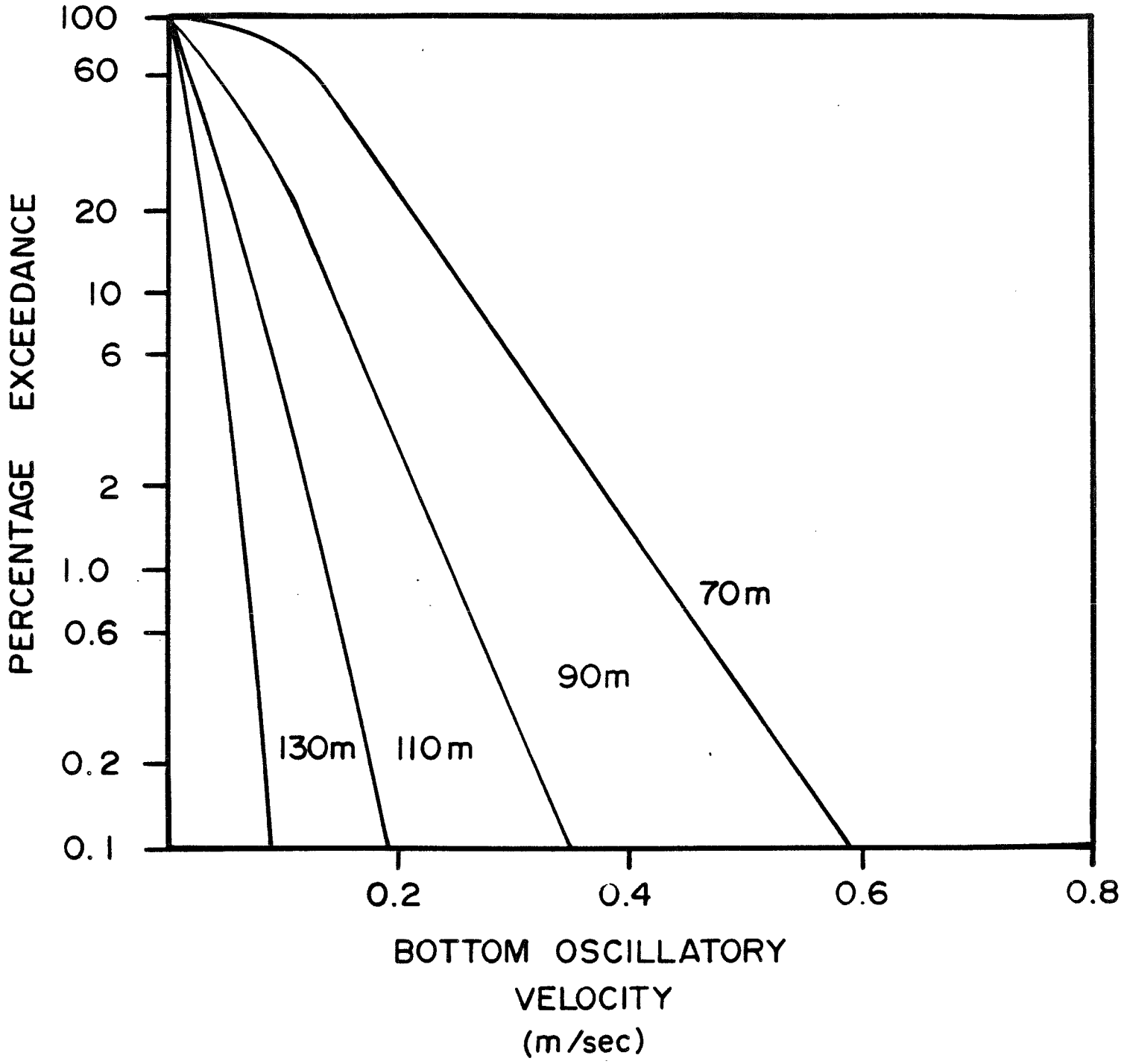
100
60
20
10
6
2
1.0
0.6
0.2
0.1
PERCENTAGE EXCEEDANCE
70m
90m
130m
110m
0.2
0.4
0.6
0.8
BOTTOM OSCILLATORY
VELOCITY
(m/sec)

Figure 23

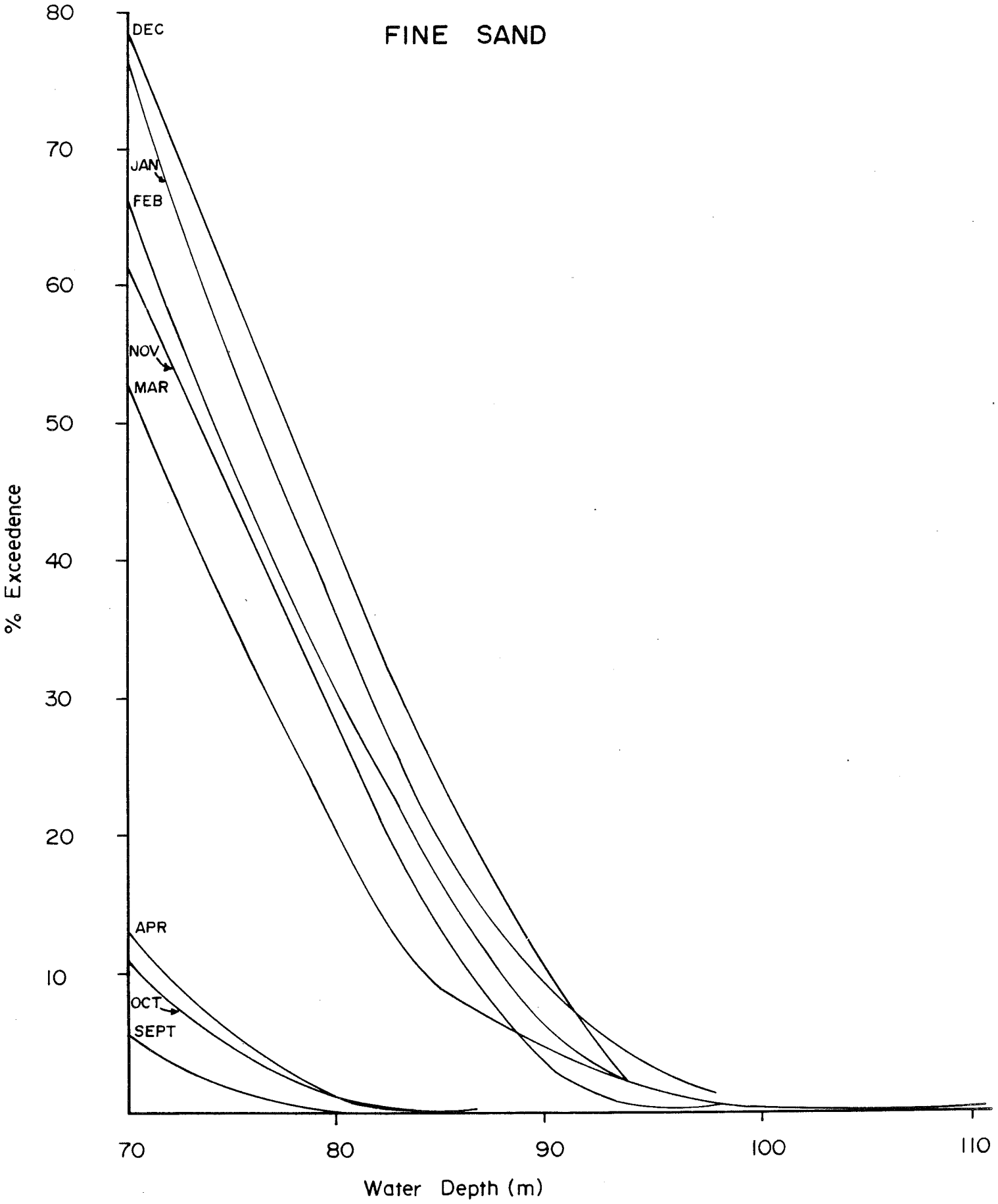
FINE SAND
DEC
JAN
FEB
NOV
MAR
APR
OCT
SEPT
% Exceedence
80
70
60
50
40
30
20
10
70
80
90
100
110
Water Depth (m)

Figure 24a

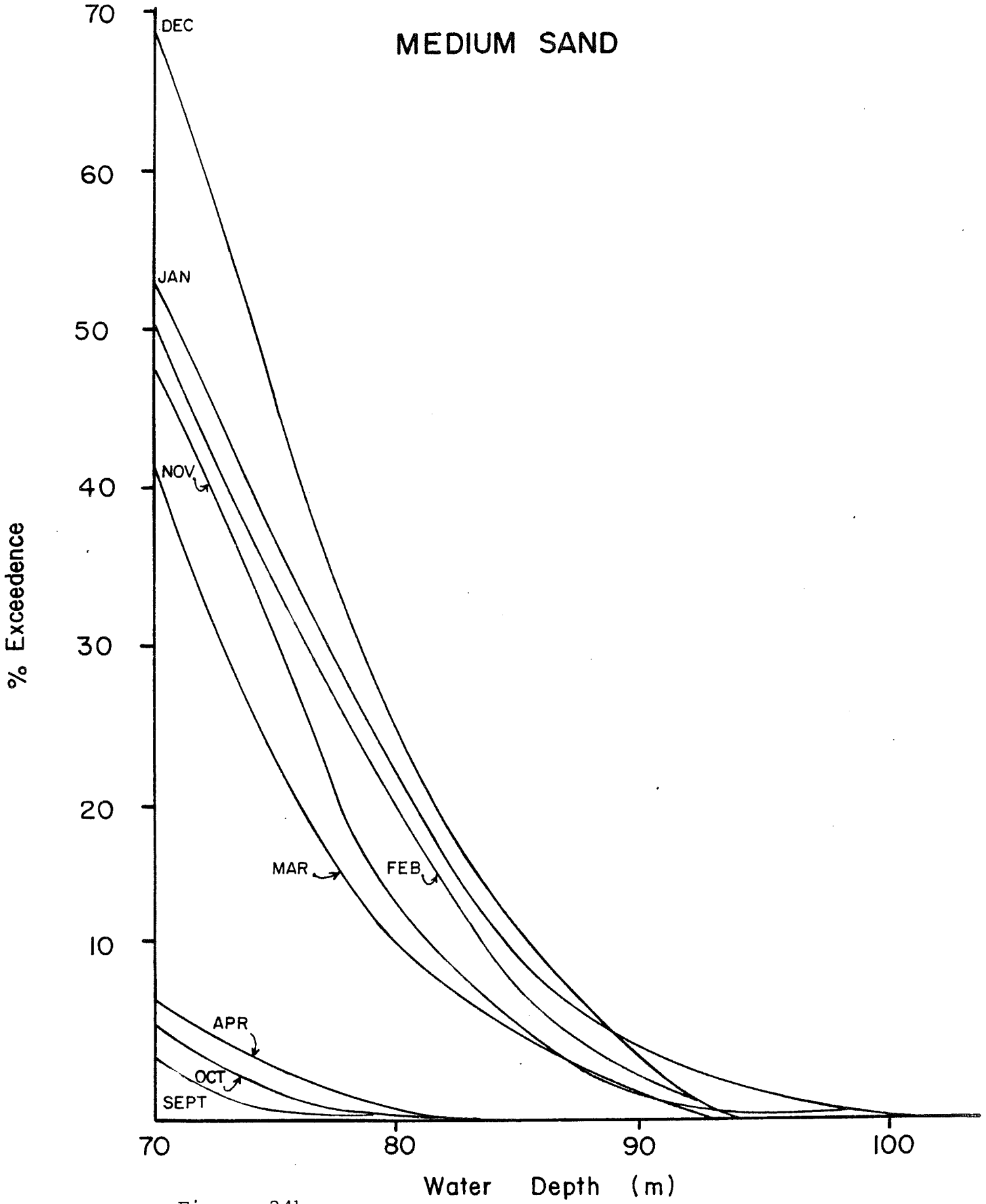
MEDIUM SAND
% Exceedence
70
60
50
40
30
20
10
DEC
JAN
NOV
MAR
FEB
APR
OCT
SEPT
70
80
90
100
Water Depth (m)

Figure 24b

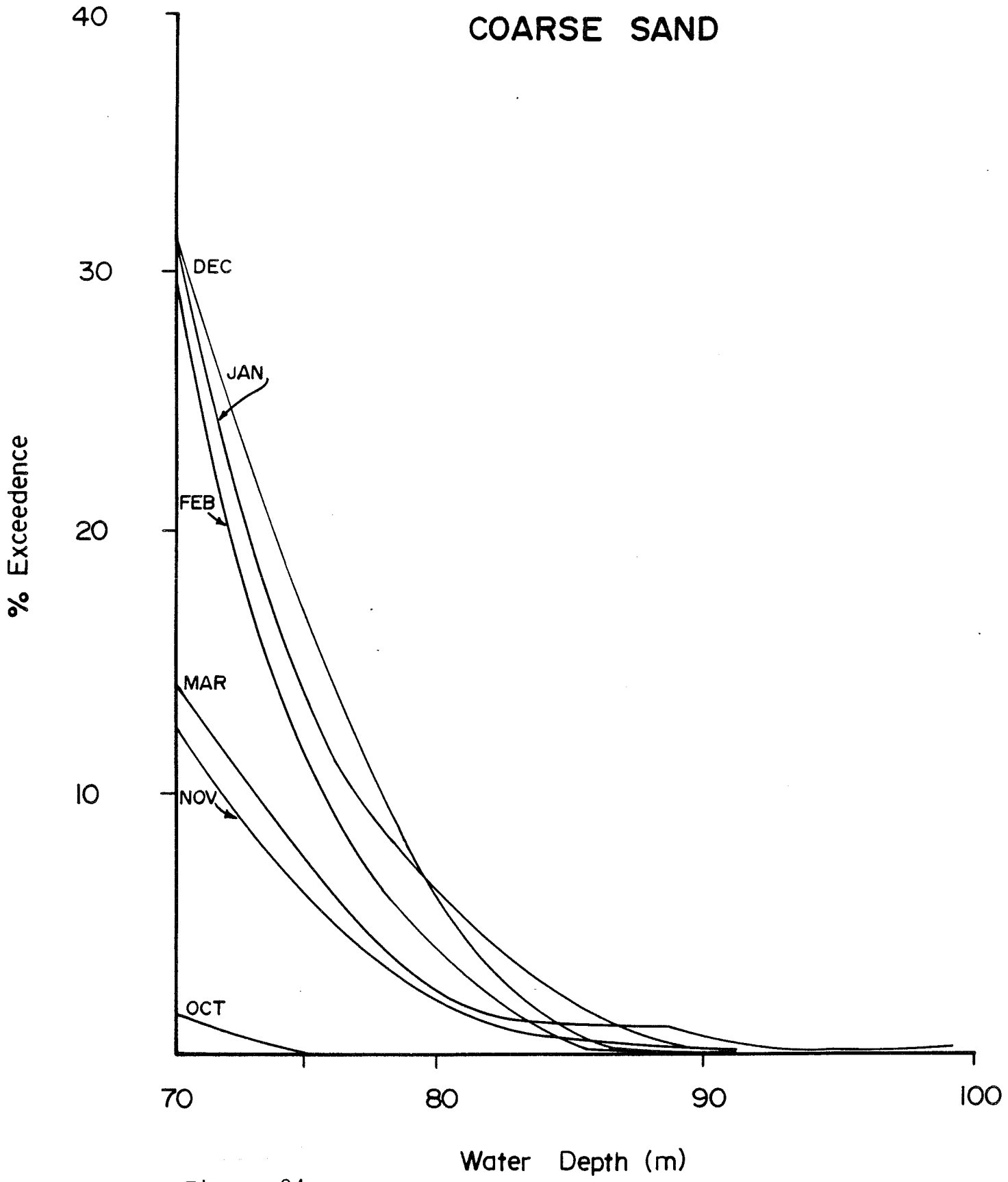
COARSE SAND
40
30
20
10
% Exceedence
DEC
JAN
FEB
MAR
NOV
OCT
70
80
90
100
Water Depth (m)

Figure 24c

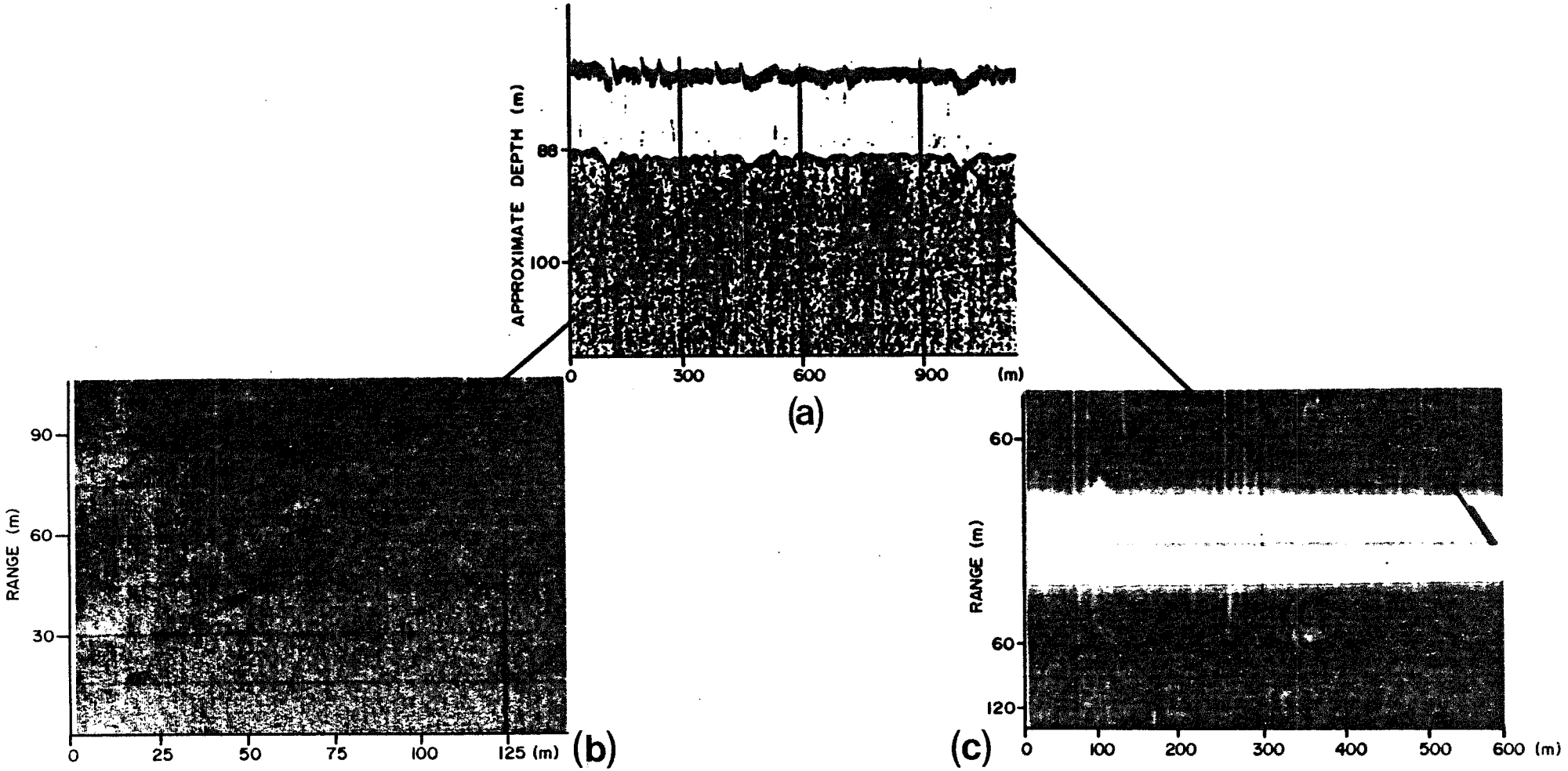
APPROXIMATE DEPTH (m)
88
100
0
300
600
900
(m)
(a)
RANGE (m)
90
60
30
0
25
50
75
100
125 (m)
(b)
RANGE (m)
60
60
120
0
100
200
300
400
500
600 (m)
(c)

Figure 25

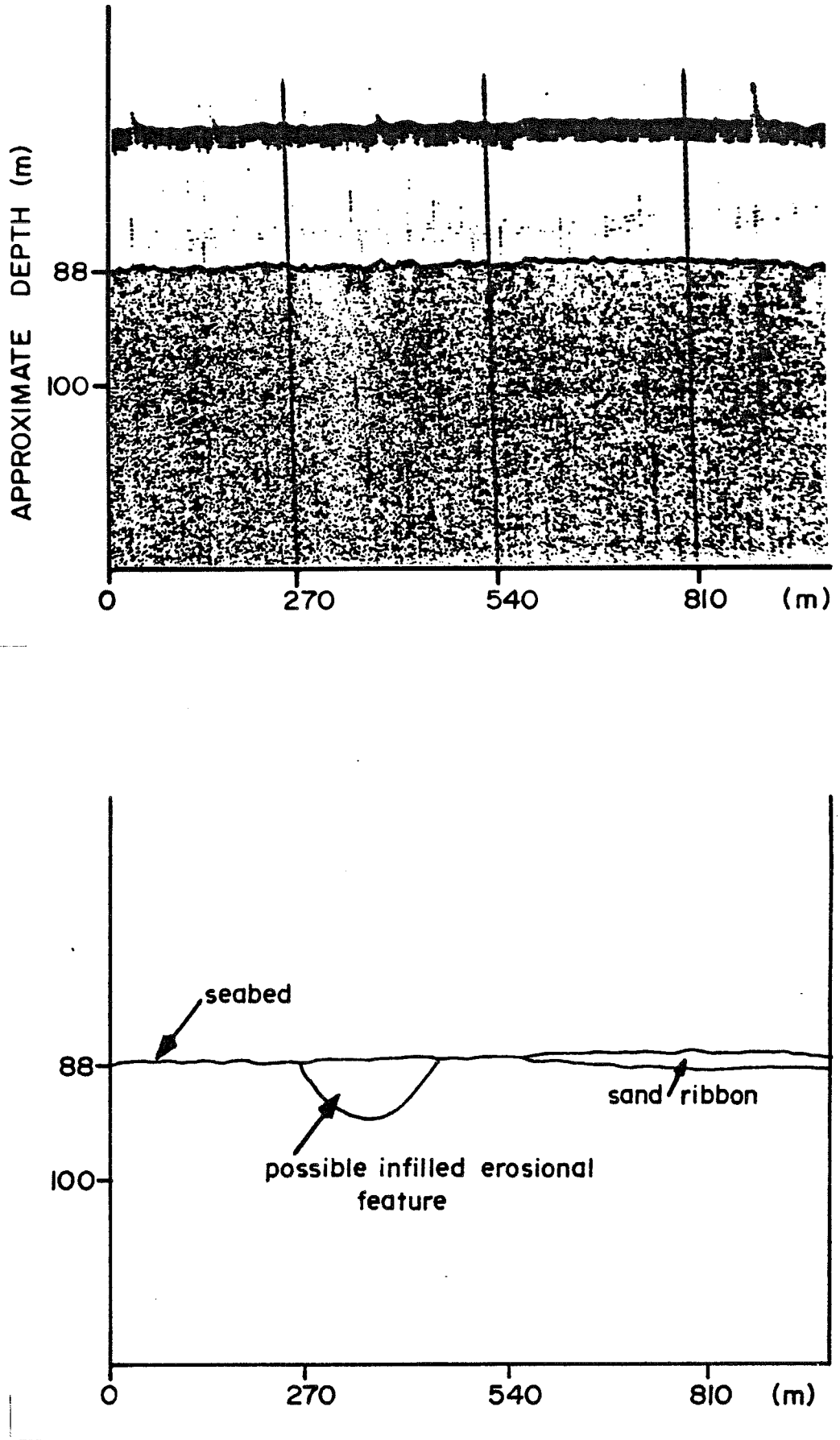
APPROXIMATE DEPTH (m)
88
100
0
270
540
810
(m)
seabed
88
sand ribbon
100
possible infilled erosional feature
0
270
540
810
(m)

Figure 26

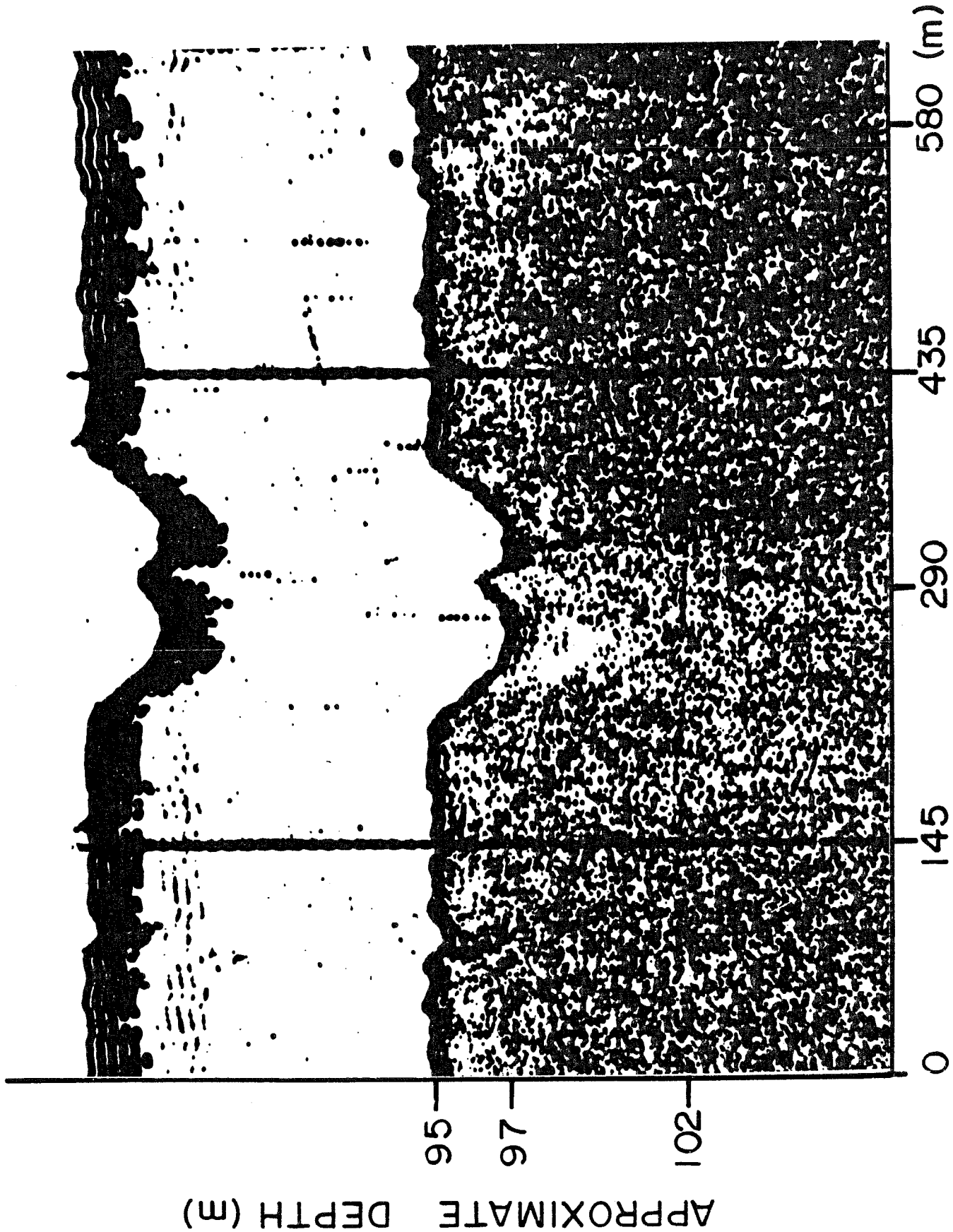

Figure 27

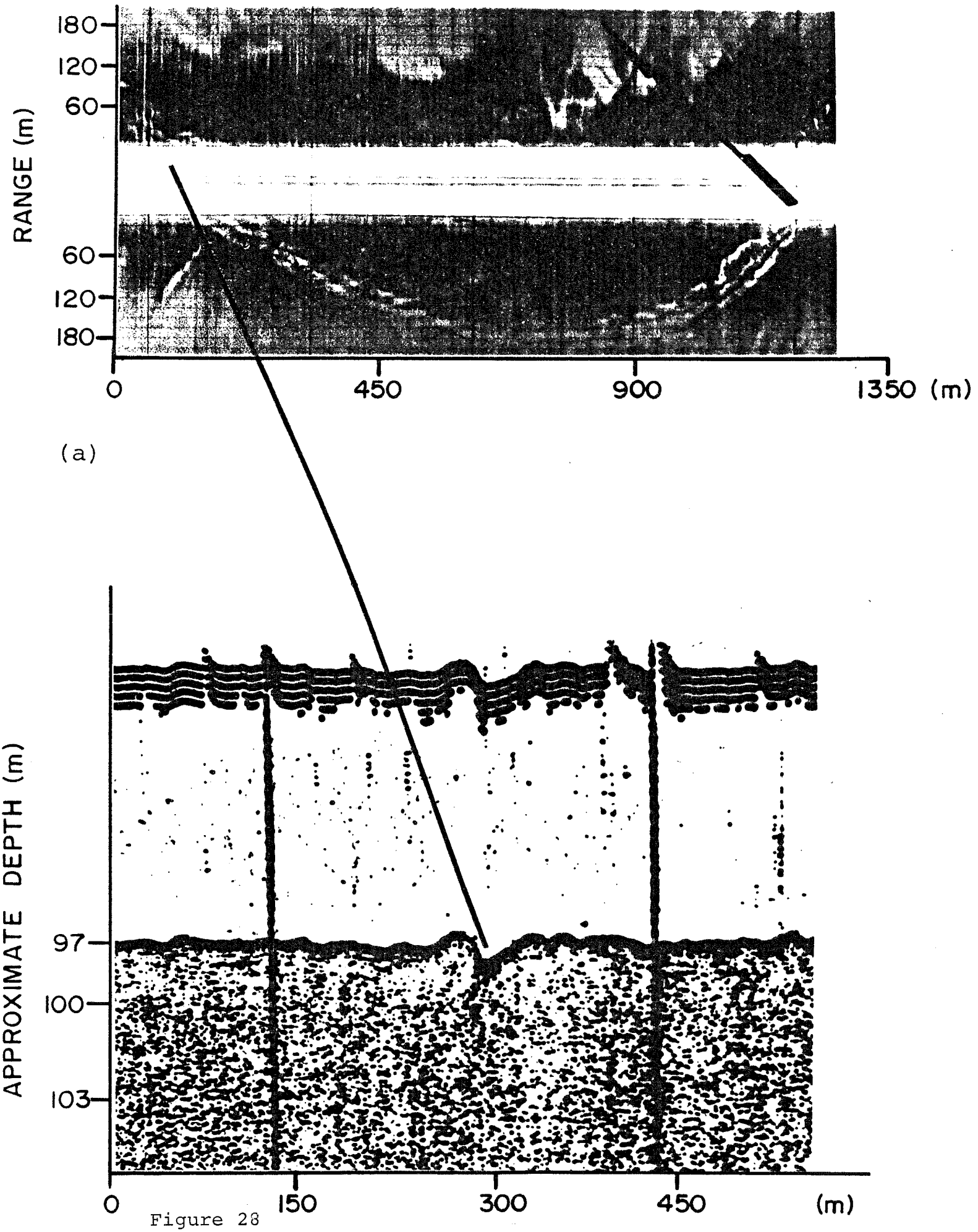
RANGE (m)
180
120
60
60
120
180
0
450
900
1350 (m)
(a)
APPROXIMATE DEPTH (m)
97
100
103
0
150
300
450
(m)

Figure 28

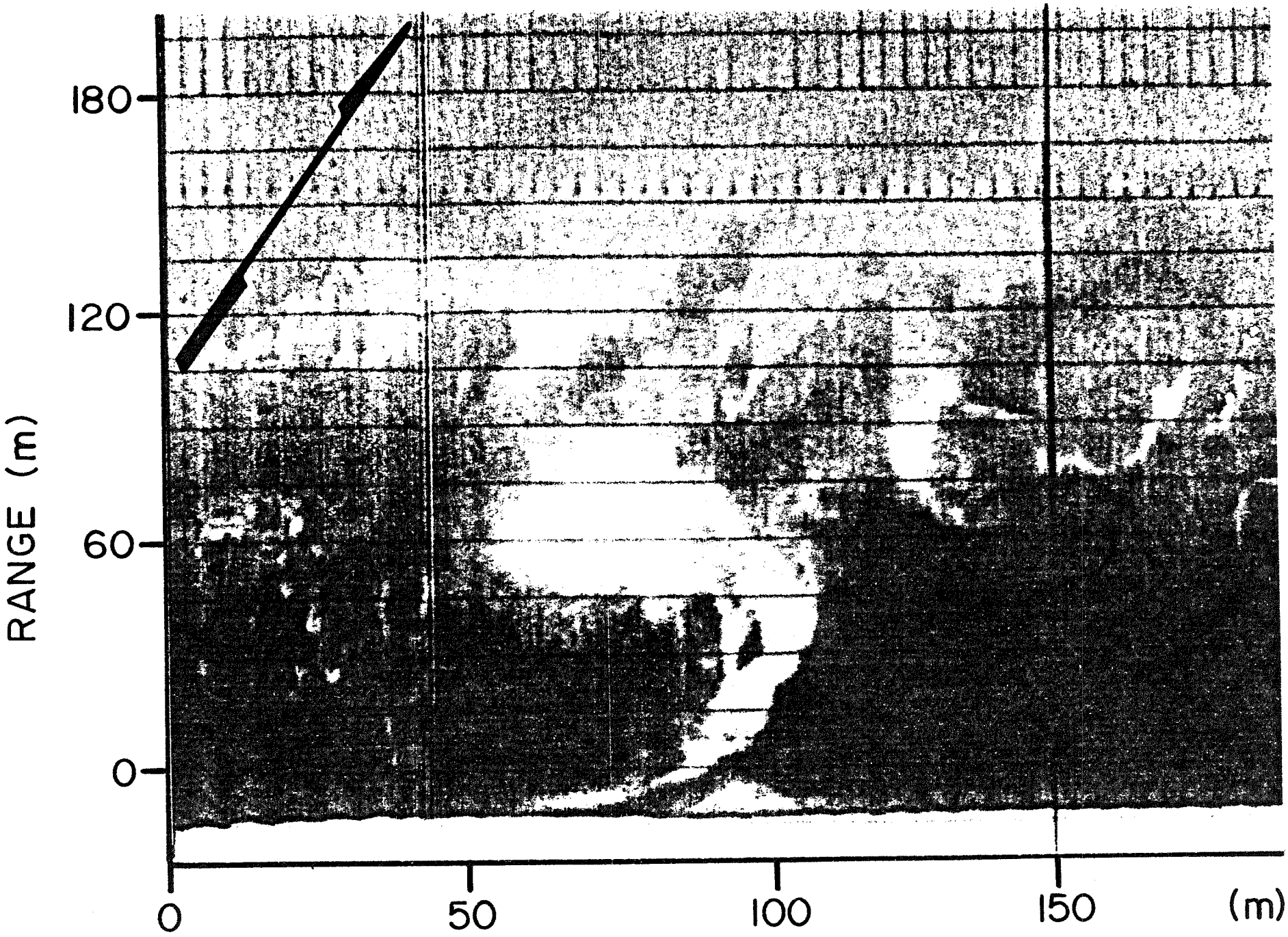

Figure 29

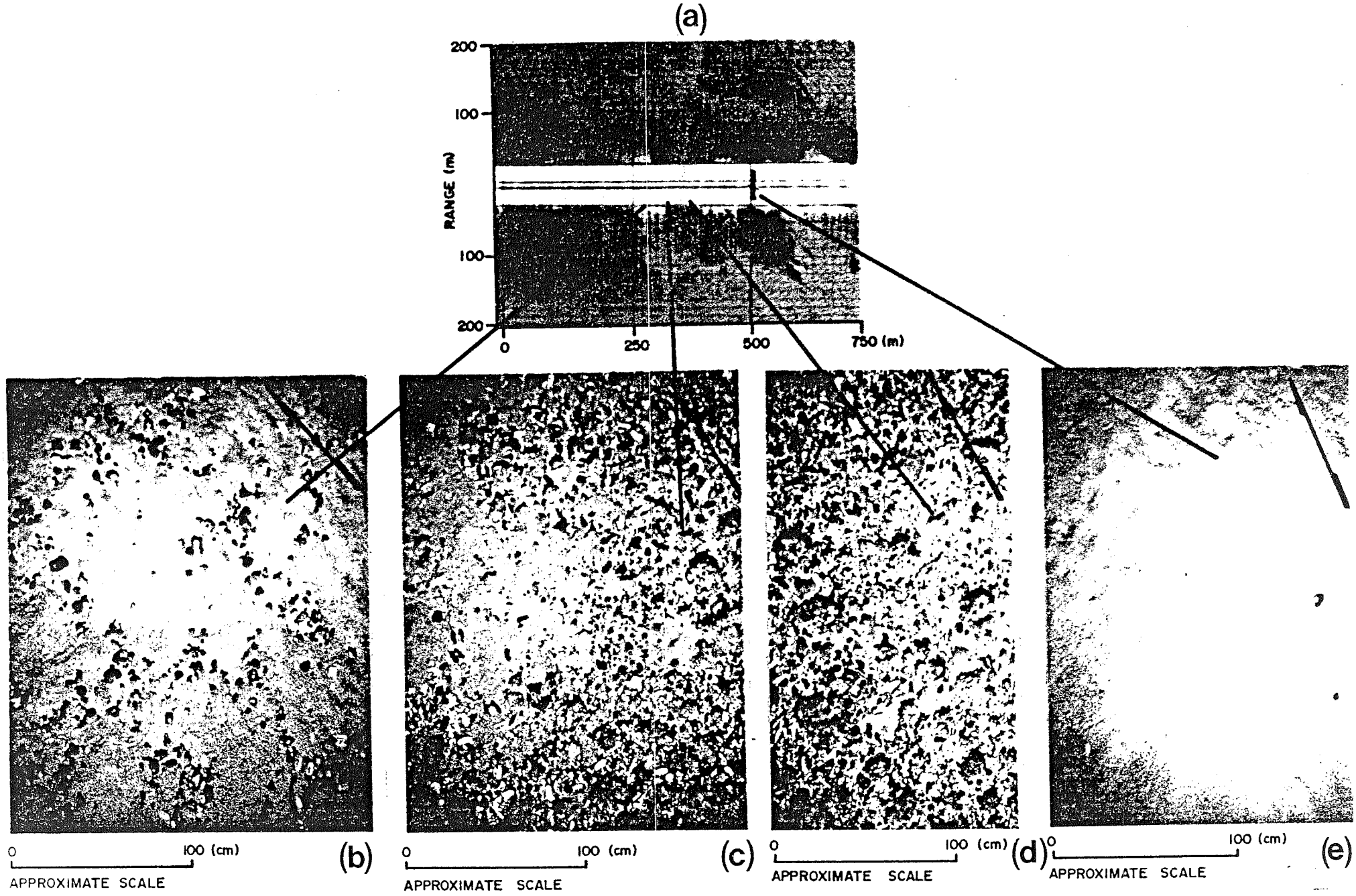
(a)
200
100
RANGE (m)
100
200
0
250
500
750 (m)
0
100 (cm)
APPROXIMATE SCALE
(b)
0
100 (cm)
APPROXIMATE SCALE
(c)
0
100 (cm)
APPROXIMATE SCALE
(d)
0
100 (cm)
APPROXIMATE SCALE
(e)

Figure 30